

# Recursive Importance Sketching for Rank Constrained Least Squares: Algorithms and High-order Convergence

Yuetian Luo<sup>1</sup>, Wen Huang<sup>2</sup>, Xudong Li<sup>3</sup>, and Anru R. Zhang<sup>1,4</sup>

December 22, 2024

## Abstract

In this paper, we propose a new *Recursive Importance Sketching* algorithm for *Rank* constrained least squares *Optimization* (RISRO). As its name suggests, the algorithm is based on a new sketching framework, recursive importance sketching. Several existing algorithms in the literature can be reinterpreted under the new sketching framework and RISRO offers clear advantages over them. RISRO is easy to implement and computationally efficient, where the core procedure in each iteration is only solving a dimension reduced least squares problem. Different from numerous existing algorithms with locally geometric convergence rate, we establish the local quadratic-linear and quadratic rate of convergence for RISRO under some mild conditions. In addition, we discover a deep connection of RISRO to Riemannian manifold optimization on fixed rank matrices. The effectiveness of RISRO is demonstrated in two applications in machine learning and statistics: low-rank matrix trace regression and phase retrieval. Simulation studies demonstrate the superior numerical performance of RISRO.

**Keywords:** Rank constrained least squares, Sketching, Quadratic convergence, Riemannian manifold optimization, Low-rank matrix recovery, Non-convex optimization

## 1 Introduction

The focus of this paper is on the rank constrained least squares:

$$\min_{\mathbf{X} \in \mathbb{R}^{p_1 \times p_2}} f(\mathbf{X}) := \frac{1}{2} \|\mathbf{y} - \mathcal{A}(\mathbf{X})\|_2^2, \quad \text{subject to} \quad \text{rank}(\mathbf{X}) = r. \quad (1)$$

Here,  $\mathbf{y} \in \mathbb{R}^n$  is the given data and  $\mathcal{A} \in \mathbb{R}^{p_1 \times p_2} \rightarrow \mathbb{R}^n$  is a known linear map that can be explicitly represented as

$$\mathcal{A}(\mathbf{X}) = [\langle \mathbf{A}_1, \mathbf{X} \rangle, \dots, \langle \mathbf{A}_n, \mathbf{X} \rangle]^\top, \quad \langle \mathbf{A}_i, \mathbf{X} \rangle = \sum_{1 \leq j \leq p_1, 1 \leq k \leq p_2} (\mathbf{A}_i)_{[j,k]} \mathbf{X}_{[j,k]} \quad (2)$$

with given measurement matrices  $\mathbf{A}_i \in \mathbb{R}^{p_1 \times p_2}$ ,  $i = 1, \dots, n$ . The expected rank is assumed to be known in Problem (1) since in some applications such as phase retrieval and blind deconvolution,

<sup>1</sup>Department of Statistics, University of Wisconsin-Madison [yluo86@wisc.edu](mailto:yluo86@wisc.edu), [anruzhang@stat.wisc.edu](mailto:anruzhang@stat.wisc.edu). Y. Luo would like to thank RAsip from Institute for Foundations of Data Science at UW-Madison.

<sup>2</sup>School of Mathematical Sciences, Xiamen University [wen.huang@xmu.edu.cn](mailto:wen.huang@xmu.edu.cn)

<sup>3</sup>School of Data Science and Shanghai Center for Mathematical Sciences, Fudan University [lixudong@fudan.edu.cn](mailto:lixudong@fudan.edu.cn)

<sup>4</sup>Department of Biostatistics and Bioinformatics, Duke University

the expected rank is known to be one. If the expected rank is unknown, it is typical to optimize over the set of fixed rank matrices using the formulation of (1) and dynamically update the rank, see, e.g., [Vandereycken and Vandewalle \(2010\)](#); [Zhou et al. \(2016\)](#).

The rank constrained least squares (1) is motivated by the widely studied low-rank matrix recovery problem, where the goal is to recovery a low-rank matrix  $\mathbf{X}^*$  from the observation  $\mathbf{y} = \mathcal{A}(\mathbf{X}^*) + \epsilon$  ( $\epsilon$  is the noise). This problem is of fundamental importance in a variety of fields such as optimization, machine learning, signal processing, scientific computation, and statistics. With different realizations of  $\mathcal{A}$ , (1) covers many applications, such as matrix trace regression ([Candès and Plan, 2011](#); [Davenport and Romberg, 2016](#)), matrix completion ([Candès and Tao, 2010](#); [Keshavan et al., 2009](#); [Koltchinskii et al., 2011](#); [Miao et al., 2016](#)), phase retrieval ([Candès et al., 2013](#); [Shechtman et al., 2015](#)), blind devolution ([Ahmed et al., 2013](#)), and matrix recovery via rank-one projections ([Cai and Zhang, 2015](#); [Chen et al., 2015](#)). To overcome the non-convexity and NP-hardness of directly solving (1) ([Recht et al., 2010](#)), various computational feasible schemes have been developed in the past decade. In particular, the convex relaxation has been a central topic of interest ([Recht et al., 2010](#); [Candès and Plan, 2011](#)):

$$\min_{\mathbf{X} \in \mathbb{R}^{p_1 \times p_2}} \frac{1}{2} \|\mathbf{y} - \mathcal{A}(\mathbf{X})\|_2^2 + \lambda \|\mathbf{X}\|_*, \quad (3)$$

where  $\|\mathbf{X}\|_* = \sum_{i=1}^{\min(p_1, p_2)} \sigma_i(\mathbf{X})$  is the nuclear norm of  $\mathbf{X}$  and  $\lambda > 0$  is a tuning parameter. Nevertheless, the convex relaxation technique has one well-documented limitation: the parameter space after relaxation is usually much larger than that of the target problem. Also, algorithms for solving the convex programming often require the singular value decomposition as the stepping stone and can be prohibitively time consuming for large-scale instances.

In addition, non-convex optimization renders another important class of algorithms for solving (1), which directly enforce the rank  $r$  constraint on the iterates. Since each iterate lies in a low dimensional space, the computation cost of the non-convex approach can be much smaller than the convex regularized approach. In the last couple of years, there is a flurry of research on non-convex methods in solving (1) ([Chen and Wainwright, 2015](#); [Hardt, 2014](#); [Jain et al., 2013](#); [Sun and Luo, 2015](#); [Tran-Dinh and Zhang, 2016](#); [Tu et al., 2016](#); [Wen et al., 2012](#); [Zhao et al., 2015](#); [Zheng and Lafferty, 2015](#)), and many of the algorithms such as gradient descent and alternating minimization are shown to have nice convergence results under proper assumptions ([Hardt, 2014](#); [Jain et al., 2013](#); [Sun and Luo, 2015](#); [Tu et al., 2016](#); [Zhao et al., 2015](#)). We refer readers to Section 1.2 for more review on recent works on convex and non-convex approaches on solving (1).

In the existing literature, many algorithms for solving (1) either require careful tuning of hyper-parameters or have a convergence rate no faster than linear. Thus, we raise the following question:

*Can we develop an easy-to-compute and efficient (hopefully has the comparable per-iteration computational complexity as the first-order methods) algorithm with provable high-order convergence guarantees (possibly converge to a stationary point due to the non-convexity) for solving (1)?*

In this paper, we give an affirmative answer to this question by making contributions to the rank constrained optimization problem (1) as outlined next.

## 1.1 Our Contributions

We introduce an easy-to-implement and computationally efficient algorithm, *Recursive Importance Sketching* for *Rank* constrained least squares *Optimization* (RISRO), for solving (1) in this paper. The proposed algorithm is tuning free and has the same per-iteration computational complexity as Alternating Minimization ([Jain et al., 2013](#)), as well as comparable complexity to many popular first-order methods such as iterative hard thresholding ([Jain et al., 2010](#)) and gradient descent

(Tu et al., 2016) when  $r \ll p_1, p_2, n$ . We then illustrate the key idea of RISRO under a general framework of recursive importance sketching. This framework also renders a platform to compare RISRO and several existing algorithms for rank constrained least squares.

Assuming  $\mathcal{A}$  satisfies the restricted isometry property (RIP), we prove that RISRO enjoys local quadratic-linear convergence in general and quadratic convergence under some extra conditions. Figure 1 provides a numerical example on the performance of RISRO in the noiseless low-rank matrix trace regression (left panel) and phase retrieval (right panel). In both problems, RISRO converges to the underlying parameter quadratically and reaches to a highly accurate solution within five iterations. We will illustrate later that RISRO has the same per-iteration complexity with other first-order methods when  $r$  is small while converges quadratically with provable guarantees. To our best knowledge, we are among the first to achieve so for the general rank constrained least squares problem.

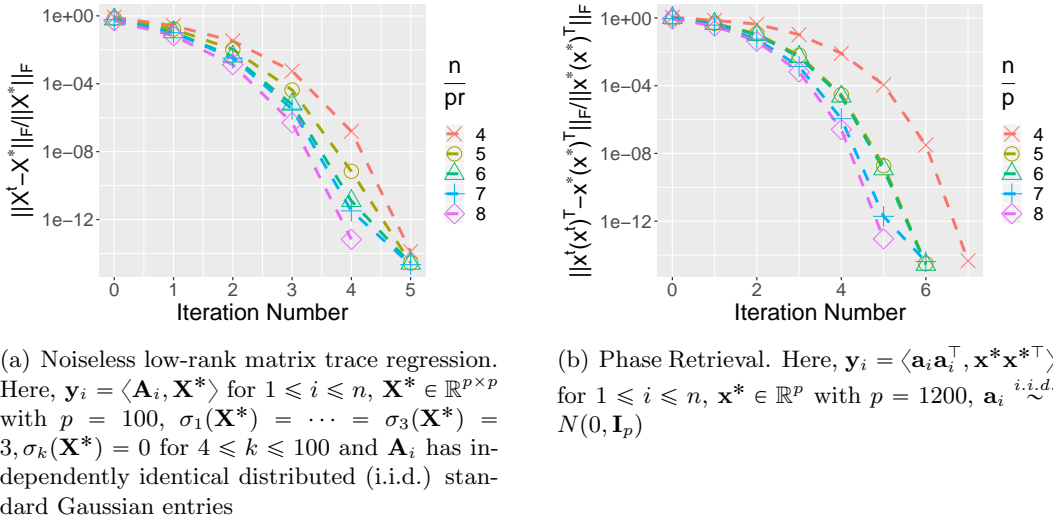


Figure 1: RISRO achieves a quadratic rate of convergence (spectral initialization is used in each setting and more details about the simulation setup is given in Section 7)

In addition, we discover a deep connection between RISRO and the optimization algorithm on Riemannian manifold. The least squares step in RISRO implicitly solves a *Fisher Scoring* or *Riemannian Gauss-Newton equation* on the Riemannian optimization of low-rank matrices and the updating rule in RISRO can be seen as a *retraction map*. With this connection, our theory on RISRO also improves the existing convergence results on the Riemannian Gauss-Newton method for the rank constrained least squares problem.

Next, we further apply RISRO to two important problems arising from machine learning and statistics: low-rank matrix trace regression and phase retrieval. In low-rank matrix trace regression, we are able to prove RISRO achieves the minimax optimal estimation error rate under the Gaussian ensemble design with only *double-logarithmic* number of iterations. In phase retrieval, where  $\mathcal{A}$  does not satisfy the RIP condition, we can still establish the local convergence of RISRO given a proper initialization.

Finally, we conduct simulation studies to support our theoretical results and compare RISRO with many existing algorithms. The simulation studies show RISRO not only offers faster and more robust convergence but also smaller sample size requirement for low-rank matrix recovery, compared to the existing approaches.

## 1.2 Related Literature

This work is related to a range of literature on low-rank matrix recovery, convex/non-convex optimization, and sketching arising from a number of communities, including optimization, machine learning, statistics and applied mathematics. We make an attempt to review the related literature without claiming the survey is exhaustive.

One class of the most popular approaches to solve (1) is the nuclear norm minimization (NNM) (3). Many algorithms have been proposed to solve NNM, such as proximal gradient descent (Toh and Yun, 2010), fixed-point continuation (FPC) (Goldfarb and Ma, 2011), and proximal point methods (Jiang et al., 2014). It has been shown that the solution of NNM has desirable properties under proper model assumptions (Cai and Zhang, 2013, 2014, 2015; Candès and Plan, 2011; Recht et al., 2010). In addition to NNM, the max norm minimization is another widely considered convex realization for the rank constrained optimization (Lee et al., 2010; Cai and Zhou, 2013). However, it is usually computationally intensive to solve these convex programs and this motivates a line of work on using non-convex approaches. Since Burer and Monteiro (2003), one of the most popular non-convex methods for solving (1) is to first factor the low-rank matrix  $\mathbf{X}$  to  $\mathbf{RL}^\top$  with two factor matrices  $\mathbf{R} \in \mathbb{R}^{p_1 \times r}, \mathbf{L} \in \mathbb{R}^{p_2 \times r}$ , then run either gradient decent or alternating minimization on  $\mathbf{R}$  and  $\mathbf{L}$  (Candès et al., 2015; Li et al., 2019b; Ma et al., 2019; Park et al., 2018; Sanghavi et al., 2017; Sun and Luo, 2015; Tu et al., 2016; Wang et al., 2017c; Zhao et al., 2015; Zheng and Lafferty, 2015; Tong et al., 2020). Others methods, such as singular value projection or iterative hard thresholding (Goldfarb and Ma, 2011; Jain et al., 2010; Tanner and Wei, 2013), Grassmann manifold optimization (Boumal and Absil, 2011; Keshavan et al., 2009), Riemannian manifold optimization (Huang and Hand, 2018; Meyer et al., 2011; Mishra et al., 2014; Vandereycken, 2013; Wei et al., 2016) have also been proposed and studied. We refer readers to the recently survey paper Chi et al. (2019) for comprehensive overview on existing literature on convex and non-convex approaches on solving (1). There are a few recent attempts in connecting the geometric structures of different approaches (Ha et al., 2020; Li et al., 2019a), and the landscape of problem (1) has also been studied in various settings (Bhojanapalli et al., 2016; Ge et al., 2017; Uschmajew and Vandereycken, 2018; Zhang et al., 2019; Zhu et al., 2018).

Our work is also related to the idea of sketching in numerical linear algebra. Performing sketching to speed up the computation via dimension reduction has been explored extensively in recent years (Mahoney, 2011; Woodruff, 2014). Sketching methods have been applied to solve a number of problems including but not limited to matrix approximation (Song et al., 2017; Zheng et al., 2012; Drineas et al., 2012), linear regression (Clarkson and Woodruff, 2017; Dobriban and Liu, 2019; Pilanci and Wainwright, 2016; Raskutti and Mahoney, 2016), ridge regression (Wang et al., 2017b), etc. In most of the sketching literature, the sketching matrices are randomly constructed (Mahoney, 2011; Woodruff, 2014). Randomized sketching matrices are easy to generate and require little storage for sparse sketching. However, randomized sketching can be suboptimal in statistical settings (Raskutti and Mahoney, 2016). To overcome this, Zhang et al. (2020) introduced an idea of importance sketching in the context of low-rank tensor regression. Contrary to the randomized sketching, importance sketching matrices are constructed deterministically with the supervision of the data and are shown capable of achieving better statistical efficiency. In this paper, we propose a more powerful recursive importance sketching algorithm where we can recursively refine the sketching matrices. Then, we provide a comprehensive convergence analysis towards the proposed algorithm and demonstrate its advantages over other algorithms for rank constrained least squares problem.

### 1.3 Organization of the Paper

The rest of this article is organized as follows. After a brief introduction of notation in Section 1.4, we present our main algorithm RISRO with an interpretation from the recursive importance sketching perspective in Section 2. The theoretical results of RISRO are given in Section 3. In Section 4, we present another interpretation for RISRO from Riemannian manifold optimization. The computational complexity of RISRO and its applications to low-rank matrix trace regression and phase retrieval are discussed in Section 5 and 6, respectively. Numerical studies of RISRO and the comparison with existing algorithms in the literature are presented in Section 7. Conclusion and future work are given in Section 8.

### 1.4 Notation

The following notation will be used throughout this article. Upper and lowercase letters (e.g.,  $A, B, a, b$ ), lowercase boldface letters (e.g.  $\mathbf{u}, \mathbf{v}$ ), uppercase boldface letters (e.g.,  $\mathbf{U}, \mathbf{V}$ ) are used to denote scalars, vectors, matrices, respectively. For any two series of numbers, say  $\{a_n\}$  and  $\{b_n\}$ , denote  $a = O(b)$  if there exists uniform constants  $C > 0$  such that  $a_n \leq Cb_n, \forall n$ . For any  $a, b \in \mathbb{R}$ , let  $a \wedge b := \min\{a, b\}, a \vee b = \max\{a, b\}$ . For any matrix  $\mathbf{X} \in \mathbb{R}^{p_1 \times p_2}$  with singular value decomposition  $\sum_{i=1}^{\min\{p_1, p_2\}} \sigma_i(\mathbf{X}) \mathbf{u}_i \mathbf{v}_i^\top$ , where  $\sigma_1(\mathbf{X}) \geq \sigma_2(\mathbf{X}) \geq \dots \geq \sigma_{\min\{p_1, p_2\}}(\mathbf{X})$ , let  $\mathbf{X}_{\max(r)} = \sum_{i=1}^r \sigma_i(\mathbf{X}) \mathbf{u}_i \mathbf{v}_i^\top$  be the best rank- $r$  approximation of  $\mathbf{X}$  and denote  $\|\mathbf{X}\|_{\text{F}} = \sqrt{\sum_i \sigma_i^2(\mathbf{X})}$  and  $\|\mathbf{X}\| = \sigma_1(\mathbf{X})$  as the Frobenius norm and spectral norm, respectively. Let  $\text{QR}(\mathbf{X})$  be the  $Q$  part of the QR decomposition outcome of  $\mathbf{X}$ .  $\text{vec}(\mathbf{X}) \in \mathbb{R}^{p_1 p_2}$  represents the vectorization of  $\mathbf{X}$  by its columns. In addition,  $\mathbf{I}_r$  is the  $r$ -by- $r$  identity matrix. Let  $\mathbb{O}_{p,r} = \{\mathbf{U} : \mathbf{U}^\top \mathbf{U} = \mathbf{I}_r\}$  be the set of all  $p$ -by- $r$  matrices with orthonormal columns. For any  $\mathbf{U} \in \mathbb{O}_{p,r}$ ,  $P_{\mathbf{U}} = \mathbf{U} \mathbf{U}^\top$  represents the orthogonal projector onto the column space of  $\mathbf{U}$ ; we also note  $\mathbf{U}_\perp \in \mathbb{O}_{p,p-r}$  as the orthonormal complement of  $\mathbf{U}$ . We use bracket subscripts to denote sub-matrices. For example,  $\mathbf{X}_{[i_1, i_2]}$  is the entry of  $\mathbf{X}$  on the  $i_1$ -th row and  $i_2$ -th column;  $\mathbf{X}_{[(r+1):p_1, :]}$  contains the  $(r+1)$ -th to the  $m$ -th rows of  $\mathbf{X}$ . For any matrix  $\mathbf{X}$ , we use  $\mathbf{X}^\dagger$  to denote its Moore-Penrose inverse. For matrices  $\mathbf{U} \in \mathbb{R}^{p_1 \times p_2}, \mathbf{V} \in \mathbb{R}^{m_1 \times m_2}$ , let

$$\mathbf{U} \otimes \mathbf{V} = \begin{bmatrix} \mathbf{U}_{[1,1]} \cdot \mathbf{V} & \dots & \mathbf{U}_{[1,p_2]} \cdot \mathbf{V} \\ \vdots & & \vdots \\ \mathbf{U}_{[p_1,1]} \cdot \mathbf{V} & \dots & \mathbf{U}_{[p_1,p_2]} \cdot \mathbf{V} \end{bmatrix} \in \mathbb{R}^{(p_1 m_1) \times (p_2 m_2)}$$

be their Kronecker product. Finally, for any given linear operator  $\mathcal{L}$ , we use  $\mathcal{L}^*$  to denote its adjoint, and use  $\text{Ran}(\mathcal{L})$  to denote its range space.

## 2 Recursive Importance Sketching for Rank Constrained Least Squares

In this section, we discuss the procedure and interpretations of RISRO, then compare it with existing algorithms from a sketching perspective.

### 2.1 RISRO Procedure and Recursive Importance Sketching

The detailed procedure of RISRO is given in Algorithm 1. RISRO includes three steps in each iteration. Specifically, in the  $t$ -th iteration, we first sketch each  $\mathbf{A}_i$  onto the subspace spanned by  $[\mathbf{U}^t \otimes \mathbf{V}^t, \mathbf{U}_\perp^t \otimes \mathbf{V}^t, \mathbf{U}^t \otimes \mathbf{V}_\perp^t]$ , which yields the sketched importance covariates  $\mathbf{U}^{t\top} \mathbf{A}_i \mathbf{V}^t, \mathbf{U}_\perp^{t\top} \mathbf{A}_i \mathbf{V}^t, \mathbf{U}^{t\top} \mathbf{A}_i \mathbf{V}_\perp^t$  in (4). See Figure 2 left panel for an illustration for the sketching scheme of RISRO. Second, we

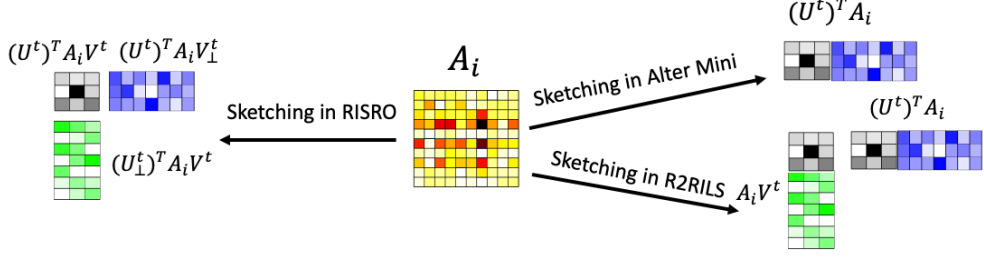


Figure 2: Illustration of RISRO (this work), Alter Mini (Hardt, 2014; Jain et al., 2013), and R2RILS (Bauch and Nadler, 2020) in a sketching perspective

solve a dimension reduced least squares problem (5) where the number of parameters is reduced to  $(p_1 + p_2 - r)r$  while the sample size remains to be  $n$ . Third, we update the sketching matrices  $\mathbf{U}^{t+1}, \mathbf{V}^{t+1}$  and  $\mathbf{X}^{t+1}$  in Step 6 and 7. Note that by construction,  $\mathbf{U}^{t+1}, \mathbf{V}^{t+1}$  capture both the column and row spans of  $\mathbf{X}^{t+1}$ . In particular, if  $\mathbf{B}^{t+1}$  is invertible, then  $\mathbf{U}^{t+1}, \mathbf{V}^{t+1}$  are exactly orthonormal bases of the column and row spans of  $\mathbf{X}^{t+1}$ , respectively.

---

**Algorithm 1** Recursive Importance Sketching for Rank Constrained Least Squares (RISRO)

---

- 1: Input:  $\mathcal{A}(\cdot) : \mathbb{R}^{p_1 \times p_2} \rightarrow \mathbb{R}^n$ ,  $\mathbf{y} \in \mathbb{R}^n$ , rank  $r$ , initialization  $\mathbf{X}^0$  which admits singular value decomposition  $\mathbf{U}^0 \Sigma^0 \mathbf{V}^{0\top}$ , where  $\mathbf{U}^0 \in \mathbb{O}_{p_1, r}$ ,  $\mathbf{V}^0 \in \mathbb{O}_{p_2, r}$ ,  $\Sigma^0 \in \mathbb{R}^{r \times r}$
- 2: **for**  $t = 0, 1, \dots$  **do**
- 3:   Perform importance sketching on  $\mathcal{A}$  and construct the covariates maps  $\mathcal{A}_B : \mathbb{R}^{r \times r} \rightarrow \mathbb{R}^n$ ,  $\mathcal{A}_{D_1} : \mathbb{R}^{(p_1-r) \times r} \rightarrow \mathbb{R}^n$  and  $\mathcal{A}_{D_2} : \mathbb{R}^{r \times (p_2-r)} \rightarrow \mathbb{R}^n$ , where for  $1 \leq i \leq n$ ,

$$(\mathcal{A}_B)_i = \mathbf{U}^{t\top} \mathbf{A}_i \mathbf{V}^t, \quad (\mathcal{A}_{D_1})_i = \mathbf{U}_\perp^{t\top} \mathbf{A}_i \mathbf{V}^t, \quad (\mathcal{A}_{D_2})_i = \mathbf{U}^{t\top} \mathbf{A}_i \mathbf{V}_\perp^t \quad (4)$$

Here,  $(\mathcal{A}_B)_i$  satisfies  $[\mathcal{A}_B(\cdot)]_i = \langle \cdot, (\mathcal{A}_B)_i \rangle$  and similarly for  $(\mathcal{A}_{D_1})_i$  and  $(\mathcal{A}_{D_2})_i$ .

- 4:   Solve the unconstrained least squares problem

$$(\mathbf{B}^{t+1}, \mathbf{D}_1^{t+1}, \mathbf{D}_2^{t+1}) = \arg \min_{\mathbf{B} \in \mathbb{R}^{r \times r}, \mathbf{D}_i \in \mathbb{R}^{(p_i-r) \times r}, i=1,2} \|\mathbf{y} - \mathcal{A}_B(\mathbf{B}) - \mathcal{A}_{D_1}(\mathbf{D}_1) - \mathcal{A}_{D_2}(\mathbf{D}_2^\top)\|_2^2 \quad (5)$$

- 5:   Compute  $\mathbf{X}_U^{t+1} = (\mathbf{U}^t \mathbf{B}^{t+1} + \mathbf{U}_\perp^t \mathbf{D}_1^{t+1})$  and  $\mathbf{X}_V^{t+1} = (\mathbf{V}^t \mathbf{B}^{t+1\top} + \mathbf{V}_\perp^t \mathbf{D}_2^{t+1})$ .
- 6:   Perform QR orthogonalization:  $\mathbf{U}^{t+1} = \text{QR}(\mathbf{X}_U^{t+1})$ ,  $\mathbf{V}^{t+1} = \text{QR}(\mathbf{X}_V^{t+1})$ .
- 7:   Update  $\mathbf{X}^{t+1} = \mathbf{X}_U^{t+1} (\mathbf{B}^{t+1})^\dagger \mathbf{X}_V^{t+1\top}$ .
- 8: **end for**

---

We give a high-level explanation of RISRO through a decomposition of  $\mathbf{y}_i$ . Suppose  $\mathbf{y}_i = \langle \mathbf{A}_i, \bar{\mathbf{X}} \rangle + \bar{\epsilon}_i$  where  $\bar{\mathbf{X}}$  is a rank  $r$  target matrix with singular value decomposition  $\bar{\mathbf{U}} \bar{\Sigma} \bar{\mathbf{V}}^\top$  with  $\bar{\mathbf{U}} \in \mathbb{O}_{p_1, r}$ ,  $\bar{\Sigma} \in \mathbb{R}^{r \times r}$  and  $\bar{\mathbf{V}} \in \mathbb{O}_{p_2, r}$ . Then

$$\begin{aligned} \mathbf{y}_i &= \langle \mathbf{U}^{t\top} \mathbf{A}_i \mathbf{V}^t, \mathbf{U}^{t\top} \bar{\mathbf{X}} \mathbf{V}^t \rangle + \langle \mathbf{U}_\perp^{t\top} \mathbf{A}_i \mathbf{V}^t, \mathbf{U}_\perp^{t\top} \bar{\mathbf{X}} \mathbf{V}^t \rangle + \langle \mathbf{U}^{t\top} \mathbf{A}_i \mathbf{V}_\perp^t, \mathbf{U}^{t\top} \bar{\mathbf{X}} \mathbf{V}_\perp^t \rangle + \langle \mathbf{U}_\perp^{t\top} \mathbf{A}_i \mathbf{V}_\perp^t, \mathbf{U}_\perp^{t\top} \bar{\mathbf{X}} \mathbf{V}_\perp^t \rangle + \bar{\epsilon}_i \\ &:= \langle \mathbf{U}^{t\top} \mathbf{A}_i \mathbf{V}^t, \mathbf{U}^{t\top} \bar{\mathbf{X}} \mathbf{V}^t \rangle + \langle \mathbf{U}_\perp^{t\top} \mathbf{A}_i \mathbf{V}^t, \mathbf{U}_\perp^{t\top} \bar{\mathbf{X}} \mathbf{V}^t \rangle + \langle \mathbf{U}^{t\top} \mathbf{A}_i \mathbf{V}_\perp^t, \mathbf{U}^{t\top} \bar{\mathbf{X}} \mathbf{V}_\perp^t \rangle + \epsilon_i^t. \end{aligned} \quad (6)$$

Here,  $\epsilon^t := \mathcal{A}(P_{\mathbf{U}_\perp^t} \bar{\mathbf{X}} P_{\mathbf{V}_\perp^t}) + \bar{\epsilon} \in \mathbb{R}^n$  can be seen as the residual of the new regression model (6),

and  $\mathbf{U}^{t\top} \mathbf{A}_i \mathbf{V}^t, \mathbf{U}_\perp^{t\top} \mathbf{A}_i \mathbf{V}^t, \mathbf{U}^{t\top} \mathbf{A}_i \mathbf{V}_\perp^t$  are exactly the importance covariates constructed in (4). Let

$$\tilde{\mathbf{B}}^t := \mathbf{U}^{t\top} \bar{\mathbf{X}} \mathbf{V}^t, \tilde{\mathbf{D}}_1^t := \mathbf{U}_\perp^{t\top} \bar{\mathbf{X}} \mathbf{V}^t, \tilde{\mathbf{D}}_2^{t\top} := \mathbf{U}^{t\top} \bar{\mathbf{X}} \mathbf{V}_\perp^t. \quad (7)$$

If  $\epsilon^t = 0$ , we have  $(\tilde{\mathbf{B}}^t, \tilde{\mathbf{D}}_1^t, \tilde{\mathbf{D}}_2^t)$  is a solution of the least squares in (5). Hence, we could set  $\mathbf{B}^{t+1} = \tilde{\mathbf{B}}^t, \mathbf{D}_1^{t+1} = \tilde{\mathbf{D}}_1^t, \mathbf{D}_2^{t+1} = \tilde{\mathbf{D}}_2^t$  and thus  $\mathbf{X}_U^{t+1} = \bar{\mathbf{X}} \mathbf{V}^t, \mathbf{X}_V^{t+1} = \bar{\mathbf{X}}^\top \mathbf{U}^t$ . Furthermore, if  $\mathbf{B}^{t+1}$  is invertible, then it holds that

$$\mathbf{X}_U^{t+1} (\mathbf{B}^{t+1})^{-1} \mathbf{X}_V^{t+1\top} = \bar{\mathbf{X}} \mathbf{V}^t (\mathbf{U}^{t\top} \bar{\mathbf{X}} \mathbf{V}^t)^{-1} (\bar{\mathbf{X}}^\top \mathbf{U}^t)^\top = \bar{\mathbf{X}}, \quad (8)$$

which means  $\bar{\mathbf{X}}$  can be exactly recovered by one iteration of RISRO.

In general,  $\epsilon^t \neq 0$ . When the column spans of  $\mathbf{U}^t, \mathbf{V}^t$  well approximate the ones of  $\bar{\mathbf{U}}, \bar{\mathbf{V}}$ , i.e., the column and row subspaces that the target parameter  $\bar{\mathbf{X}}$  lie on, we expect  $\mathbf{U}_\perp^{t\top} \bar{\mathbf{X}} \mathbf{V}_\perp^t$  and  $\epsilon_i^t = \langle \mathbf{U}_\perp^{t\top} \mathbf{A}_i \mathbf{V}_\perp^t, \mathbf{U}_\perp^{t\top} \bar{\mathbf{X}} \mathbf{V}_\perp^t \rangle + \bar{\epsilon}_i$  to have a small amplitude, then  $\mathbf{B}^{t+1}, \mathbf{D}_1^{t+1}, \mathbf{D}_2^{t+1}$ , the outcome of the least squares problem (5), can well approximate  $\tilde{\mathbf{B}}^t, \tilde{\mathbf{D}}_1^t, \tilde{\mathbf{D}}_2^t$ . In Lemma 1, we give a precise characterization for this approximation. Before that, let us introduce a convenient notation so that (5) can be written in a more compact way.

Define the linear operator  $\mathcal{L}_t$  as

$$\mathcal{L}_t : \mathbf{W} = \begin{bmatrix} \mathbf{W}_0 \in \mathbb{R}^{r \times r} & \mathbf{W}_2 \in \mathbb{R}^{r \times (p_2-r)} \\ \mathbf{W}_1 \in \mathbb{R}^{(p_1-r) \times r} & \mathbf{0}_{(p_1-r) \times (p_2-r)} \end{bmatrix} \rightarrow [\mathbf{U}^t \quad \mathbf{U}_\perp^t] \begin{bmatrix} \mathbf{W}_0 & \mathbf{W}_2 \\ \mathbf{W}_1 & \mathbf{0} \end{bmatrix} [\mathbf{V}^t \quad \mathbf{V}_\perp^t]^\top, \quad (9)$$

and it is easy to compute its adjoint  $\mathcal{L}_t^* : \mathbf{M} \in \mathbb{R}^{p_1 \times p_2} \rightarrow \begin{bmatrix} \mathbf{U}^{t\top} \mathbf{M} \mathbf{V}^t & \mathbf{U}^{t\top} \mathbf{M} \mathbf{V}_\perp^t \\ (\mathbf{U}_\perp^{t\top} \mathbf{M} \mathbf{V}^t)^\top & \mathbf{0} \end{bmatrix}$ . Then, the least squares problem in (5) can be written as

$$(\mathbf{B}^{t+1}, \mathbf{D}_1^{t+1}, \mathbf{D}_2^{t+1}) = \arg \min_{\mathbf{B} \in \mathbb{R}^{r \times r}, \mathbf{D}_i \in \mathbb{R}^{(p_i-r) \times r}, i=1,2} \left\| \mathbf{y} - \mathcal{A} \mathcal{L}_t \left( \begin{bmatrix} \mathbf{B} & \mathbf{D}_2^\top \\ \mathbf{D}_1 & \mathbf{0} \end{bmatrix} \right) \right\|_2^2. \quad (10)$$

**Lemma 1 (Iteration Error Analysis for RISRO)** *Let  $\bar{\mathbf{X}}$  be any given target matrix. Recall the definition of  $\epsilon^t = \bar{\epsilon} + \mathcal{A}(P_{\mathbf{U}_\perp^t} \bar{\mathbf{X}} P_{\mathbf{V}_\perp^t})$  from (6). If the operator  $\mathcal{L}_t^* \mathcal{A}^* \mathcal{A} \mathcal{L}_t$  is invertible over  $\text{Ran}(\mathcal{L}_t^*)$ , then  $\mathbf{B}^{t+1}, \mathbf{D}_1^{t+1}, \mathbf{D}_2^{t+1}$  in (5) satisfy*

$$\begin{bmatrix} \mathbf{B}^{t+1} - \tilde{\mathbf{B}}^t & \mathbf{D}_2^{t+1\top} - \tilde{\mathbf{D}}_2^{t\top} \\ \mathbf{D}_1^{t+1} - \tilde{\mathbf{D}}_1^t & \mathbf{0} \end{bmatrix} = (\mathcal{L}_t^* \mathcal{A}^* \mathcal{A} \mathcal{L}_t)^{-1} \mathcal{L}_t^* \mathcal{A}^* \epsilon^t, \quad (11)$$

and

$$\|\mathbf{B}^{t+1} - \tilde{\mathbf{B}}^t\|_F^2 + \sum_{k=1}^2 \|\mathbf{D}_k^{t+1} - \tilde{\mathbf{D}}_k^t\|_F^2 = \|(\mathcal{L}_t^* \mathcal{A}^* \mathcal{A} \mathcal{L}_t)^{-1} \mathcal{L}_t^* \mathcal{A}^* \epsilon^t\|_F^2. \quad (12)$$

In view of Lemma 1, the approximation errors of  $\mathbf{B}^{t+1}, \mathbf{D}_1^{t+1}, \mathbf{D}_2^{t+1}$  to  $\tilde{\mathbf{B}}^t, \tilde{\mathbf{D}}_1^t, \tilde{\mathbf{D}}_2^t$  are driven by the least squares residual  $\|(\mathcal{L}_t^* \mathcal{A}^* \mathcal{A} \mathcal{L}_t)^{-1} \mathcal{L}_t^* \mathcal{A}^* \epsilon^t\|_F^2$ . This fact plays a key role in the proof for the high-order convergence theory of RISRO.

**Remark 1 (Comparison with Randomized Sketching)** *The importance sketching in RISRO is significantly different from the randomized sketching in the literature (see surveys [Mahoney \(2011\)](#); [Woodruff \(2014\)](#) and the references therein). The randomized sketching matrices are often randomly generated and reduce the sample size ( $n$ ), the importance sketching matrices are deterministically constructed under supervision of  $\mathbf{y}$  and reduce the dimension of parameter space ( $p_1 p_2$ ). See ([Zhang et al., 2020](#), Section 1.3 and 2) for more comparison of randomized and importance sketchings.*

## 2.2 Comparison with More Algorithms in View of Sketching

In addition to RISRO, several classic algorithms for rank constrained least squares can be interpreted from a recursive importance sketching perspective. Through the lens of the sketching, RISRO exhibits advantages over these existing algorithms.

We first focus on Alternating Minimization (Alter Mini) proposed and studied in Hardt (2014); Jain et al. (2013); Zhao et al. (2015). Suppose  $\mathbf{U}^t$  is the left singular vectors of  $\mathbf{X}^t$ , the outcome of the  $t$ -th iteration, Alter Mini solves the following least squares problems to update  $\mathbf{U}$  and  $\mathbf{V}$ ,

$$\begin{aligned}\check{\mathbf{V}}^{t+1} &= \arg \min_{\mathbf{V} \in \mathbb{R}^{p_2 \times r}} \sum_{i=1}^n (\mathbf{y}_i - \langle \mathbf{A}_i, \mathbf{U}^t \mathbf{V}^\top \rangle)^2 = \arg \min_{\mathbf{V} \in \mathbb{R}^{p_2 \times r}} \sum_{i=1}^n (\mathbf{y}_i - \langle \mathbf{U}^{t\top} \mathbf{A}_i, \mathbf{V}^\top \rangle)^2, \\ \check{\mathbf{U}}^{t+1} &= \arg \min_{\mathbf{U} \in \mathbb{R}^{p_1 \times r}} \sum_{i=1}^n (\mathbf{y}_i - \langle \mathbf{A}_i, \mathbf{U} (\mathbf{V}^{t+1})^\top \rangle)^2 = \arg \min_{\mathbf{U} \in \mathbb{R}^{p_1 \times r}} \sum_{i=1}^n (\mathbf{y}_i - \langle \mathbf{A}_i \mathbf{V}^{t+1}, \mathbf{U} \rangle)^2, \\ \mathbf{V}^{t+1} &= \text{QR}(\check{\mathbf{V}}^{t+1}), \quad \mathbf{U}^{t+1} = \text{QR}(\check{\mathbf{U}}^{t+1}).\end{aligned}\tag{13}$$

Then, Alter Mini essentially solves least squares problems with sketched covariates  $\mathbf{U}^{t\top} \mathbf{A}_i, \mathbf{A}_i \mathbf{V}^{t+1}$  to update  $\check{\mathbf{V}}^{t+1}, \check{\mathbf{U}}^{t+1}$  alternatively and iteratively. The number of parameters of the least squares in (13) are  $rp_2$  and  $rp_1$  as opposed to  $p_1 p_2$ , the number of parameters in the original least squares problem. See Figure 2 upper right panel for an illustration of the sketching scheme in Alter Mini. Consider the following decomposition of  $\mathbf{y}_i$ ,

$$\mathbf{y}_i = \langle \mathbf{A}_i, P_{\mathbf{U}^t} \bar{\mathbf{X}} \rangle + \langle \mathbf{A}_i, P_{\mathbf{U}_\perp^t} \bar{\mathbf{X}} \rangle + \bar{\epsilon}_i = \langle \mathbf{U}^{t\top} \mathbf{A}_i, \mathbf{U}^{t\top} \bar{\mathbf{X}} \rangle + \langle \mathbf{A}_i, P_{\mathbf{U}_\perp^t} \bar{\mathbf{X}} \rangle + \bar{\epsilon}_i := \langle \mathbf{U}^{t\top} \mathbf{A}_i, \mathbf{U}^{t\top} \bar{\mathbf{X}} \rangle + \check{\epsilon}_i^t,\tag{14}$$

where  $\check{\epsilon}^t := \mathcal{A}(P_{\mathbf{U}_\perp^t} \bar{\mathbf{X}}) + \bar{\epsilon} \in \mathbb{R}^n$ . Define  $\check{\mathbf{A}}^t \in \mathbb{R}^{n \times p_2 r}$  with  $\check{\mathbf{A}}_{[i,:]} = \text{vec}(\mathbf{U}^{t\top} \mathbf{A}_i)$ . Similar to how Lemma 1 is proved, we can show  $\|\check{\mathbf{V}}^{t+1\top} - \mathbf{U}^{t\top} \bar{\mathbf{X}}\|_F^2 = \|(\check{\mathbf{A}}^{t\top} \check{\mathbf{A}}^t)^{-1} \check{\mathbf{A}}^{t\top} \check{\epsilon}^t\|_2^2$ , which implies the approximation error of  $\mathbf{V}^{t+1} = \text{QR}(\check{\mathbf{V}}^{t+1})$  (i.e., the outcome of one iteration Alter Mini) to  $\bar{\mathbf{V}}$  (i.e., true row span of the target matrix  $\bar{\mathbf{X}}$ ) is driven by  $\check{\epsilon}^t = \mathcal{A}(P_{\mathbf{U}_\perp^t} \bar{\mathbf{X}}) + \bar{\epsilon}$ , i.e., the residual of least squares problem (14). Recall for RISRO, Lemma 1 shows the approximation error of  $\mathbf{V}^{t+1}$  is driven by  $\epsilon^t = \mathcal{A}(P_{\mathbf{U}_\perp^t} \bar{\mathbf{X}} P_{\mathbf{V}_\perp^t}) + \bar{\epsilon}$ . Since  $\|P_{\mathbf{U}_\perp^t} \bar{\mathbf{X}} P_{\mathbf{V}_\perp^t}\|_F \leq \|P_{\mathbf{U}_\perp^t} \bar{\mathbf{X}}\|_F$ , the approximation error in per iteration of RISRO can be smaller than the one of Alter Mini. Such a difference between RISRO and Alter Mini is due to the following fact: in Alter Mini, the sketching captures the importance covariates correspond to only the row (or column) span of  $\mathbf{X}^t$  in updating  $\mathbf{V}^{t+1}$  (or  $\mathbf{U}^{t+1}$ ), while the importance sketching of RISRO in (4) catches the importance covariates from both the row span and column span of  $\mathbf{X}^t$ . As a consequence, Alter Mini iterations yield first order convergence while RISRO iterations render high-order convergence as will be established in Section 3.

**Remark 2** Recently, Kümmerle and Sigl (2018) proposed a harmonic mean iterative reweighted least squares (HM-IRLS) method for low-rank matrix recovery via solving  $\min_{\mathbf{X} \in \mathbb{R}^{p_1 \times p_2}} \|\mathbf{X}\|_q^q$ , subject to  $\mathbf{y} = \mathcal{A}(\mathbf{X})$ , where  $\|\mathbf{X}\|_q = (\sum_i \sigma_i^q(\mathbf{X}))^{1/q}$  is the Schatten- $q$  norm of the matrix  $\mathbf{X}$ . Compared to the original iterative reweighted least squares (IRLS) (Fornasier et al., 2011; Mohan and Fazel, 2012), which only uses the column span of  $\mathbf{X}^t$  in constructing the reweight matrix, HM-IRLS uses both the column and row spans of  $\mathbf{X}^t$  in constructing the reweight matrix and results in better performance. Such a comparison of HM-IRLS versus IRLS shares the same spirit as RISRO versus Alter Mini: the importance sketching of RISRO captures the information of both column and row spans of  $\mathbf{X}^t$  and achieves a better performance.

Another example is the rank  $2r$  iterative least squares (R2RILS) proposed in [Bauch and Nadler \(2020\)](#) for solving ill-conditioned matrix completion problems. In particular, at  $t$ -th iteration, Step 1 of R2RILS solves the following least squares problem

$$\min_{\mathbf{M} \in \mathbb{R}^{p_1 \times r}, \mathbf{N} \in \mathbb{R}^{p_2 \times r}} \sum_{(i,j) \in \Omega} \left\{ (\mathbf{U}^t \mathbf{N}^\top + \mathbf{M} \mathbf{V}^{t\top} - \mathbf{X})_{[i,j]} \right\}^2, \quad (15)$$

where  $\Omega$  is the set of index pairs of the observed entries. In the matrix completion setting, it turns out the following equivalence holds (proof given in Appendix)

$$\begin{aligned} & \arg \min_{\mathbf{M} \in \mathbb{R}^{p_1 \times r}, \mathbf{N} \in \mathbb{R}^{p_2 \times r}} \sum_{(i,j) \in \Omega} \left\{ (\mathbf{U}^t \mathbf{N}^\top + \mathbf{M} \mathbf{V}^{t\top} - \mathbf{X})_{[i,j]} \right\}^2 \\ &= \arg \min_{\mathbf{M} \in \mathbb{R}^{p_1 \times r}, \mathbf{N} \in \mathbb{R}^{p_2 \times r}} \sum_{(i,j) \in \Omega} (\langle \mathbf{U}^{t\top} \mathbf{A}^{ij}, \mathbf{N}^\top \rangle + \langle \mathbf{M}, \mathbf{A}^{ij} \mathbf{V}^t \rangle - \mathbf{X}_{[i,j]})^2, \end{aligned} \quad (16)$$

where  $\mathbf{A}^{ij} \in \mathbb{R}^{p_1 \times p_2}$  is the special covariate in matrix completion satisfying  $(\mathbf{A}^{ij})_{[k,l]} = 1$  if  $(i,j) = (k,l)$  and  $(\mathbf{A}^{ij})_{[k,l]} = 0$  otherwise. This equivalence reveals that the least squares step (15) in R2RILS can be seen as an implicit sketched least squares problem similar to (5) and (13) with covariates  $\mathbf{U}^{t\top} \mathbf{A}^{ij}$  and  $\mathbf{A}^{ij} \mathbf{V}^t$  for  $(i,j) \in \Omega$ .

We give a pictorial illustration for the sketching interpretation of R2RILS on the bottom right part of Figure 2. Different from the sketching in RISRO, R2RILS incorporates the core sketch  $\mathbf{U}^{t\top} \mathbf{A}^{ij} \mathbf{V}^t$  twice, which results in the rank deficiency in the least squares problem (15) and brings difficulties in both implementation and theoretical analysis. RISRO overcomes this issue by performing a better designed sketching and covers more general low-rank matrix recovery settings than R2RILS. With the new sketching scheme, we are able to give a new and solid theory for RISRO with high-order convergence.

### 3 Theoretical Analysis

In this section, we provide convergence analysis for the proposed algorithm. For technical convenience, we assume  $\mathcal{A}$  satisfies the Restricted Isometry Property (RIP) ([Candès, 2008](#)). The RIP condition, first introduced in compressed sensing, has been widely used as one of the most standard assumptions in the low-rank matrix recovery literature ([Cai and Zhang, 2013, 2014; Candès and Plan, 2011; Chen and Wainwright, 2015; Jain et al., 2010; Recht et al., 2010; Tu et al., 2016; Zhao et al., 2015](#)). It also plays a critical role in analyzing the landscape of the rank constrained optimization problem (1) ([Bhojanapalli et al., 2016; Ge et al., 2017; Uschmajew and Vandereycken, 2018; Zhang et al., 2019; Zhu et al., 2018](#)). Moreover, it is practically useful as the condition has been shown to be satisfied with desired sample size in random design ([Candès and Plan, 2011; Recht et al., 2010](#)).

**Definition 1 (Restricted Isometry Property (RIP))** *Let  $\mathcal{A} : \mathbb{R}^{p_1 \times p_2} \rightarrow \mathbb{R}^n$  be a linear map. For every integer  $r$  with  $1 \leq r \leq \min(p_1, p_2)$ , define the  $r$ -restricted isometry constant to be the smallest number  $R_r$  such that  $(1 - R_r) \|\mathbf{Z}\|_F^2 \leq \|\mathcal{A}(\mathbf{Z})\|_2^2 \leq (1 + R_r) \|\mathbf{Z}\|_F^2$  holds for all  $\mathbf{Z}$  of rank at most  $r$ . And  $\mathcal{A}$  is said to satisfy the  $r$ -restricted isometry property ( $r$ -RIP) if  $0 \leq R_r < 1$ .*

Note that, by definition,  $R_r \leq R_{r'}$  for  $r \leq r'$ . By assuming RIP for  $\mathcal{A}$ , we can show the linear operator  $\mathcal{L}_t^* \mathcal{A}^* \mathcal{A} \mathcal{L}_t$  mentioned in Lemma 1 is always invertible over  $\text{Ran}(\mathcal{L}_t^*)$  (i.e. the least squares (5) has the unique solution). In fact, we could give explicit lower and upper bounds for the spectrum of this operator.

**Lemma 2 (Bounds for Spectrum of  $\mathcal{L}_t^* \mathcal{A}^* \mathcal{A} \mathcal{L}_t$ )** Recall the definition of  $\mathcal{L}_t$  in (9). It holds that

$$\|\mathcal{L}_t(\mathbf{M})\|_F = \|\mathbf{M}\|_F, \quad \forall \mathbf{M} \in \text{Ran}(\mathcal{L}_t^*). \quad (17)$$

Suppose the linear map  $\mathcal{A}$  satisfies the  $2r$ -RIP. Then, it holds that for any matrix  $\mathbf{M} \in \text{Ran}(\mathcal{L}_t^*)$ ,

$$(1 - R_{2r})\|\mathbf{M}\|_F \leq \|\mathcal{L}_t^* \mathcal{A}^* \mathcal{A} \mathcal{L}_t(\mathbf{M})\|_F \leq (1 + R_{2r})\|\mathbf{M}\|_F.$$

**Remark 3 (Bounds for spectrum of  $(\mathcal{L}_t^* \mathcal{A}^* \mathcal{A} \mathcal{L}_t)^{-1}$ )** By the relationship of the spectrum of an operator and its inverse, from Lemma 2, we also have the spectrum of  $(\mathcal{L}_t^* \mathcal{A}^* \mathcal{A} \mathcal{L}_t)^{-1}$  is lower and upper bounded by  $\frac{1}{(1+R_{2r})}$  and  $\frac{1}{(1-R_{2r})}$ , respectively.

In the following Proposition 1, we bound the iteration approximation error given in Lemma 1.

**Proposition 1 (Upper Bound for Iteration Approximation Error)** Let  $\bar{\mathbf{X}}$  be a given target rank  $r$  matrix and  $\bar{\epsilon} = \mathbf{y} - \mathcal{A}(\bar{\mathbf{X}})$ . Suppose that  $\mathcal{A}$  satisfies the  $3r$ -RIP. Then at  $t$ -th iteration of RISRO, the approximation error (12) has the following upper bound:

$$\begin{aligned} & \|(\mathcal{L}_t^* \mathcal{A}^* \mathcal{A} \mathcal{L}_t)^{-1} \mathcal{L}_t^* \mathcal{A}^* \bar{\epsilon}\|_F^2 \\ & \leq \frac{R_{3r}^2 \|\mathbf{X}^t - \bar{\mathbf{X}}\|^2 \|\mathbf{X}^t - \bar{\mathbf{X}}\|_F^2}{(1 - R_{2r})^2 \sigma_r^2(\bar{\mathbf{X}})} + \frac{\|\mathcal{L}_t^* \mathcal{A}^*(\bar{\epsilon})\|_F^2}{(1 - R_{2r})^2} + \|\mathcal{L}_t^* \mathcal{A}^*(\bar{\epsilon})\|_F \frac{2R_{3r} \|\mathbf{X}^t - \bar{\mathbf{X}}\| \|\mathbf{X}^t - \bar{\mathbf{X}}\|_F}{\sigma_r(\bar{\mathbf{X}})(1 - R_{2r})^2}. \end{aligned} \quad (18)$$

Note that Proposition 1 is rather general in the sense that it applies to any  $\bar{\mathbf{X}}$  of rank  $r$  and we will pick different choices of  $\bar{\mathbf{X}}$  depending on our purposes. For example, in studying the convergence of RISRO, e.g., the upcoming Theorem 1, we treat  $\bar{\mathbf{X}}$  as a stationary point and in the setting of estimating the model parameter in matrix trace regression, we take  $\bar{\mathbf{X}}$  to be the ground truth (see Theorem 3).

Now, we are ready to establish the deterministic convergence theory for RISRO. For problem (1), we use the following definition of stationary points: a rank  $r$  matrix  $\bar{\mathbf{X}}$  is said to be a stationary point of (1) if  $\nabla f(\bar{\mathbf{X}})^\top \bar{\mathbf{U}} = 0$  and  $\nabla f(\bar{\mathbf{X}}) \bar{\mathbf{V}} = 0$  where  $\nabla f(\bar{\mathbf{X}}) = \mathcal{A}^*(\mathcal{A}(\bar{\mathbf{X}}) - \mathbf{y})$ , and  $\bar{\mathbf{U}}, \bar{\mathbf{V}}$  are the left and right singular vectors of  $\bar{\mathbf{X}}$ . See also Ha et al. (2020). In Theorem 1, we show that given any target stationary point  $\bar{\mathbf{X}}$  and proper initialization, RISRO has a local quadratic-linear convergence rate in general and quadratic convergence rate if  $\mathbf{y} = \mathcal{A}(\bar{\mathbf{X}})$ .

**Theorem 1 (Local Quadratic-Linear and Quadratic Convergence of RISRO)** Let  $\bar{\mathbf{X}}$  be a stationary point to problem (1) and  $\bar{\epsilon} = \mathbf{y} - \mathcal{A}(\bar{\mathbf{X}})$ . Suppose that  $\mathcal{A}$  satisfies the  $3r$ -RIP, and the initialization  $\mathbf{X}^0$  satisfies

$$\|\mathbf{X}^0 - \bar{\mathbf{X}}\|_F \leq \left( \frac{1}{4} \wedge \frac{1 - R_{2r}}{4\sqrt{5}R_{3r}} \right) \sigma_r(\bar{\mathbf{X}}), \quad (19)$$

and  $\|\mathcal{A}^*(\bar{\epsilon})\|_F \leq \frac{1 - R_{2r}}{4\sqrt{5}} \sigma_r(\bar{\mathbf{X}})$ . Then, we have  $\{\mathbf{X}^t\}$ , the sequence generated by RISRO (Algorithm 1), converges  $Q$ -linearly to  $\bar{\mathbf{X}}$ :  $\|\mathbf{X}^{t+1} - \bar{\mathbf{X}}\|_F \leq \frac{3}{4} \|\mathbf{X}^t - \bar{\mathbf{X}}\|_F, \quad \forall t \geq 0$ .

More precisely, it holds that  $\forall t \geq 0$ :

$$\|\mathbf{X}^{t+1} - \bar{\mathbf{X}}\|_F^2 \leq \frac{5\|\mathbf{X}^t - \bar{\mathbf{X}}\|^2}{(1 - R_{2r})^2 \sigma_r^2(\bar{\mathbf{X}})} \cdot (R_{3r}^2 \|\mathbf{X}^t - \bar{\mathbf{X}}\|_F^2 + 4R_{3r} \|\mathcal{A}^*(\bar{\epsilon})\|_F \|\mathbf{X}^t - \bar{\mathbf{X}}\|_F + 4\|\mathcal{A}^*(\bar{\epsilon})\|_F^2). \quad (20)$$

In particular, if  $\bar{\epsilon} = 0$ , then  $\{\mathbf{X}^t\}$  converges quadratically to  $\bar{\mathbf{X}}$  as

$$\|\mathbf{X}^{t+1} - \bar{\mathbf{X}}\|_F \leq \frac{\sqrt{5}R_{3r}}{(1 - R_{2r})\sigma_r(\bar{\mathbf{X}})} \|\mathbf{X}^t - \bar{\mathbf{X}}\|_F^2, \quad \forall t \geq 0.$$

**Remark 4 (Quadratic-linear and Quadratic Convergence of RISRO)** We call the convergence in (20) quadratic-linear since the sequence  $\{\mathbf{X}^t\}$  generated by RISRO exhibits a phase transition from quadratic to linear convergence: when  $\|\mathbf{X}^t - \bar{\mathbf{X}}\|_F \gg \|\mathcal{A}^*(\bar{\epsilon})\|_F$ , the algorithm has a quadratic convergence rate; when  $\mathbf{X}^t$  becomes close to  $\bar{\mathbf{X}}$  such that  $\|\mathbf{X}^t - \bar{\mathbf{X}}\|_F \leq c\|\mathcal{A}^*(\bar{\epsilon})\|_F$  for some  $c > 0$ , the convergence rate becomes linear. Moreover, as  $\bar{\epsilon}$  becomes smaller, the stage of quadratic convergence becomes longer (see Section 7.1 for a numerical illustration of this convergence pattern). In the extreme case  $\bar{\epsilon} = 0$ , Theorem 1 covers the widely studied matrix sensing problem under the RIP framework (Chen and Wainwright, 2015; Jain et al., 2010; Park et al., 2018; Recht et al., 2010; Tu et al., 2016; Zhao et al., 2015; Zheng and Lafferty, 2015). It shows as long as the initialization error is within a constant factor of  $\sigma_r(\bar{\mathbf{X}})$ , Algorithm RISRO enjoys quadratic convergence to the target matrix  $\bar{\mathbf{X}}$ . To our best knowledge, we are among the first to give quadratic-linear algorithmic convergence guarantees for general rank constrained least squares and quadratic convergence for matrix sensing. Recently, Charisopoulos et al. (2019) formulated (1) as a non-convex composite optimization problem based on  $\mathbf{X} = \mathbf{R}\mathbf{L}^\top$  factorization and showed that the prox-linear algorithm (Burke, 1985; Lewis and Wright, 2016) achieves local quadratic convergence when  $\bar{\epsilon} = 0$ . Note that in each iteration therein, a carefully tuned convex programming problem needs to be solved exactly. In contrast, the proposed RISRO is tuning free, only solves a dimension-reduced least squares in each step, and can be as cheap as many first-order methods. See Section 5 for a detailed discussion on the computational complexity of RISRO.

It is noteworthy that a quadratic-linear convergence rate appears in the recent Newton Sketch algorithm (Pilanci and Wainwright, 2017). However, Pilanci and Wainwright (2017) studied a convex problem using randomized sketching, which is significantly different from our settings, i.e., the recursive importance sketching and the non-convex matrix optimization.

**Remark 5 (Initialization and global convergence of RISRO)** The convergence theory in Theorem 1 requires a good initialization condition. Practically, the spectral method often provides a sufficiently good initialization that meets the requirement in (19) in many statistical applications. In Section 6 and 7, we will illustrate this point from two applications: matrix trace regression and phase retrieval.

Moreover, our main finding in the next section, i.e., RISRO can be interpreted as a Riemannian manifold optimization method, implies that standard globalization strategies in manifold optimization such as the line search or the trust region scheme (Absil et al., 2009; Nocedal and Wright, 2006) can be used to guarantee the global convergence of RISRO.

**Remark 6 (Small residual condition in Theorem 1)** In addition to the initialization condition, the small residual condition  $\|\mathcal{A}^*(\bar{\epsilon})\|_F \leq \frac{1-R_{2r}}{4\sqrt{5}}\sigma_r(\bar{\mathbf{X}})$  is also needed in Theorem 1. This condition essentially means that the signal strength at point  $\bar{\mathbf{X}}$  needs to dominate the noise. If  $\bar{\epsilon} = \mathbf{y} - \mathcal{A}(\bar{\mathbf{X}}) = 0$ , then the aforementioned small residual condition holds automatically.

## 4 A Riemannian Manifold Optimization Interpretation of RISRO

We give an interpretation of RISRO by recursive importance sketching in Section 2 and develop the convergence results in Section 3. The superior performance of RISRO yields the following question:

*Is there a connection of RISRO to any class of optimization algorithms in the literature?*

In this section, we give an affirmative answer to this question. We show RISRO can be viewed as a Riemannian optimization algorithm on the manifold  $\mathcal{M}_r := \{\mathbf{X} \in \mathbb{R}^{p_1 \times p_2} \mid \text{rank}(\mathbf{X}) = r\}$ . We find the sketched least squares in (5) in RISRO actually solves the *Fisher Scoring* or *Riemannian*

*Gauss-Newton equation* and Step 7 in RISRO performs a type of *retraction* under the framework of Riemannian optimization.

Riemannian optimization concerns optimizing a real-valued function  $f$  defined on a Riemannian manifold  $\mathcal{M}$ . One commonly-encountered manifold is a submanifold of  $\mathbb{R}^n$ . Under such circumstance, a manifold can be viewed as a smooth subset of  $\mathbb{R}^n$ . When a smooth-varying inner product is further defined on the subset, the subset together with the inner product is called a Riemannian manifold. We refer to [Absil et al. \(2009\)](#) for the rigorous definition of Riemannian manifolds. Optimization on a Riemannian manifold often relies on the notion of Riemannian gradient and Riemannian Hessian, which are used for finding a search direction, and the notion of retraction, which is defined for motion of iterates on the manifold. The remaining of this section describes the required Riemannian optimization tools and the connection of RISRO to Riemannian optimization.

It has been shown in [\(Lee, 2013, Example 8.14\)](#) that the set  $\mathcal{M}_r$  is a smooth submanifold of  $\mathbb{R}^{p_1 \times p_2}$  and the tangent space is also given therein. The result is given in [Proposition 2](#) for completeness.

**Proposition 2** [\(Lee, 2013, Example 8.14\)](#)  $\mathcal{M}_r = \{\mathbf{X} \in \mathbb{R}^{p_1 \times p_2} : \text{rank}(\mathbf{X}) = r\}$  is a smooth submanifold of dimension  $(p_1 + p_2 - r)r$ . Its tangent space  $T_{\mathbf{X}}\mathcal{M}_r$  at  $\mathbf{X} \in \mathcal{M}_r$  with the SVD decomposition  $\mathbf{X} = \mathbf{U}\Sigma\mathbf{V}^\top$  ( $\mathbf{U} \in \mathbb{O}_{p_1, r}$  and  $\mathbf{V} \in \mathbb{O}_{p_2, r}$ ) is given by:

$$T_{\mathbf{X}}\mathcal{M}_r = \left\{ [\mathbf{U} \quad \mathbf{U}_\perp] \begin{bmatrix} \mathbb{R}^{r \times r} & \mathbb{R}^{r \times (p_2-r)} \\ \mathbb{R}^{(p_1-r) \times r} & \mathbf{0}_{(p_1-r) \times (p_2-r)} \end{bmatrix} [\mathbf{V} \quad \mathbf{V}_\perp]^\top \right\}. \quad (21)$$

The Riemannian metric of  $\mathcal{M}_r$  that we use throughout this paper is the Euclidean inner product, i.e.,  $\langle \mathbf{U}, \mathbf{V} \rangle = \text{trace}(\mathbf{U}^\top \mathbf{V})$ .

In the Euclidean setting, the update formula in an iterative algorithm is  $\mathbf{X}^t + \alpha\eta^t$ , where  $\alpha$  is the stepsize and  $\eta^t$  is a descent direction. However, in the framework of Riemannian optimization,  $\mathbf{X}^t + \alpha\eta^t$  is generally neither well-defined nor lying in the manifold. To overcome this difficulty, the notion of retraction is used, see e.g., [Absil et al. \(2009\)](#). Considering the manifold  $\mathcal{M}_r$ , we have the definition that a retraction  $R$  is a smooth map from  $T\mathcal{M}_r$  to  $\mathcal{M}_r$  satisfying i)  $R(\mathbf{X}, 0) = \mathbf{X}$  and ii)  $\frac{d}{dt}R(\mathbf{X}, t\eta)|_{t=0} = \eta$  for all  $\mathbf{X} \in \mathcal{M}_r$  and  $\eta \in T_{\mathbf{X}}\mathcal{M}_r$ , where  $T\mathcal{M}_r = \{(\mathbf{X}, T_{\mathbf{X}}\mathcal{M}_r) : \mathbf{X} \in \mathcal{M}_r\}$ , is the tangent bundle of  $\mathcal{M}_r$ . The two conditions guarantee that  $R(\mathbf{X}, t\eta)$  stays in  $\mathcal{M}_r$  and  $R(\mathbf{X}, t\eta)$  is a first order approximation of  $\mathbf{X} + t\eta$  at  $t = 0$ .

Next, we show that Step 7 in RISRO performs the orthographic retraction on the manifold of fixed-rank matrices given in [Absil and Malick \(2012\)](#). Suppose at iteration  $t + 1$ ,  $\mathbf{B}^{t+1}$  is invertible (this is true under the RIP framework, see Step 2 in the proof of [Theorem 1](#)). We can show by some algebraic calculations that the update  $\mathbf{X}^{t+1}$  in Step 7 can be rewritten as

$$\mathbf{X}^{t+1} = \mathbf{X}_U^{t+1} (\mathbf{B}^{t+1})^{-1} \mathbf{X}_V^{t+1\top} = [\mathbf{U}^t \quad \mathbf{U}_\perp^t] \begin{bmatrix} \mathbf{B}^{t+1} & \mathbf{D}_2^{t+1\top} \\ \mathbf{D}_1^{t+1} & \mathbf{D}_1^{t+1}(\mathbf{B}^{t+1})^{-1} \mathbf{D}_2^{t+1\top} \end{bmatrix} [\mathbf{V}^t \quad \mathbf{V}_\perp^t]^\top. \quad (22)$$

Let  $\eta^t \in T_{\mathbf{X}^t}\mathcal{M}_r$  be the update direction and  $\mathbf{X}^t + \eta^t$  has the following representation,

$$\mathbf{X}^t + \eta^t = [\mathbf{U}^t \quad \mathbf{U}_\perp^t] \begin{bmatrix} \mathbf{B}^{t+1} & \mathbf{D}_2^{t+1\top} \\ \mathbf{D}_1^{t+1} & \mathbf{0} \end{bmatrix} [\mathbf{V}^t \quad \mathbf{V}_\perp^t]^\top. \quad (23)$$

Comparing (22) and (23), we can view the update of  $\mathbf{X}^{t+1}$  from  $\mathbf{X}^t + \eta^t$  as simply completing the  $\mathbf{0}$  matrix in  $\begin{bmatrix} \mathbf{B}^{t+1} & \mathbf{D}_2^{t+1\top} \\ \mathbf{D}_1^{t+1} & \mathbf{0} \end{bmatrix}$  by  $\mathbf{D}_1^{t+1}(\mathbf{B}^{t+1})^{-1} \mathbf{D}_2^{t+1\top}$ . This operation maps the tangent vector on

$T_{\mathbf{X}^t} \mathcal{M}_r$  back to the manifold  $\mathcal{M}_r$  and it turns out that it coincides with the orthographic retraction

$$R(\mathbf{X}^t, \eta^t) = [\mathbf{U}^t \quad \mathbf{U}_\perp^t] \begin{bmatrix} \mathbf{B}^{t+1} & \mathbf{D}_2^{t+1\top} \\ \mathbf{D}_1^{t+1} & \mathbf{D}_1^{t+1}(\mathbf{B}^{t+1})^{-1} \mathbf{D}_2^{t+1\top} \end{bmatrix} [\mathbf{V}^t \quad \mathbf{V}_\perp^t]^\top \quad (24)$$

on the set of fixed-rank matrices (Absil and Malick, 2012). Therefore, we have  $\mathbf{X}^{t+1} = R(\mathbf{X}^t, \eta^t)$ .

**Remark 7** Although the orthographic retraction defined in Absil and Malick (2012) requires that  $\mathbf{U}^t$  and  $\mathbf{V}^t$  are left and right singular vectors of  $\mathbf{X}^t$ , one can verify that even if the  $\mathbf{U}^t$  and  $\mathbf{V}^t$  are not exactly the left and right singular vectors but satisfy  $\mathbf{U}^t = \tilde{\mathbf{U}}^t \mathbf{O}$ ,  $\mathbf{V}^t = \tilde{\mathbf{V}}^t \mathbf{Q}$ , then the mapping (24) is equivalent to the orthographic retraction in Absil and Malick (2012). Here,  $\mathbf{O}, \mathbf{Q} \in \mathbb{O}_{r,r}$ , and  $\tilde{\mathbf{U}}^t$  and  $\tilde{\mathbf{V}}^t$  are left and right singular vectors of  $\mathbf{X}^t$ .

The Riemannian gradient of a smooth function  $f : \mathcal{M}_r \rightarrow \mathbb{R}$  at  $\mathbf{X} \in \mathcal{M}_r$  is defined as the unique tangent vector  $\text{grad } f(\mathbf{X}) \in T_{\mathbf{X}} \mathcal{M}_r$  such that  $\langle \text{grad } f(\mathbf{X}), \mathbf{Z} \rangle = Df(\mathbf{X})[\mathbf{Z}]$ ,  $\forall \mathbf{Z} \in T_{\mathbf{X}} \mathcal{M}_r$ , where  $Df(\mathbf{X})[\mathbf{Z}]$  denotes the directional derivative of  $f$  at point  $\mathbf{X}$  along the direction  $\mathbf{Z}$ . Since  $\mathcal{M}_r$  is an embedded submanifold of  $\mathbb{R}^{p_1 \times p_2}$  and the Euclidean metric is used, from (Absil et al., 2009, (3.37)), we know in our problem,

$$\text{grad } f(\mathbf{X}) = P_{T_{\mathbf{X}}}(\mathcal{A}^*(\mathcal{A}(\mathbf{X}) - \mathbf{y})), \quad (25)$$

and here  $P_{T_{\mathbf{X}}}$  is the orthogonal projector onto the tangent space at  $\mathbf{X}$  defined as follows

$$P_{T_{\mathbf{X}}}(\mathbf{Z}) = P_{\mathbf{U}} \mathbf{Z} P_{\mathbf{V}} + P_{\mathbf{U}_\perp} \mathbf{Z} P_{\mathbf{V}} + P_{\mathbf{U}} \mathbf{Z} P_{\mathbf{V}_\perp}, \quad \forall \mathbf{Z} \in \mathbb{R}^{p_1 \times p_2}, \quad (26)$$

where  $\mathbf{U} \in \mathbb{O}_{p_1, r}$ ,  $\mathbf{V} \in \mathbb{O}_{p_2, r}$  are the left and right singular vectors of  $\mathbf{X}$ .

Next, we introduce the Riemannian Hessian. The Riemannian Hessian of  $f$  at  $\mathbf{X} \in \mathcal{M}_r$  is the linear map  $\text{Hess } f(\mathbf{X})$  of  $T_{\mathbf{X}} \mathcal{M}_r$  onto itself defined as  $\text{Hess } f(\mathbf{X})[\mathbf{Z}] = \bar{\nabla}_{\mathbf{Z}} \text{grad } f(\mathbf{X})$ ,  $\forall \mathbf{Z} \in T_{\mathbf{X}} \mathcal{M}_r$ , where  $\bar{\nabla}$  is the Riemannian connection on  $\mathcal{M}_r$  (Absil et al., 2009, Section 5.3). Lemma 3 gives an explicit formula for Riemannian Hessian in our problem.

**Lemma 3 (Riemannian Hessian)** Consider  $f(\mathbf{X})$  in (1). If  $\mathbf{X} \in \mathcal{M}_r$  has singular value decomposition  $\mathbf{U} \Sigma \mathbf{V}^\top$  and  $\mathbf{Z} \in T_{\mathbf{X}} \mathcal{M}_r$  has representation

$$\mathbf{Z} = [\mathbf{U} \quad \mathbf{U}_\perp] \begin{bmatrix} \mathbf{Z}_B & \mathbf{Z}_{D_2}^\top \\ \mathbf{Z}_{D_1} & 0 \end{bmatrix} [\mathbf{V} \quad \mathbf{V}_\perp]^\top,$$

then the Hessian operator in this setting satisfies

$$\begin{aligned} \text{Hess } f(\mathbf{X})[\mathbf{Z}] = & P_{T_{\mathbf{X}}}(\mathcal{A}^*(\mathcal{A}(\mathbf{Z}))) + P_{\mathbf{U}_\perp} \mathcal{A}^*(\mathcal{A}(\mathbf{X}) - \mathbf{y}) \mathbf{V}_p \Sigma^{-1} \mathbf{V}^\top P_{\mathbf{V}} \\ & + P_{\mathbf{U}} \mathbf{U} \Sigma^{-1} \mathbf{U}_p^\top \mathcal{A}^*(\mathcal{A}(\mathbf{X}) - \mathbf{y}) P_{\mathbf{V}_\perp}, \end{aligned} \quad (27)$$

where  $\mathbf{U}_p = \mathbf{U}_\perp \mathbf{Z}_{D_1}$ ,  $\mathbf{V}_p = \mathbf{V}_\perp \mathbf{Z}_{D_2}$ .

Next, we show that the update direction  $\eta^t$ , implicitly encoded in (23), finds the Riemannian Gauss-Newton direction in the manifold optimization of  $\mathcal{M}_r$ . Similar as the classic Newton's method, at  $t$ -th iteration, the Riemannian Newton method aims to find the Riemannian Newton direction  $\eta_{\text{Newton}}^t$  in  $T_{\mathbf{X}^t} \mathcal{M}_r$  that solves the following Newton equation

$$-\text{grad } f(\mathbf{X}^t) = \text{Hess } f(\mathbf{X}^t)[\eta_{\text{Newton}}^t]. \quad (28)$$

If the residual  $(\mathbf{y} - \mathcal{A}(\mathbf{X}^t))$  is small, the last two terms in  $\text{Hess}f(\mathbf{X}^t)[\eta]$  of (27) are expected to be small, which means we can approximately solve the Riemannian Newton direction via

$$-\text{grad}f(\mathbf{X}^t) = P_{T_{\mathbf{X}^t}}(\mathcal{A}^*(\mathcal{A}(\eta))), \quad \eta \in T_{\mathbf{X}^t}\mathcal{M}_r. \quad (29)$$

In fact, Equation (29) has a interpretation from the *Fisher scoring* algorithm. Consider the statistical setting  $\mathbf{y} = \mathcal{A}(\mathbf{X}) + \boldsymbol{\epsilon}$ , where  $\mathbf{X}$  is a fixed low-rank matrix and  $\boldsymbol{\epsilon}_i \stackrel{i.i.d.}{\sim} N(0, \sigma^2)$ . Then for any  $\eta$ ,

$$\{\mathbb{E}(\text{Hess}f(\mathbf{X})[\eta])\}|_{\mathbf{X}=\mathbf{X}^t} = P_{T_{\mathbf{X}^t}}(\mathcal{A}^*(\mathcal{A}(\eta))),$$

where on the left hand side, the expression is evaluated at  $\mathbf{X}^t$  after taking expectation. In the literature, the *Fisher Scoring* algorithm computes the update direction via solving the modified Newton equation which replaces the Hessian with its expected value (Lange, 2010), i.e.,

$$\{\mathbb{E}(\text{Hess}f(\mathbf{X})[\eta])\}|_{\mathbf{X}=\mathbf{X}^t} = -\text{grad}f(\mathbf{X}^t), \quad \eta \in T_{\mathbf{X}^t}\mathcal{M}_r,$$

which exactly becomes (29) in our setting. Meanwhile, it is not difficult to show that the Fisher Scoring algorithm here is equivalent to the Riemannian Gauss-Newton method for solving nonlinear least squares (Lange, 2010, Section 14.6) and (Absil et al., 2009, Section 8.4). Thus,  $\eta$  that solves the equation (29) is also the *Riemannian Gauss-Newton direction*.

It turns out that the update direction  $\eta^t$  (23) of RISRO solves the Fisher Scoring or Riemannian Gauss-Newton equation (29):

**Theorem 2** *Let  $\{\mathbf{X}^t\}$  be the sequence generated by RISRO under the same assumptions as in Theorem 1. Then, for all  $t \geq 0$ , the implicitly encoded update direction  $\eta^t$  in (23) solves the Riemannian Gauss-Newton equation (29).*

Theorem 2 together with the retraction explanation in (24) establishes the connection of RISRO and Riemannian manifold optimization. Following this connection, we further show that each  $\eta_t$  is always a decent direction in the next Proposition 3. By incorporating the globalization scheme discussed in Remark 5, this fact is useful in boosting the local convergence of RISRO to the global convergence.

**Proposition 3** *For all  $t \geq 0$ , the update direction  $\eta^t \in T_{\mathbf{X}^t}\mathcal{M}_r$  in (23) satisfies  $\langle \text{grad}f(\mathbf{X}^t), \eta^t \rangle < 0$ , i.e.,  $\eta_t$  is a descent direction. If  $\mathcal{A}$  satisfies the  $2r$ -RIP, then the direction sequence  $\{\eta^t\}$  is gradient related.*

**Remark 8** *The convergence of Riemannian Gauss-Newton was studied in a recent work Breiding and Vannieuwenhoven (2018). Our results are significantly different from and offer improvements to Breiding and Vannieuwenhoven (2018) in the following ways. First, Breiding and Vannieuwenhoven (2018) considered a more general Riemannian Gauss-Newton setting, while their convergence results are established for a local minima, which is a much stronger and less practical requirement than the stationary point assumption we need. Second, the initialization condition and convergence rate in Breiding and Vannieuwenhoven (2018) can be suboptimal in our rank constrained least squares setting. Third, the proof technique of ours are quite different from Breiding and Vannieuwenhoven (2018). The proof of Breiding and Vannieuwenhoven (2018) is based on the manifold optimization, while our proof is motivated from the insight of recursive importance sketching introduced in Section 2 and in particular, the approximation error of sketched least squares established in Lemma 1 plays a key role. Fourth, our recursive importance sketching framework provides new sketching interpretations for several classical algorithms for rank constrained least squares. In Section 6 we also apply RISRO in popular statistical models and establish the statistical convergence results. It is however not immediately clear how to utilize the results in Breiding and Vannieuwenhoven (2018) in these statistical settings.*

|                          | Alter Mini            | SVP       | GD        | RISRO (this work)     |
|--------------------------|-----------------------|-----------|-----------|-----------------------|
| Complexity per iteration | $O(np^2r^2 + (pr)^3)$ | $O(np^2)$ | $O(np^2)$ | $O(np^2r^2 + (pr)^3)$ |
| Convergence rate         | Linear                | Linear    | Linear    | Quadratic-(linear)    |

Table 1: Computational complexity per iteration and convergence rate for Alternating Minimization (Alter Mini) (Jain et al., 2013), singular value projection (SVP) (Jain et al., 2010), gradient descent (GD) (Tu et al., 2016), and RISRO

## 5 Computational Complexity of RISRO

In this section, we discuss the computational complexity of RISRO. Suppose  $p_1 = p_2 = p$ , the computational complexity of RISRO per iteration is  $O(np^2r^2 + (pr)^3)$  in the general setting. A comparison on computational complexity of RISRO and other common algorithms is provided in Table 1. Here the main complexity of RISRO and Alter Mini is from solving the least squares. The main complexity of the singular value projection (SVP) (Jain et al., 2010) and gradient descent (Tu et al., 2016) is from computing the gradient. From Table 1, we can see RISRO has the same per-iteration complexity as Alter Mini and comparable complexity with SVP and GD when  $n \geq pr$  and  $r$  is much less than  $n$  and  $p$ . On the other hand, RISRO and Alter Mini are tuning free, while a proper step size is crucial for SVP and GD to have fast convergence. Finally, RISRO enjoys a high-order convergence as we have shown in Section 3, and the convergence rates of all other algorithms are limited to be linear.

The main computational bottleneck of RISRO is solving the least squares, which can be alleviated by using iterative linear system solvers, such as the (preconditioned) conjugate gradient method, when the linear operator  $\mathcal{A}$  has special structures. Such special structures occur, for example, in matrix completion problem ( $\mathcal{A}$  is sparse) (Vandereycken, 2013), phase retrieval for X-ray crystallography imaging ( $\mathcal{A}$  involves fast Fourier transforms) (Huang et al., 2017b), and blind deconvolution for imaging deblurring ( $\mathcal{A}$  involves fast Fourier transforms and Haar wavelet transforms) (Huang and Hand, 2018).

To utilize these structures, we introduce an intrinsic representation of tangent vectors in  $\mathcal{M}_r$ : if  $\mathbf{U}, \mathbf{V}$  are the left and right singular vectors of a rank- $r$  matrix  $\mathbf{X}$ , an orthonormal basis of  $T_{\mathbf{X}}\mathcal{M}_r$  can be

$$\begin{aligned} & \left\{ [\mathbf{U} \quad \mathbf{U}_\perp] \begin{bmatrix} \mathbf{e}_i \mathbf{e}_j^\top & \mathbf{0}_{r \times (p-r)} \\ \mathbf{0}_{(p-r) \times r} & \mathbf{0}_{(p-r) \times (p-r)} \end{bmatrix} [\mathbf{V} \quad \mathbf{V}_\perp]^\top, i = 1, \dots, r, j = 1, \dots, r \right\} \cup \\ & \left\{ [\mathbf{U} \quad \mathbf{U}_\perp] \begin{bmatrix} \mathbf{0}_{r \times r} & \mathbf{e}_i \tilde{\mathbf{e}}_j^\top \\ \mathbf{0}_{(p-r) \times r} & \mathbf{0}_{(p-r) \times (p-r)} \end{bmatrix} [\mathbf{V} \quad \mathbf{V}_\perp]^\top, i = 1, \dots, r, j = 1, \dots, p-r \right\} \cup \\ & \left\{ [\mathbf{U} \quad \mathbf{U}_\perp] \begin{bmatrix} \mathbf{0}_{r \times r} & \mathbf{0}_{r \times (p-r)} \\ \tilde{\mathbf{e}}_i \mathbf{e}_j^\top & \mathbf{0}_{(p-r) \times (p-r)} \end{bmatrix} [\mathbf{V} \quad \mathbf{V}_\perp]^\top, i = 1, \dots, p-r, j = 1, \dots, r \right\}, \end{aligned}$$

where  $\mathbf{e}_i$  and  $\tilde{\mathbf{e}}_i$  denote the  $i$ -th canonical basis of  $\mathbb{R}^r$  and  $\mathbb{R}^{p-r}$ , respectively. It follows that any tangent vector in  $T_{\mathbf{X}}\mathcal{M}_r$  can be uniquely represented by a coefficient vector in  $\mathbb{R}^{(2p-r)r}$  via the basis above. This representation is called the intrinsic representation (Huang et al., 2017a). Computing the intrinsic representations of a Riemannian gradient can be computationally efficient. For example, the complexity of computing the Riemannian gradient in matrix completion is  $O(nr + pr^2)$  and its intrinsic representation can be computed by an additional  $O(pr^2)$  operations (Vandereycken, 2013). The complexities of computing intrinsic representations of the Riemannian gradients of the

phase retrieval and the blind deconvolution are both  $O(n \log(n)r + pr^2)$  (Huang et al., 2017b; Huang and Hand, 2018).

By Theorem 2, the least squares problem (5) of RISRO is equivalent to solve  $\eta \in T_{\mathbf{X}^t} \mathcal{M}_r$  such that  $P_{T_{\mathbf{X}^t}} \mathcal{A}^*(\mathcal{A}(\eta)) = -\text{grad}f(\mathbf{X}^t)$ . Reformulating this equation by intrinsic representation yields

$$-\text{grad}f(\mathbf{X}^t) = P_{T_{\mathbf{X}^t}} \mathcal{A}^*(\mathcal{A}(\eta)) \implies -u = \mathcal{B}_{\mathbf{X}}^*(\mathcal{A}^*(\mathcal{A}(\mathcal{B}_{\mathbf{X}}v))), \quad (30)$$

where  $u, v$  are the intrinsic representations of  $\text{grad}f(\mathbf{X}^t)$  and  $\eta$ , the mapping  $\mathcal{B}_{\mathbf{X}} : \mathbb{R}^{(2p-r)r} \rightarrow T_{\mathbf{X}} \mathcal{M}_r \subset \mathbb{R}^{p \times p}$  converts an intrinsic representation to the corresponding tangent vector, and  $\mathcal{B}_{\mathbf{X}}^* : \mathbb{R}^{p \times p} \rightarrow \mathbb{R}^{(2p-r)r}$  is the adjoint operator of  $\mathcal{B}_{\mathbf{X}}$ . The computational complexity of using conjugate gradient method to solve (30) is determined by the complexity of evaluating the operator  $\mathcal{B}_{\mathbf{X}}^* \circ (\mathcal{A}^* \mathcal{A}) \circ \mathcal{B}_{\mathbf{X}}$  on a given vector. With the intrinsic representation, it can be shown that this evaluation costs  $O(nr + pr^2)$  in matrix completion and  $O(n \log(n)r + pr^2)$  in the phase retrieval and blind deconvolution. Thus, when solving (30) via the conjugate gradient method, the complexity is  $O(k(nr + pr^2))$  in the matrix completion and  $O(k(n \log(n)r + pr^2))$  in the phase retrieval and the blind deconvolution, where  $k$  is the number of conjugate gradient iterations and is provably at most  $(2p-r)r$ . Hence, for special applications such as matrix completion, phase retrieval and blind deconvolution, by using the conjugate gradient method with the intrinsic representation, the per iteration complexity of RISRO can be greatly reduced. This point will be further exploited in our future research.

## 6 Recursive Importance Sketching under Statistical Models

In this section, we study the applications of RISRO in machine learning and statistics. We specifically investigate the low-rank matrix trace regression and phase retrieval, while our key ideas can be applied to more problems.

### 6.1 Low-Rank Matrix Trace Regression

Consider the low-rank matrix trace regression model:

$$\mathbf{y}_i = \langle \mathbf{A}_i, \mathbf{X}^* \rangle + \epsilon_i, \quad \text{for } 1 \leq i \leq n, \quad (31)$$

where  $\mathbf{X}^* \in \mathbb{R}^{p_1 \times p_2}$  is the true model parameter and  $\text{rank}(\mathbf{X}^*) = r$ . The goal is to estimate  $\mathbf{X}^*$  from  $\{\mathbf{y}_i, \mathbf{A}_i\}_{i=1}^n$ . Due to the noise  $\epsilon_i$ ,  $\mathbf{X}^*$  usually cannot be exactly recovered.

The following Theorem 3 shows RISRO converges quadratic-linearly to  $\mathbf{X}^*$  up to some statistical error given a proper initialization. Moreover, under the Gaussian ensemble design, RISRO with spectral initialization achieves the minimax optimal estimation error rate.

**Theorem 3 (RISRO in Matrix Trace Regression)** *Consider the low-rank matrix trace regression problem (31). Suppose that  $\mathcal{A}$  satisfies the  $3r$ -RIP, the initialization of RISRO satisfies*

$$\|\mathbf{X}^0 - \mathbf{X}^*\|_{\text{F}} \leq \left( \frac{1}{4} \wedge \frac{1 - R_{2r}}{2\sqrt{5}R_{3r}} \right) \sigma_r(\mathbf{X}^*), \quad (32)$$

and

$$\sigma_r(\mathbf{X}^*) \geq \left( 16\sqrt{5} \vee \frac{40\sqrt{2}R_{3r}}{1 - R_{2r}} \right) \frac{\|(\mathcal{A}^*(\epsilon))_{\max(r)}\|_{\text{F}}}{1 - R_{2r}}. \quad (33)$$

Then the iterations of RISRO converge as follows

$$\|\mathbf{X}^{t+1} - \mathbf{X}^*\|_F^2 \leq 10 \frac{R_{3r}^2 \|\mathbf{X}^t - \mathbf{X}^*\|_F^4}{(1 - R_{2r})^2 \sigma_r^2(\mathbf{X}^*)} + \frac{20 \|(\mathcal{A}^*(\epsilon))_{\max(r)}\|_F^2}{(1 - R_{2r})^2}, \quad \forall t \geq 0. \dots \quad (34)$$

Moreover, if we assume  $(\mathbf{A}_i)_{[j,k]} \stackrel{i.i.d.}{\sim} N(0, 1/n)$  and  $\epsilon_i \stackrel{i.i.d.}{\sim} N(0, \sigma^2/n)$ . Then there exist universal constants  $C_1, C_2, C', c > 0$  such that as long as  $n \geq C_1(p_1 + p_2)r(\frac{\sigma^2}{\sigma_r^2(\mathbf{X}^*)} \vee r\kappa^2)$  (here  $\kappa = \frac{\sigma_1(\mathbf{X}^*)}{\sigma_r(\mathbf{X}^*)}$  is the condition number of  $\mathbf{X}^*$ ) and  $t_{\max} \geq C_2 \log \log(\frac{\sigma_r^2(\mathbf{X}^*)n}{r(p_1 + p_2)\sigma^2}) \vee 1$ , the output of RISRO with spectral initialization  $\mathbf{X}^0 = (\mathcal{A}^*(\mathbf{y}))_{\max(r)}$  satisfies  $\|\mathbf{X}^{t_{\max}} - \mathbf{X}^*\|_F^2 \leq c \frac{r(p_1 + p_2)}{n} \sigma^2$  with probability at least  $1 - \exp(-C'(p_1 + p_2))$ .

**Remark 9 (Quadratic Convergence, Statistical Error, and Robustness)** Note that in (34), there are two terms in the upper bound of  $\|\mathbf{X}^t - \mathbf{X}^*\|_F^2$ . The first term corresponds to the optimization error, which quadratically decreases over iteration  $t$ ; the second term  $O(\|(\mathcal{A}^*(\epsilon))_{\max(r)}\|_F^2)$  is the essential statistical error that is independent of the optimization algorithm.

In addition, (34) shows the error contraction factor is independent of the condition number  $\kappa$ , which demonstrates the robustness of RISRO to the ill-conditioning of the underlying low-rank matrix. We will further demonstrate this point by simulation studies in Section 7.2.

**Remark 10 (Optimal Statistical Error)** Under the Gaussian ensemble design, RISRO with spectral initialization achieves the rate of estimation error  $cr(p_1 + p_2)\sigma^2/n$  after double-logarithmic number of iterations when  $n \geq C_1(p_1 + p_2)r(\frac{\sigma^2}{\sigma_r^2(\mathbf{X}^*)} \vee r\kappa^2)$ . Compared with the lower bound of the estimation error

$$\min_{\hat{\mathbf{X}}} \max_{\text{rank}(\mathbf{X}^*) \leq r} \mathbb{E} \|\hat{\mathbf{X}} - \mathbf{X}^*\|_F^2 \geq c' \frac{r(p_1 + p_2)\sigma^2}{n}$$

for some  $c' > 0$  in [Candès and Plan \(2011\)](#), RISRO achieves the minimax optimal estimation error. To the best of our knowledge, RISRO is the first provable algorithm that achieves the minimax rate-optimal estimation error with only a double-logarithmic number of iterations.

## 6.2 Phase Retrieval

In this section, we consider RISRO for solving the following quadratic equation system

$$\mathbf{y}_i = |\langle \mathbf{a}_i, \mathbf{x}^* \rangle|^2 \quad \text{for } 1 \leq i \leq n, \quad (35)$$

where  $\mathbf{y} \in \mathbb{R}^n$  and covariates  $\{\mathbf{a}_i\}_{i=1}^n \in \mathbb{R}^p$  (or  $\mathbb{C}^p$ ) are known whereas  $\mathbf{x}^* \in \mathbb{R}^p$  (or  $\mathbb{C}^p$ ) are unknown. The goal is to recover  $\mathbf{x}^*$  based on  $\{\mathbf{y}_i, \mathbf{a}_i\}_{i=1}^n$ . One important application is known as *phase retrieval* arising from physical science due to the nature of optical sensors ([Fienup, 1982](#)). In the literature, various approaches have been proposed for phase retrieval with provable guarantees, such as convex relaxation ([Candès et al., 2013; Huang et al., 2017b; Waldspurger et al., 2015](#)) and non-convex approaches ([Candès et al., 2015; Chen and Candès, 2017; Gao and Xu, 2017; Ma et al., 2019; Netrapalli et al., 2013; Sanghavi et al., 2017; Wang et al., 2017a; Duchi and Ruan, 2019](#)).

For ease of exposition, we focus on the real-value model, i.e.,  $\mathbf{x}^* \in \mathbb{R}^n$  and  $\mathbf{a}_i \in \mathbb{R}^n$ , while a simple trick in [Sanghavi et al. \(2017\)](#) can recast the problem (35) in the complex model into a rank-2 real value matrix recovery problem, then our approach still applies. In the real-valued setting, we can rewrite model (35) into a low-rank matrix recovery model

$$\mathbf{y} = \mathcal{A}(\mathbf{X}^*) \text{ with } \mathbf{X}^* = \mathbf{x}^* \mathbf{x}^{*\top} \text{ and } [\mathcal{A}(\mathbf{X}^*)]_i = \langle \mathbf{a}_i \mathbf{a}_i^\top, \mathbf{x}^* \mathbf{x}^{*\top} \rangle. \quad (36)$$

There are two challenges in phase retrieval compared to the low-rank matrix trace regression considered previously. First, due to the symmetry of sensing matrices  $\mathbf{a}_i \mathbf{a}_i^\top$  and  $\mathbf{x}^* \mathbf{x}^{*\top}$  in phase retrieval, the importance covariates  $\mathcal{A}_{D_1}$  and  $\mathcal{A}_{D_2}$  in (4) are exactly the same and an adaptation of Algorithm 1 is thus needed. Second, in phase retrieval, the mapping  $\mathcal{A}$  no longer satisfies a proper RIP condition in general (Cai and Zhang, 2015; Candès et al., 2013), so new theory is needed. To this end, we introduce a modified RISRO for phase retrieval in Algorithm 2. Particularly in Step 4 of Algorithm 2, we multiply the importance covariates  $\mathbf{A}_2$  by an extra factor 2 to account for the duplicate importance covariates due to symmetry.

---

**Algorithm 2** RISRO for Phase Retrieval

---

- 1: Input: design vectors  $\{\mathbf{a}_i\}_{i=1}^n \in \mathbb{R}^p$ ,  $\mathbf{y} \in \mathbb{R}^n$ , initialization  $\mathbf{X}^0$  that admits eigenvalue decomposition  $\sigma_1^0 \mathbf{u}^0 \mathbf{u}^{0\top}$
- 2: **for**  $t = 0, 1, \dots$ , **do**
- 3:   Perform importance sketching on  $\mathbf{a}_i$  and construct the covariates  $\mathbf{A}_1 \in \mathbb{R}^n$ ,  $\mathbf{A}_2 \in \mathbb{R}^{n \times (p-1)}$ , where for  $1 \leq i \leq n$ ,  $(\mathbf{A}_1)_i = (\mathbf{a}_i^\top \mathbf{u}^t)^2$ ,  $(\mathbf{A}_2)_{[i,:]} = \mathbf{u}_\perp^{t\top} \mathbf{a}_i \mathbf{a}_i^\top \mathbf{u}^t$ .
- 4:   Solve the unconstrained least squares problem  $(\mathbf{b}^{t+1}, \mathbf{d}^{t+1}) = \arg \min_{\mathbf{b} \in \mathbb{R}, \mathbf{d} \in \mathbb{R}^{(p-1)}} \|\mathbf{y} - \mathbf{A}_1 \mathbf{b} - 2\mathbf{A}_2 \mathbf{d}\|_2^2$ .
- 5:   Compute the eigenvalue decomposition of  $[\mathbf{u}^t \mathbf{u}_\perp^t] \begin{bmatrix} \mathbf{b}^{t+1} & \mathbf{d}^{t+1\top} \\ \mathbf{d}^{t+1} & \mathbf{0} \end{bmatrix} [\mathbf{u}^t \mathbf{u}_\perp^t]^\top$ , and denote it as  $[\mathbf{v}_1 \mathbf{v}_2] \begin{bmatrix} \lambda_1 & 0 \\ 0 & \lambda_2 \end{bmatrix} [\mathbf{v}_1 \mathbf{v}_2]^\top$  with  $\lambda_1 \geq \lambda_2$ .
- 6:   Update  $\mathbf{u}^{t+1} = \mathbf{v}_1$  and  $\mathbf{X}^{t+1} = \lambda_1 \mathbf{u}^{t+1} \mathbf{u}^{t+1\top}$ .
- 7: **end for**

---

Next, we show under Gaussian ensemble design, given the sample number  $n = O(p \log p)$  and proper initialization, the sequence  $\{\mathbf{X}^t\}$  generated by Algorithm 2 converges quadratically to  $\mathbf{X}^*$ .

**Theorem 4 (Local Quadratic Convergence of RISRO for Phase Retrieval)** *In the phase retrieval problem (35), assume that  $\{\mathbf{a}_i\}_{i=1}^n$  are independently generated from  $N(0, \mathbf{I}_p)$ . Then for any  $\delta_1, \delta_2 \in (0, 1)$ , there exist  $c, C(\delta_1), C' > 0$  such that when  $p \geq c \log n, n \geq C(\delta_1)p \log p$ , if  $\|\mathbf{X}^0 - \mathbf{X}^*\|_F \leq \frac{(1-\delta_1)}{C'(1+\delta_2)p} \|\mathbf{X}^*\|_F$ , with probability at least  $1 - C_1 \exp(-C_2(\delta_1, \delta_2)n) - C_3 n^{-p}$ , the sequence  $\{\mathbf{X}^t\}$  generated by Algorithm 2 satisfies*

$$\|\mathbf{X}^{t+1} - \mathbf{X}^*\|_F \leq \frac{C'(1+\delta_2)p}{(1-\delta_1)\|\mathbf{X}^*\|_F} \|\mathbf{X}^t - \mathbf{X}^*\|_F^2, \quad \forall t \geq 0 \quad (37)$$

for some  $C_1, C_2(\delta_1, \delta_2), C_3 > 0$ .

**Remark 11 (Initialization Condition)** *In Theorem 4, we assume  $\|\mathbf{X}^0 - \mathbf{X}^*\|_F \leq O(\|\mathbf{X}^*\|_F/p)$  to show the quadratic convergence for RISRO. This initialization assumption is used to handle some technical difficulties without the proper restricted isometry property in phase retrieval. Although in theory it is difficult to prove that the spectral initialization satisfies this assumption, we find by simulation that the spectral initialization is sufficiently good to guarantee quadratic convergence in the subsequent updates. We leave the convergence theory under weaker initialization assumption as future work.*

## 7 Numerical Studies

In this section, we conduct simulation studies to investigate the numerical performance of RISRO. We specifically consider two settings:

- Matrix trace regression. Let  $p = p_1 = p_2$  and  $\mathbf{y}_i = \langle \mathbf{X}^*, \mathbf{A}_i \rangle + \boldsymbol{\epsilon}_i$ , where  $\mathbf{A}_i$ s are constructed with independent standard normal entries and  $\boldsymbol{\epsilon}_i \stackrel{i.i.d.}{\sim} N(0, \sigma^2)$ .  $\mathbf{X}^* = \mathbf{U}^* \boldsymbol{\Sigma}^* \mathbf{V}^{*\top}$  where  $\mathbf{U}^*, \mathbf{V}^* \in \mathbb{O}_{p,r}$  are randomly generated,  $\boldsymbol{\Sigma} = \text{diag}(\lambda_1, \dots, \lambda_r)$ . Also, we set  $\lambda_1 = 3$  and  $\lambda_i = \frac{\lambda_1}{\kappa^{i/r}}$  for  $i = 2, \dots, r$ , so the condition number of  $\mathbf{X}^*$  is  $\kappa$ . We initialize  $\mathbf{X}^0$  via  $(\mathcal{A}^*(\mathbf{y}))_{\max(r)}$ .
- Phase retrieval. Let  $\mathbf{y}_i = \langle \mathbf{a}_i, \mathbf{x}^* \rangle^2$ , where  $\mathbf{x}^* \in \mathbb{R}^p$  is a randomly generated unit vector,  $\mathbf{a}_i \stackrel{i.i.d.}{\sim} N(0, \mathbf{I}_p)$ . We initialize  $\mathbf{X}^0$  via truncated spectral initialization (Chen and Candès, 2017).

Throughout the simulation studies, we consider errors in two metrics: (1)  $\|\mathbf{X}^t - \mathbf{X}^{t_{\max}}\|_F / \|\mathbf{X}^{t_{\max}}\|_F$ , which measures the convergence error; (2)  $\|\mathbf{X}^t - \mathbf{X}^*\|_F / \|\mathbf{X}^*\|_F$ , which is the relative root mean-squared error (Relative RMSE) that measures the estimation error for  $\mathbf{X}^*$ . The algorithm is terminated when it reaches the maximum number of iterations  $t_{\max} = 300$  or the corresponding error metric is less than  $10^{-12}$ . Unless otherwise noted, the reported results are based on the averages of 50 simulations and on a computer with Intel Xeon E5-2680 2.5GHz CPU.

## 7.1 Properties of RISRO

We first study the convergence rate of RISRO. Specifically, set  $p = 100, r = 3, n \in \{1200, 1500, 1800, 2100, 2400\}, \kappa = 1, \sigma = 0$  for low-rank matrix trace regression and  $p = 1200, n \in \{4800, 6000, 7200, 8400, 9600\}$  for phase retrieval. The convergence performance of RISRO (Algorithm 1 in low-rank matrix trace regression and Algorithm 2 in phase retrieval) is plotted in Figure 1. We can see RISRO with the (truncated) spectral initialization converges quadratically to the true parameter  $\mathbf{X}^*$  in both problems, which is in line with the theory developed in previous sections. Although our theory on phase retrieval in Theorem 4 is based a stronger initialization assumption, the truncated spectral initialization achieves great empirical performance.

In another setting, we examine the quadratic-linear convergence for RISRO under the noisy setting. Consider the matrix trace regression problem, where  $\sigma = 10^\alpha, \alpha \in \{0, -1, -2, -3, -5, -14\}$ ,  $n = 1500$ , and  $p, r, \kappa$  are the same as the previous setting. The simulation results in Figure 3 show the gradient norm  $\|\text{grad}f(\mathbf{X}^t)\|$  of the iterates converges to zero, which demonstrates the convergence of the algorithm. Meanwhile, since the observations are noisy, RISRO exhibits the quadratic-linear convergence as we discussed in Remark 4: when  $\alpha = 0$ , i.e.,  $\sigma = 1$ , RISRO converges quadratically in the first 2-3 steps and then reduces to linear convergence afterwards; as  $\sigma$  gets smaller, we can see RISRO enjoys a longer path of quadratic convergence, which matches our theoretical prediction in Remark 4.

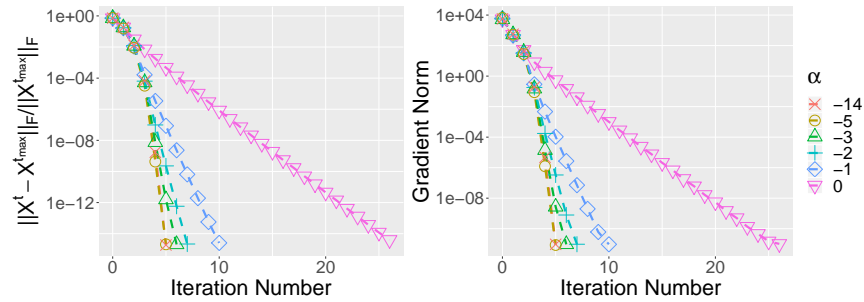


Figure 3: Convergence plot of RISRO in matrix trace regression.  $p = 100, r = 3, n = 1500, \kappa = 1, \sigma = 10^\alpha$  with varying  $\alpha$

Finally, we study the performance of RISRO under the large-scale setting of the matrix trace regression. Fix  $n = 7000, r = 3, \kappa = 1, \sigma = 0$  and let dimension  $p$  grow from 100 to 500. For the largest case, the space cost of storing  $\mathcal{A}$  reaches  $7000 \cdot 500 \cdot 500 \cdot 8B = 13.04\text{GB}$ . Figure 4 shows the relative RMSE of the output of RISRO and runtime versus the dimension. We can clearly see the relative RMSE of the output is stable and the runtime scales reasonably well as the dimension  $p$  grows.

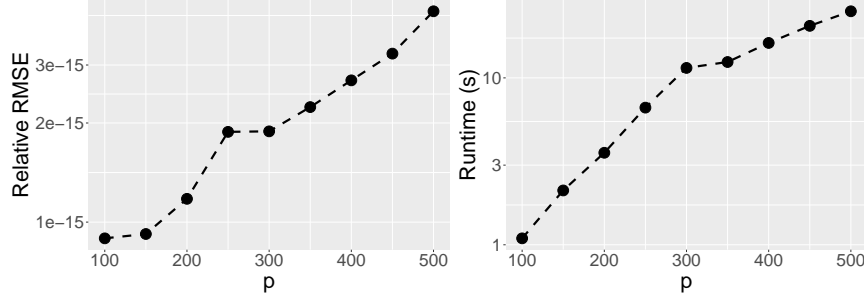


Figure 4: Relative RMSE and runtime of RISRO in matrix trace regression.  $p \in [100, 500], r = 3, n = 7000, \kappa = 1, \sigma = 0$

## 7.2 Comparison of RISRO with Other Algorithms in Literature

In this subsection, we further compare RISRO with existing algorithms in the literature. In the matrix trace regression, we compare our algorithm with singular value projection (SVP) (Goldfarb and Ma, 2011; Jain et al., 2010), Alternating Minimization (Alter Mini) (Jain et al., 2013; Zhao et al., 2015), gradient descent (GD) (Park et al., 2018; Tu et al., 2016; Zheng and Lafferty, 2015), and convex nuclear norm minimization (NNM) (3) (Toh and Yun, 2010). We consider the setting with  $p = 100, r = 3, n = 1500, \kappa \in \{1, 50, 500\}, \sigma = 0$  (noiseless case) or  $\sigma = 10^{-6}$  (noisy case). Following Zheng and Lafferty (2015), in the implementation of GD and SVP, we evaluate three choices of step size,  $\{5 \times 10^{-3}, 10^{-3}, 5 \times 10^{-4}\}$ , then choose the best one. In phase retrieval, we compare Algorithm 2 with Wirtinger Flow (WF) (Candès et al., 2015) and Truncated Wirtinger Flow (TWF) (Chen and Candès, 2017) with  $p = 1200, n = 6000$ . We use the codes of the accelerated proximal gradient for NNM, WF and TWF from the corresponding authors' websites and implement the other algorithms by ourselves. The stopping criteria of all procedures are the same as RISRO mentioned in the previous simulation settings.

We compare the performance of various procedures on noiseless matrix trace regression in Figure 5. For all different choices of  $\kappa$ , RISRO converges quadratically to  $\mathbf{X}^*$  in 7 iterations with high accuracy, while the other baseline algorithms converge much slower in a linear rate. When  $\kappa$  (condition number of  $\mathbf{X}^*$ ) increases from 1 to 50 and 500 so that the problem becomes more ill-conditioned, RISRO, Alter Mini, and SVP perform robustly, while GD converges more slowly. In Theorem 3, we have shown the quadratic convergence rate of RISRO is robust to the condition number (see Remark 9). As we expect, the non-convex optimization methods converge much faster than the convex relaxation method. Moreover, to achieve a relative RMSE of  $10^{-10}$ , RISRO only takes about 1/5 runtime compared to other algorithms if  $\kappa = 1$  and this factor is even smaller in the ill-conditioned cases that  $\kappa = 50$  and 500.

The comparison of RISRO, WF, and TWF in phase retrieval is plotted in Figure 6. We can also see RISRO can recover the underlying true signal with high accuracy in much less time than the other baseline methods.

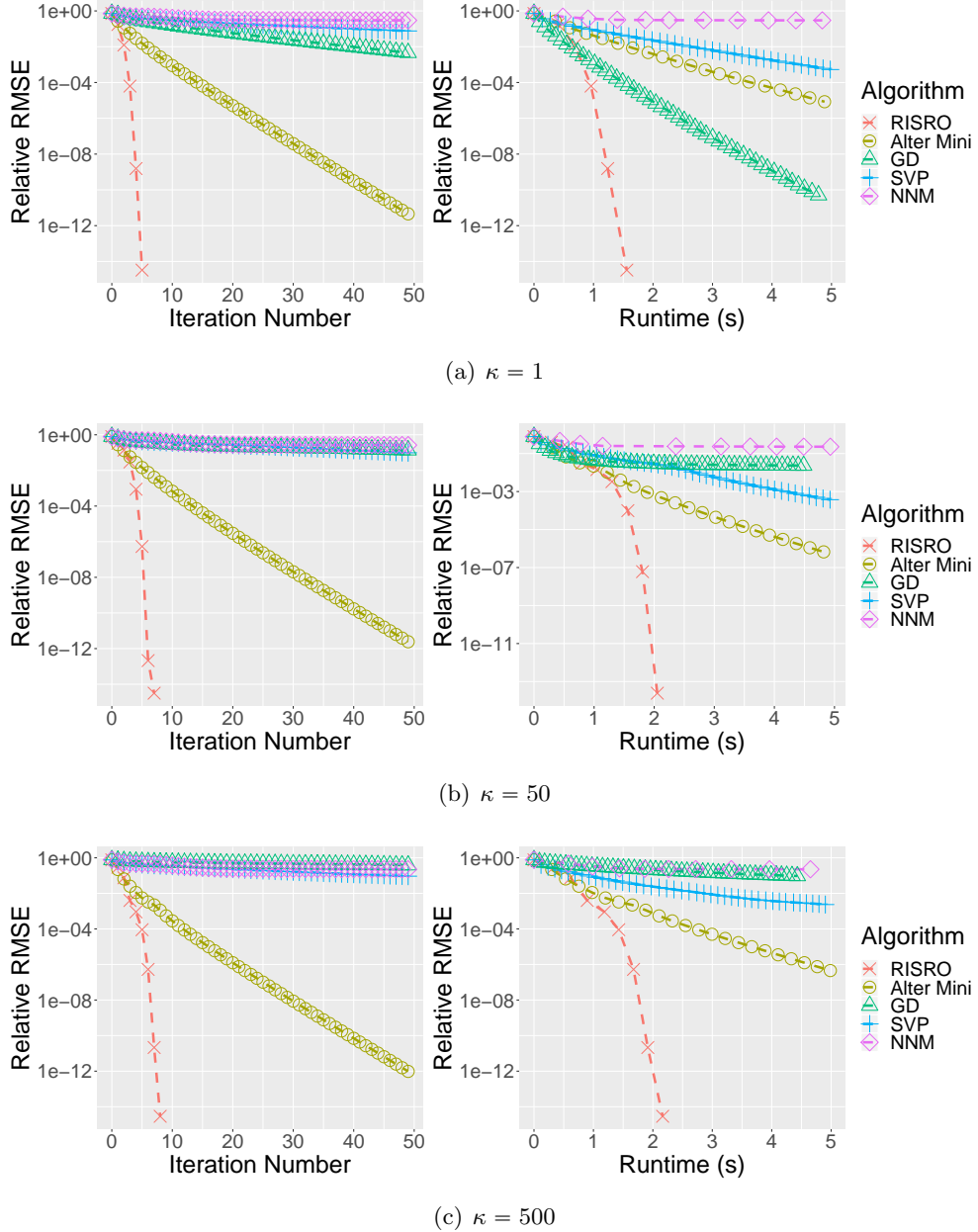


Figure 5: Relative RMSE of RISRO, singular value projection (SVP), Alternating Minimization (Alter Mini), gradient descent (GD), and Nuclear Norm Minimization (NNM) in low-rank matrix trace regression. Here,  $p = 100, r = 3, n = 1500, \sigma = 0, \kappa \in \{1, 50, 500\}$ .

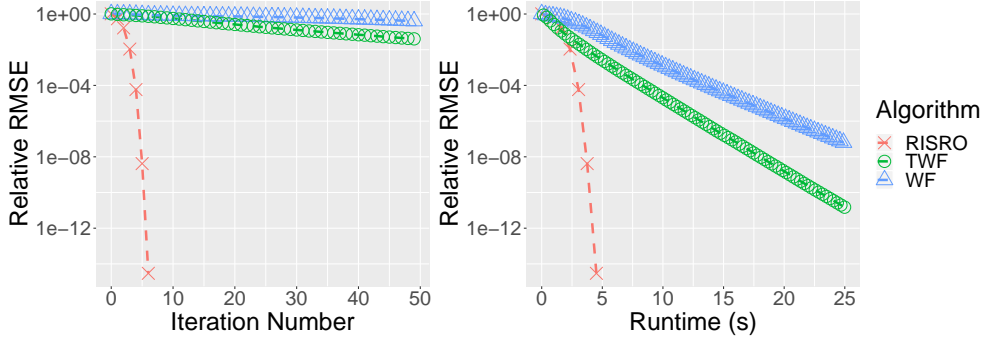


Figure 6: Relative RMSE of RISRO, Wirtinger Flow (WF), Truncated Wirtinger Flow (TWF) in phase retrieval. Here,  $p = 1200, n = 6000$

Next, we compare the performance of RISRO with other algorithms in the noisy setting,  $\sigma = 10^{-6}$ , in the low-rank matrix trace regression. We can see from the results in Figure 7 that due to the noise, the estimation error first decreases then stabilizes after reaching at a certain level. Meanwhile, we can also find RISRO converges in a much faster quadratic-linear rate before reaching at the stable level compared to all other algorithms.

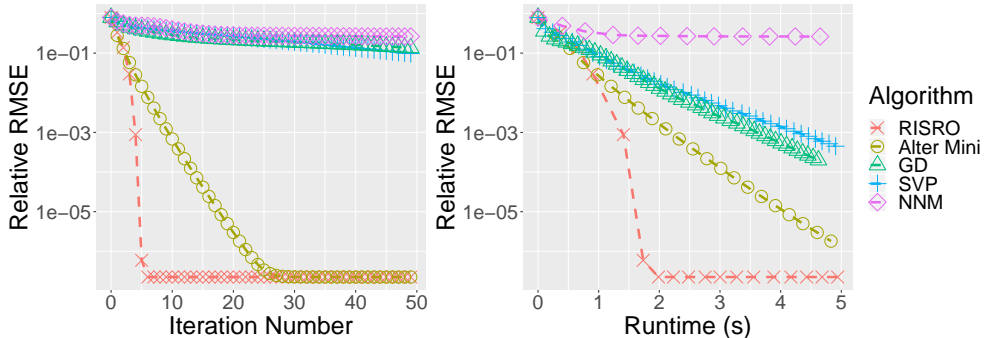


Figure 7: Relative RMSE of RISRO, singular value projection (SVP), Alternating Minimization (Alter Mini), gradient descent (GD), and Nuclear Norm Minimization (NNM) in low-rank matrix trace regression. Here,  $p = 100, r = 3, n = 1500, \kappa = 5, \sigma = 10^{-6}$

Finally, we study the required sample size to guarantee successful recovery by RISRO and other algorithms. We set  $p = 100, r = 3, \kappa = 5, n \in [600, 1500]$  in the noiseless matrix trace regression and  $p = 1200, n \in [2400, 6000]$  in phase retrieval. We say the algorithm achieves successful recovery if the relative RMSE is less than  $10^{-2}$  when the algorithm terminates. The simulation results in Figure 8 show RISRO requires the minimum sample size to achieve a successful recovery in both matrix trace regression and phase retrieval; Alter Mini has similar performance to RISRO; and both RISRO and Alter Mini require smaller sample size than the rest of algorithms for successful recovery.

## 8 Conclusion and Discussion

In this paper, we propose a new algorithm, RISRO, for solving rank constrained least squares. RISRO is based on a novel algorithmic framework, recursive importance sketching, which also

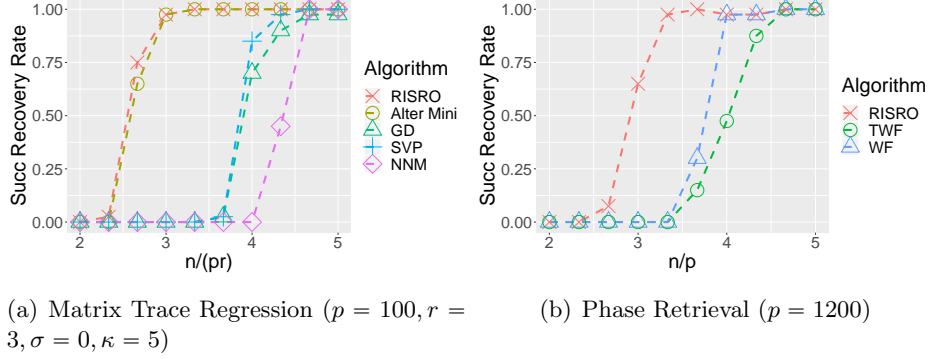


Figure 8: Successful recovery rate comparison

provides new sketching interpretations for several existing algorithms for rank constrained least squares. RISRO is easy to implement and computationally efficient. Under some reasonable assumptions, local quadratic-linear and quadratic convergence are established for RISRO. Simulation studies demonstrate the superior performance of RISRO.

There are many interesting extensions to the results in this paper to be explored in the future. First, our current convergence theory on RISRO relies on RIP assumption, which may not hold in many scenarios, such as phase retrieval and matrix completion. In this paper, we give some theoretical guarantees of RISRO in phase retrieval with a strong initialization assumption as we discussed in Remark 11. However, such an initialization requirement may be unnecessary and spectral initialization is good enough to guarantee quadratic convergence as we observe in the simulation studies. Also in matrix completion, the analysis will become more delicate as the additional incoherence condition on  $\mathbf{X}^*$  is needed to guarantee recovery. To improve and establish theoretical guarantees for RISRO in phase retrieval and matrix completion, we think some extra properties such as “implicit regularization” (Ma et al., 2019) need to be incorporated in the analysis for RISRO and it is an interesting future work. Also, this paper focuses on the squared error loss in (1), while the other loss functions may be of interest in different settings, such as the  $\ell_1$  loss in robust low-rank matrix recovery (Charisopoulos et al., 2019; Li et al., 2020a,b), which is worth exploring.

## References

Absil, P.-A., Mahony, R., and Sepulchre, R. (2009). *Optimization algorithms on matrix manifolds*. Princeton University Press.

Absil, P.-A. and Malick, J. (2012). Projection-like retractions on matrix manifolds. *SIAM Journal on Optimization*, 22(1):135–158.

Ahmed, A., Recht, B., and Romberg, J. (2013). Blind deconvolution using convex programming. *IEEE Transactions on Information Theory*, 60(3):1711–1732.

Bauch, J. and Nadler, B. (2020). Rank  $2r$  iterative least squares: efficient recovery of ill-conditioned low rank matrices from few entries. *to appear, SIAM Journal on the Mathematics of Data Science*.

Bhojanapalli, S., Neyshabur, B., and Srebro, N. (2016). Global optimality of local search for low rank matrix recovery. In *Advances in Neural Information Processing Systems*, pages 3873–3881.

Boumal, N. and Absil, P.-a. (2011). Rtrmc: A Riemannian trust-region method for low-rank matrix completion. In *Advances in neural information processing systems*, pages 406–414.

Breiding, P. and Vannieuwenhoven, N. (2018). Convergence analysis of Riemannian Gauss–Newton methods and its connection with the geometric condition number. *Applied Mathematics Letters*, 78:42–50.

Burer, S. and Monteiro, R. D. (2003). A nonlinear programming algorithm for solving semidefinite programs via low-rank factorization. *Mathematical Programming*, 95(2):329–357.

Burke, J. V. (1985). Descent methods for composite nondifferentiable optimization problems. *Mathematical Programming*, 33(3):260–279.

Cai, T. T. and Zhang, A. (2013). Sharp RIP bound for sparse signal and low-rank matrix recovery. *Applied and Computational Harmonic Analysis*, 35(1):74–93.

Cai, T. T. and Zhang, A. (2014). Sparse representation of a polytope and recovery of sparse signals and low-rank matrices. *IEEE transactions on information theory*, 60(1):122–132.

Cai, T. T. and Zhang, A. (2015). ROP: Matrix recovery via rank-one projections. *The Annals of Statistics*, 43(1):102–138.

Cai, T. T. and Zhang, A. (2018). Rate-optimal perturbation bounds for singular subspaces with applications to high-dimensional statistics. *The Annals of Statistics*, 46(1):60–89.

Cai, T. T. and Zhou, W.-X. (2013). A max-norm constrained minimization approach to 1-bit matrix completion. *The Journal of Machine Learning Research*, 14(1):3619–3647.

Candès, E. J. (2008). The restricted isometry property and its implications for compressed sensing. *Comptes rendus mathematique*, 346(9-10):589–592.

Candès, E. J., Li, X., and Soltanolkotabi, M. (2015). Phase retrieval via Wirtinger flow: Theory and algorithms. *IEEE Transactions on Information Theory*, 61(4):1985–2007.

Candès, E. J. and Plan, Y. (2011). Tight oracle inequalities for low-rank matrix recovery from a minimal number of noisy random measurements. *IEEE Transactions on Information Theory*, 57(4):2342–2359.

Candès, E. J., Strohmer, T., and Voroninski, V. (2013). Phaselift: Exact and stable signal recovery from magnitude measurements via convex programming. *Communications on Pure and Applied Mathematics*, 66(8):1241–1274.

Candès, E. J. and Tao, T. (2010). The power of convex relaxation: Near-optimal matrix completion. *IEEE Transactions on Information Theory*, 56(5):2053–2080.

Charisopoulos, V., Chen, Y., Davis, D., Díaz, M., Ding, L., and Drusvyatskiy, D. (2019). Low-rank matrix recovery with composite optimization: good conditioning and rapid convergence. *arXiv preprint arXiv:1904.10020*.

Chen, Y. and Candès, E. J. (2017). Solving random quadratic systems of equations is nearly as easy as solving linear systems. *Communications on Pure and Applied Mathematics*, 70(5):822–883.

Chen, Y., Chi, Y., and Goldsmith, A. J. (2015). Exact and stable covariance estimation from quadratic sampling via convex programming. *IEEE Transactions on Information Theory*, 61(7):4034–4059.

Chen, Y. and Wainwright, M. J. (2015). Fast low-rank estimation by projected gradient descent: General statistical and algorithmic guarantees. *arXiv preprint arXiv:1509.03025*.

Chi, Y., Lu, Y. M., and Chen, Y. (2019). Nonconvex optimization meets low-rank matrix factorization: An overview. *IEEE Transactions on Signal Processing*, 67(20):5239–5269.

Clarkson, K. L. and Woodruff, D. P. (2017). Low-rank approximation and regression in input sparsity time. *Journal of the ACM (JACM)*, 63(6):54.

Davenport, M. A. and Romberg, J. (2016). An overview of low-rank matrix recovery from incomplete observations. *IEEE Journal of Selected Topics in Signal Processing*, 10(4):608–622.

Dobriban, E. and Liu, S. (2019). Asymptotics for sketching in least squares regression. In *Advances in Neural Information Processing Systems*, pages 3675–3685.

Drineas, P., Magdon-Ismail, M., Mahoney, M. W., and Woodruff, D. P. (2012). Fast approximation of matrix coherence and statistical leverage. *Journal of Machine Learning Research*, 13(Dec):3475–3506.

Duchi, J. C. and Ruan, F. (2019). Solving (most) of a set of quadratic equalities: Composite optimization for robust phase retrieval. *Information and Inference: A Journal of the IMA*, 8(3):471–529.

Fienup, J. R. (1982). Phase retrieval algorithms: a comparison. *Applied optics*, 21(15):2758–2769.

Fornasier, M., Rauhut, H., and Ward, R. (2011). Low-rank matrix recovery via iteratively reweighted least squares minimization. *SIAM Journal on Optimization*, 21(4):1614–1640.

Gao, B. and Xu, Z. (2017). Phaseless recovery using the Gauss–Newton method. *IEEE Transactions on Signal Processing*, 65(22):5885–5896.

Ge, R., Jin, C., and Zheng, Y. (2017). No spurious local minima in nonconvex low rank problems: A unified geometric analysis. In *Proceedings of the 34th International Conference on Machine Learning-Volume 70*, pages 1233–1242. JMLR. org.

Goldfarb, D. and Ma, S. (2011). Convergence of fixed-point continuation algorithms for matrix rank minimization. *Foundations of Computational Mathematics*, 11(2):183–210.

Ha, W., Liu, H., and Barber, R. F. (2020). An equivalence between critical points for rank constraints versus low-rank factorizations. *SIAM Journal on Optimization*, 30(4):2927–2955.

Hardt, M. (2014). Understanding alternating minimization for matrix completion. In *2014 IEEE 55th Annual Symposium on Foundations of Computer Science*, pages 651–660. IEEE.

Huang, W., Absil, P.-A., and Gallivan, K. A. (2017a). Intrinsic representation of tangent vectors and vector transports on matrix manifolds. *Numerische Mathematik*, 136(2):523–543.

Huang, W., Gallivan, K. A., and Zhang, X. (2017b). Solving phaselift by low-rank Riemannian optimization methods for complex semidefinite constraints. *SIAM Journal on Scientific Computing*, 39(5):B840–B859.

Huang, W. and Hand, P. (2018). Blind deconvolution by a steepest descent algorithm on a quotient manifold. *SIAM Journal on Imaging Sciences*, 11(4):2757–2785.

Jain, P., Meka, R., and Dhillon, I. S. (2010). Guaranteed rank minimization via singular value projection. In *Advances in Neural Information Processing Systems*, pages 937–945.

Jain, P., Netrapalli, P., and Sanghavi, S. (2013). Low-rank matrix completion using alternating minimization. In *Proceedings of the forty-fifth annual ACM symposium on Theory of computing*, pages 665–674. ACM.

Jiang, K., Sun, D., and Toh, K.-C. (2014). A partial proximal point algorithm for nuclear norm regularized matrix least squares problems. *Mathematical Programming Computation*, 6(3):281–325.

Keshavan, R. H., Oh, S., and Montanari, A. (2009). Matrix completion from a few entries. In *2009 IEEE International Symposium on Information Theory*, pages 324–328. IEEE.

Koltchinskii, V., Lounici, K., Tsybakov, A. B., et al. (2011). Nuclear-norm penalization and optimal rates for noisy low-rank matrix completion. *The Annals of Statistics*, 39(5):2302–2329.

Kümmerle, C. and Sigl, J. (2018). Harmonic mean iteratively reweighted least squares for low-rank matrix recovery. *The Journal of Machine Learning Research*, 19(1):1815–1863.

Lange, K. (2010). *Numerical analysis for statisticians*. Springer Science & Business Media.

Lee, J. D., Recht, B., Srebro, N., Tropp, J., and Salakhutdinov, R. R. (2010). Practical large-scale optimization for max-norm regularization. In *Advances in Neural Information Processing Systems*, pages 1297–1305.

Lee, J. M. (2013). Smooth manifolds. In *Introduction to Smooth Manifolds*, pages 1–31. Springer.

Lewis, A. S. and Wright, S. J. (2016). A proximal method for composite minimization. *Mathematical Programming*, 158(1-2):501–546.

Li, Q., Zhu, Z., and Tang, G. (2019a). The non-convex geometry of low-rank matrix optimization. *Information and Inference: A Journal of the IMA*, 8(1):51–96.

Li, X., Ling, S., Strohmer, T., and Wei, K. (2019b). Rapid, robust, and reliable blind deconvolution via nonconvex optimization. *Applied and computational harmonic analysis*, 47(3):893–934.

Li, X., Zhu, Z., Man-Cho So, A., and Vidal, R. (2020a). Nonconvex robust low-rank matrix recovery. *SIAM Journal on Optimization*, 30(1):660–686.

Li, Y., Chi, Y., Zhang, H., and Liang, Y. (2020b). Non-convex low-rank matrix recovery with arbitrary outliers via median-truncated gradient descent. *Information and Inference: A Journal of the IMA*, 9(2):289–325.

Luo, Y. and Zhang, A. R. (2020). A schatten- $q$  matrix perturbation theory via perturbation projection error bound. *arXiv preprint arXiv:2008.01312*.

Ma, C., Wang, K., Chi, Y., and Chen, Y. (2019). Implicit regularization in nonconvex statistical estimation: Gradient descent converges linearly for phase retrieval, matrix completion, and blind deconvolution. *Foundations of Computational Mathematics*, pages 1–182.

Mahoney, M. W. (2011). Randomized algorithms for matrices and data. *Foundations and Trends® in Machine Learning*, 3(2):123–224.

Meyer, G., Bonnabel, S., and Sepulchre, R. (2011). Linear regression under fixed-rank constraints: a Riemannian approach. In *Proceedings of the 28th international conference on machine learning*.

Miao, W., Pan, S., and Sun, D. (2016). A rank-corrected procedure for matrix completion with fixed basis coefficients. *Mathematical Programming*, 159(1):289–338.

Mishra, B., Meyer, G., Bonnabel, S., and Sepulchre, R. (2014). Fixed-rank matrix factorizations and Riemannian low-rank optimization. *Computational Statistics*, 29(3-4):591–621.

Mohan, K. and Fazel, M. (2012). Iterative reweighted algorithms for matrix rank minimization. *The Journal of Machine Learning Research*, 13(1):3441–3473.

Netrapalli, P., Jain, P., and Sanghavi, S. (2013). Phase retrieval using alternating minimization. In *Advances in Neural Information Processing Systems*, pages 2796–2804.

Nocedal, J. and Wright, S. (2006). *Numerical optimization*. Springer Science & Business Media.

Park, D., Kyriolidis, A., Caramanis, C., and Sanghavi, S. (2018). Finding low-rank solutions via nonconvex matrix factorization, efficiently and provably. *SIAM Journal on Imaging Sciences*, 11(4):2165–2204.

Pilanci, M. and Wainwright, M. J. (2016). Iterative Hessian sketch: Fast and accurate solution approximation for constrained least-squares. *The Journal of Machine Learning Research*, 17(1):1842–1879.

Pilanci, M. and Wainwright, M. J. (2017). Newton sketch: A near linear-time optimization algorithm with linear-quadratic convergence. *SIAM Journal on Optimization*, 27(1):205–245.

Raskutti, G. and Mahoney, M. W. (2016). A statistical perspective on randomized sketching for ordinary least-squares. *The Journal of Machine Learning Research*, 17(1):7508–7538.

Recht, B., Fazel, M., and Parrilo, P. A. (2010). Guaranteed minimum-rank solutions of linear matrix equations via nuclear norm minimization. *SIAM review*, 52(3):471–501.

Sanghavi, S., Ward, R., and White, C. D. (2017). The local convexity of solving systems of quadratic equations. *Results in Mathematics*, 71(3-4):569–608.

Shechtman, Y., Eldar, Y. C., Cohen, O., Chapman, H. N., Miao, J., and Segev, M. (2015). Phase retrieval with application to optical imaging: a contemporary overview. *IEEE signal processing magazine*, 32(3):87–109.

Song, Z., Woodruff, D. P., and Zhong, P. (2017). Low rank approximation with entrywise  $l_1$ -norm error. In *Proceedings of the 49th Annual ACM SIGACT Symposium on Theory of Computing*, pages 688–701. ACM.

Sun, J., Qu, Q., and Wright, J. (2018). A geometric analysis of phase retrieval. *Foundations of Computational Mathematics*, 18(5):1131–1198.

Sun, R. and Luo, Z.-Q. (2015). Guaranteed matrix completion via nonconvex factorization. In *Foundations of Computer Science (FOCS), 2015 IEEE 56th Annual Symposium on*, pages 270–289. IEEE.

Tanner, J. and Wei, K. (2013). Normalized iterative hard thresholding for matrix completion. *SIAM Journal on Scientific Computing*, 35(5):S104–S125.

Toh, K.-C. and Yun, S. (2010). An accelerated proximal gradient algorithm for nuclear norm regularized linear least squares problems. *Pacific Journal of Optimization*, 6(615-640):15.

Tong, T., Ma, C., and Chi, Y. (2020). Low-rank matrix recovery with scaled subgradient methods: Fast and robust convergence without the condition number. *arXiv preprint arXiv:2010.13364*.

Tran-Dinh, Q. and Zhang, Z. (2016). Extended Gauss-Newton and Gauss-Newton-ADMM algorithms for low-rank matrix optimization. *arXiv preprint arXiv:1606.03358*.

Tu, S., Boczar, R., Simchowitz, M., Soltanolkotabi, M., and Recht, B. (2016). Low-rank solutions of linear matrix equations via Procrustes flow. In *International Conference on Machine Learning*, pages 964–973.

Uschmajew, A. and Vandeheycken, B. (2018). On critical points of quadratic low-rank matrix optimization problems. *IMA Journal of Numerical Analysis*.

Vandereycken, B. (2013). Low-rank matrix completion by Riemannian optimization. *SIAM Journal on Optimization*, 23(2):1214–1236.

Vandereycken, B. and Vandewalle, S. (2010). A Riemannian optimization approach for computing low-rank solutions of lyapunov equations. *SIAM Journal on Matrix Analysis and Applications*, 31(5):2553–2579.

Vershynin, R. (2010). Introduction to the non-asymptotic analysis of random matrices. *arXiv preprint arXiv:1011.3027*.

Waldspurger, I., d’Aspremont, A., and Mallat, S. (2015). Phase recovery, maxcut and complex semidefinite programming. *Mathematical Programming*, 149(1-2):47–81.

Wang, G., Giannakis, G. B., and Eldar, Y. C. (2017a). Solving systems of random quadratic equations via truncated amplitude flow. *IEEE Transactions on Information Theory*, 64(2):773–794.

Wang, J., Lee, J. D., Mahdavi, M., Kolar, M., Srebro, N., et al. (2017b). Sketching meets random projection in the dual: A provable recovery algorithm for big and high-dimensional data. *Electronic Journal of Statistics*, 11(2):4896–4944.

Wang, L., Zhang, X., and Gu, Q. (2017c). A unified computational and statistical framework for nonconvex low-rank matrix estimation. In *Artificial Intelligence and Statistics*, pages 981–990.

Wei, K., Cai, J.-F., Chan, T. F., and Leung, S. (2016). Guarantees of Riemannian optimization for low rank matrix recovery. *SIAM Journal on Matrix Analysis and Applications*, 37(3):1198–1222.

Wen, Z., Yin, W., and Zhang, Y. (2012). Solving a low-rank factorization model for matrix completion by a nonlinear successive over-relaxation algorithm. *Mathematical Programming Computation*, 4(4):333–361.

Woodruff, D. P. (2014). Sketching as a tool for numerical linear algebra. *Foundations and Trends® in Theoretical Computer Science*, 10(1–2):1–157.

Zhang, A. R., Luo, Y., Raskutti, G., and Yuan, M. (2020). ISLET: Fast and optimal low-rank tensor regression via importance sketching. *SIAM Journal on Mathematics of Data Science*, 2(2):444–479.

Zhang, R. Y., Sojoudi, S., and Lavaei, J. (2019). Sharp restricted isometry bounds for the inexistence of spurious local minima in nonconvex matrix recovery. *Journal of Machine Learning Research*, 20(114):1–34.

Zhao, T., Wang, Z., and Liu, H. (2015). A nonconvex optimization framework for low rank matrix estimation. In *Advances in Neural Information Processing Systems*, pages 559–567.

Zheng, Q. and Lafferty, J. (2015). A convergent gradient descent algorithm for rank minimization and semidefinite programming from random linear measurements. In *Advances in Neural Information Processing Systems*, pages 109–117.

Zheng, Y., Liu, G., Sugimoto, S., Yan, S., and Okutomi, M. (2012). Practical low-rank matrix approximation under robust  $l_1$ -norm. In *2012 IEEE Conference on Computer Vision and Pattern Recognition*, pages 1410–1417. IEEE.

Zhou, G., Huang, W., Gallivan, K. A., Van Dooren, P., and Absil, P.-A. (2016). A Riemannian rank-adaptive method for low-rank optimization. *Neurocomputing*, 192:72–80.

Zhu, Z., Li, Q., Tang, G., and Wakin, M. B. (2018). Global optimality in low-rank matrix optimization. *IEEE Transactions on Signal Processing*, 66(13):3614–3628.

## 9 Proof of the Main Results in the Paper

**Proof of Lemma 1.** First by the decomposition of (6), we have

$$\mathbf{y} = \mathcal{A}\mathcal{L}_t \begin{pmatrix} \tilde{\mathbf{B}}^t & \tilde{\mathbf{D}}_2^{t\top} \\ \tilde{\mathbf{D}}_1^t & \mathbf{0} \end{pmatrix} + \boldsymbol{\epsilon}^t. \quad (38)$$

In view of (10), if the operator  $\mathcal{L}_t^* \mathcal{A}^* \mathcal{A} \mathcal{L}_t$  is invertible, the output of least squares in (5) satisfies

$$\begin{bmatrix} \mathbf{B}^{t+1} & \mathbf{D}_2^{t+1\top} \\ \mathbf{D}_1^{t+1} & \mathbf{0} \end{bmatrix} = (\mathcal{L}_t^* \mathcal{A}^* \mathcal{A} \mathcal{L}_t)^{-1} \mathcal{L}_t^* \mathcal{A}^* \mathbf{y} = \begin{bmatrix} \tilde{\mathbf{B}}^t & \tilde{\mathbf{D}}_2^{t\top} \\ \tilde{\mathbf{D}}_1^t & \mathbf{0} \end{bmatrix} + (\mathcal{L}_t^* \mathcal{A}^* \mathcal{A} \mathcal{L}_t)^{-1} \mathcal{L}_t^* \mathcal{A}^* \boldsymbol{\epsilon}^t,$$

where the second equality is due to (38). This finishes the proof.  $\blacksquare$

**Proof of Lemma 2.** Equation (17) can be directly verified from definitions of  $\mathcal{L}_t$  and  $\mathcal{L}_t^*$  in (9).

The second conclusion holds if  $\mathbf{M}$  is a zero matrix. When  $\mathbf{M}$  is not zero, to prove the claim it is equivalent to show the spectrum of  $\mathcal{L}_t^* \mathcal{A}^* \mathcal{A} \mathcal{L}_t$  is upper and lower bounded by  $1 + R_{2r}$  and  $1 - R_{2r}$ , respectively, in the range of  $\mathcal{L}_t^*$ . Since  $\mathcal{L}_t^* \mathcal{A}^* \mathcal{A} \mathcal{L}_t$  is a symmetric operator, the upper and lower bounds of its spectrum are given below

$$\begin{aligned} \sup_{\mathbf{Z} \in \text{Ran}(\mathcal{L}_t^*): \|\mathbf{Z}\|_F=1} \langle \mathbf{Z}, \mathcal{L}_t^* \mathcal{A}^* \mathcal{A} \mathcal{L}_t(\mathbf{Z}) \rangle &= \sup_{\mathbf{Z} \in \text{Ran}(\mathcal{L}_t^*): \|\mathbf{Z}\|_F=1} \|\mathcal{A} \mathcal{L}_t(\mathbf{Z})\|_2^2 \stackrel{(a)}{\leqslant} 1 + R_{2r} \\ \inf_{\mathbf{Z} \in \text{Ran}(\mathcal{L}_t^*): \|\mathbf{Z}\|_F=1} \langle \mathbf{Z}, \mathcal{L}_t^* \mathcal{A}^* \mathcal{A} \mathcal{L}_t(\mathbf{Z}) \rangle &= \inf_{\mathbf{Z} \in \text{Ran}(\mathcal{L}_t^*): \|\mathbf{Z}\|_F=1} \|\mathcal{A} \mathcal{L}_t(\mathbf{Z})\|_2^2 \stackrel{(b)}{\geqslant} 1 - R_{2r}. \end{aligned}$$

Here (a) and (b) are due to the RIP condition of  $\mathcal{A}$ ,  $\mathcal{L}_t(\mathbf{Z})$  is a at most rank  $2r$  matrix by the definition of  $\mathcal{L}_t$  and (17). This finishes the proof.  $\blacksquare$

**Proof of Proposition 1.** Since  $\mathcal{A}$  satisfies 3r-RIP,  $R_{2r} \leqslant R_{3r} < 1$ . Then, by Lemma 2,  $\mathcal{L}_t^* \mathcal{A}^* \mathcal{A} \mathcal{L}_t$  is invertible over  $\text{Ran}(\mathcal{L}_t^*)$ . With a slight abuse of notation, define  $P_{\mathbf{X}^t}$  as

$$P_{\mathbf{X}^t}(\mathbf{Z}) := \mathcal{L}_t \mathcal{L}_t^*(\mathbf{Z}) = P_{\mathbf{U}^t} \mathbf{Z} P_{\mathbf{V}^t} + P_{\mathbf{U}_\perp^t} \mathbf{Z} P_{\mathbf{V}^t} + P_{\mathbf{U}^t} \mathbf{Z} P_{\mathbf{V}_\perp^t}, \quad \forall \mathbf{Z} \in \mathbb{R}^{p_1 \times p_2}, \quad (39)$$

where  $\mathbf{U}^t, \mathbf{V}^t$  are the updated sketching matrices at iteration  $t$  defined in Step 7 of Algorithm 1. We can verify  $P_{\mathbf{X}^t}$  is an orthogonal projector. Let  $P_{(\mathbf{X}^t)_\perp}(\mathbf{Z}) := \mathbf{Z} - P_{\mathbf{X}^t}(\mathbf{Z}) = P_{\mathbf{U}_\perp^t} \mathbf{Z} P_{\mathbf{V}_\perp^t}$ . Recall  $\boldsymbol{\epsilon}^t = \mathcal{A}(P_{\mathbf{U}_\perp^t} \bar{\mathbf{X}} P_{\mathbf{V}_\perp^t}) + \bar{\boldsymbol{\epsilon}} = \mathcal{A}P_{(\mathbf{X}^t)_\perp}(\bar{\mathbf{X}}) + \bar{\boldsymbol{\epsilon}}$  from (6), we have

$$\begin{aligned} & \|(\mathcal{L}_t^* \mathcal{A}^* \mathcal{A} \mathcal{L}_t)^{-1} \mathcal{L}_t^* \mathcal{A}^* \boldsymbol{\epsilon}^t\|_F^2 \\ & \stackrel{(a)}{\leqslant} \frac{1}{(1 - R_{2r})^2} \|\mathcal{L}_t^* \mathcal{A}^* (\mathcal{A}(P_{(\mathbf{X}^t)_\perp} \bar{\mathbf{X}}) + \bar{\boldsymbol{\epsilon}})\|_F^2 \\ & = \frac{1}{(1 - R_{2r})^2} \left( \overbrace{\|\mathcal{L}_t^* \mathcal{A}^* \mathcal{A}(P_{(\mathbf{X}^t)_\perp} \bar{\mathbf{X}})\|_F^2}^{(1)} + \overbrace{\|\mathcal{L}_t^* \mathcal{A}^* (\bar{\boldsymbol{\epsilon}})\|_F^2}^{(2)} + \overbrace{2 \langle \mathcal{L}_t^* \mathcal{A}^* \mathcal{A} P_{(\mathbf{X}^t)_\perp} \bar{\mathbf{X}}, \mathcal{L}_t^* \mathcal{A}^* (\bar{\boldsymbol{\epsilon}}) \rangle}^{(3)} \right), \end{aligned} \quad (40)$$

where (a) is due to Lemma 2 and the definition of  $\boldsymbol{\epsilon}^t$ .

Notice term (2) is the target term we want, next we bound (1) and (3) at the right hand side of (40).

**Bound for (1).**

$$\begin{aligned}
\|\mathcal{L}_t^* \mathcal{A}^* \mathcal{A}(P_{(\mathbf{X}^t)_\perp} \bar{\mathbf{X}})\|_F^2 &= \langle \mathcal{L}_t^* \mathcal{A}^* \mathcal{A}(P_{(\mathbf{X}^t)_\perp} \bar{\mathbf{X}}), \mathcal{L}_t^* \mathcal{A}^* \mathcal{A}(P_{(\mathbf{X}^t)_\perp} \bar{\mathbf{X}}) \rangle \\
&= \langle \mathcal{A}(P_{(\mathbf{X}^t)_\perp} \bar{\mathbf{X}}), \mathcal{A}P_{\mathbf{X}^t} \mathcal{A}^* \mathcal{A}(P_{(\mathbf{X}^t)_\perp} \bar{\mathbf{X}}) \rangle \\
&\stackrel{(a)}{\leq} R_{3r} \|P_{(\mathbf{X}^t)_\perp} \bar{\mathbf{X}}\|_F \|P_{\mathbf{X}^t} \mathcal{A}^* \mathcal{A}(P_{(\mathbf{X}^t)_\perp} \bar{\mathbf{X}})\|_F \\
&= R_{3r} \|P_{(\mathbf{X}^t)_\perp} \bar{\mathbf{X}}\|_F \|\mathcal{L}_t^* \mathcal{A}^* \mathcal{A}(P_{(\mathbf{X}^t)_\perp} \bar{\mathbf{X}})\|_F,
\end{aligned} \tag{41}$$

where (a) is due to the Lemma 8 and the fact that  $\langle P_{(\mathbf{X}^t)_\perp} \bar{\mathbf{X}}, P_{\mathbf{X}^t} \mathcal{A}^* \mathcal{A}P_{(\mathbf{X}^t)_\perp} \bar{\mathbf{X}} \rangle = 0$ ,  $\text{rank}(P_{(\mathbf{X}^t)_\perp} \bar{\mathbf{X}}) \leq r$  and  $\text{rank}(P_{\mathbf{X}^t} \mathcal{A}^* \mathcal{A}P_{(\mathbf{X}^t)_\perp} \bar{\mathbf{X}}) \leq 2r$ . Note that

$$\begin{aligned}
P_{(\mathbf{X}^t)_\perp} \bar{\mathbf{X}} &= \bar{\mathbf{X}} - P_{\mathbf{X}^t} \bar{\mathbf{X}} \\
&\stackrel{(a)}{=} P_{\bar{\mathbf{U}}} \bar{\mathbf{X}} + \bar{\mathbf{X}} P_{\bar{\mathbf{V}}} - P_{\bar{\mathbf{U}}} \bar{\mathbf{X}} P_{\bar{\mathbf{V}}} - P_{\mathbf{U}^t} \bar{\mathbf{X}} - \bar{\mathbf{X}} P_{\mathbf{V}^t} + P_{\mathbf{U}^t} \bar{\mathbf{X}} P_{\mathbf{V}^t} \\
&= (P_{\bar{\mathbf{U}}} - P_{\mathbf{U}^t}) \bar{\mathbf{X}} + \bar{\mathbf{X}} (P_{\bar{\mathbf{V}}} - P_{\mathbf{V}^t}) - P_{\bar{\mathbf{U}}} \bar{\mathbf{X}} P_{\bar{\mathbf{V}}} + P_{\bar{\mathbf{U}}} \bar{\mathbf{X}} P_{\mathbf{V}^t} - P_{\bar{\mathbf{U}}} \bar{\mathbf{X}} P_{\mathbf{V}^t} + P_{\mathbf{U}^t} \bar{\mathbf{X}} P_{\mathbf{V}^t} \\
&= (P_{\bar{\mathbf{U}}} - P_{\mathbf{U}^t}) \bar{\mathbf{X}} (\mathbf{I} - P_{\mathbf{V}^t}) + (\mathbf{I} - P_{\bar{\mathbf{U}}}) \bar{\mathbf{X}} (P_{\bar{\mathbf{V}}} - P_{\mathbf{V}^t}) \\
&\stackrel{(b)}{=} (P_{\bar{\mathbf{U}}} - P_{\mathbf{U}^t}) \bar{\mathbf{X}} (\mathbf{I} - P_{\mathbf{V}^t}) \\
&\stackrel{(c)}{=} (P_{\bar{\mathbf{U}}} - P_{\mathbf{U}^t}) (\bar{\mathbf{X}} - \mathbf{X}^t) (\mathbf{I} - P_{\mathbf{V}^t}),
\end{aligned} \tag{42}$$

where  $\bar{\mathbf{U}}, \bar{\mathbf{V}}$  are left and right singular vectors of  $\bar{\mathbf{X}}$ , (a) is because  $\bar{\mathbf{X}} = P_{\bar{\mathbf{U}}} \bar{\mathbf{X}} + \bar{\mathbf{X}} P_{\bar{\mathbf{V}}} - P_{\bar{\mathbf{U}}} \bar{\mathbf{X}} P_{\bar{\mathbf{V}}}$ , (b) is due to the fact that  $(\mathbf{I} - P_{\bar{\mathbf{U}}}) \bar{\mathbf{X}} (P_{\bar{\mathbf{V}}} - P_{\mathbf{V}^t}) = 0$  and (c) is because  $\mathbf{X}^t (\mathbf{I} - P_{\mathbf{V}^t}) = 0$ . Now, from (41), we get

$$\begin{aligned}
\|\mathcal{L}_t^* \mathcal{A}^* \mathcal{A}(P_{(\mathbf{X}^t)_\perp} \bar{\mathbf{X}})\|_F &\leq R_{3r} \|P_{(\mathbf{X}^t)_\perp} \bar{\mathbf{X}}\|_F \\
&\stackrel{(a)}{\leq} R_{3r} \|(P_{\bar{\mathbf{U}}} - P_{\mathbf{U}^t}) (\bar{\mathbf{X}} - \mathbf{X}^t) (\mathbf{I} - P_{\mathbf{V}^t})\|_F \\
&\leq R_{3r} \|P_{\bar{\mathbf{U}}} - P_{\mathbf{U}^t}\| \|\bar{\mathbf{X}} - \mathbf{X}^t\|_F \\
&\stackrel{(b)}{\leq} R_{3r} \frac{\|\mathbf{X}^t - \bar{\mathbf{X}}\| \|\mathbf{X}^t - \bar{\mathbf{X}}\|_F}{\sigma_r(\bar{\mathbf{X}})},
\end{aligned} \tag{43}$$

here (a) is due to (42) and (b) is due to the singular subspace perturbation inequality  $\|P_{\bar{\mathbf{U}}} - P_{\mathbf{U}^t}\| \leq \|\mathbf{X}^t - \bar{\mathbf{X}}\|/\sigma_r(\bar{\mathbf{X}})$  obtained from Lemma 9.

**Bound for (3).**

$$\begin{aligned}
2 \langle \mathcal{L}_t^* \mathcal{A}^* \mathcal{A}P_{(\mathbf{X}^t)_\perp} \bar{\mathbf{X}}, \mathcal{L}_t^* \mathcal{A}^* (\bar{\epsilon}) \rangle &= 2 \langle \mathcal{A}P_{(\mathbf{X}^t)_\perp} \bar{\mathbf{X}}, \mathcal{A}P_{\mathbf{X}^t} \mathcal{A}^* (\bar{\epsilon}) \rangle \\
&\stackrel{(a)}{\leq} 2R_{3r} \|P_{(\mathbf{X}^t)_\perp} \bar{\mathbf{X}}\|_F \|\mathcal{L}_t^* \mathcal{A}^* (\bar{\epsilon})\|_F \\
&\stackrel{(b)}{\leq} 2R_{3r} \frac{\|\mathbf{X}^t - \bar{\mathbf{X}}\| \|\mathbf{X}^t - \bar{\mathbf{X}}\|_F}{\sigma_r(\bar{\mathbf{X}})} \|\mathcal{L}_t^* \mathcal{A}^* (\bar{\epsilon})\|_F,
\end{aligned} \tag{44}$$

here (a) and (b) are by the same arguments in (41) and (43), respectively.

Plugging (44) and (43) into (40), we get (18). This finishes the proof of this Proposition.  $\blacksquare$

**Proof of Theorem 1.** First notice that quadratic convergence result follows easily from (20) when we set  $\bar{\epsilon} = 0$ . So the rest of the proof is devoted to prove (20) and we also prove the Q-linear convergence along the way. The proof can be divided into four steps. In Step 1, we use Proposition 1 and give an upper bound for the approximation error in the case  $\bar{\mathbf{X}}$  is a stationary point. Then, we use induction to show the main results in Step 2,3,4. To start, similar as (39), define

$$P_{\bar{\mathbf{X}}}(Z) = P_{\bar{\mathbf{U}}} \mathbf{Z} P_{\bar{\mathbf{V}}} + P_{\bar{\mathbf{U}}_\perp} \mathbf{Z} P_{\bar{\mathbf{V}}} + P_{\bar{\mathbf{U}}} \mathbf{Z} P_{\bar{\mathbf{V}}_\perp}, \quad \forall \mathbf{Z} \in \mathbb{R}^{p_1 \times p_2},$$

where  $\bar{\mathbf{U}}, \bar{\mathbf{V}}$  are left and right singular vectors of  $\bar{\mathbf{X}}$ .

**Step 1.** In this step, we apply Proposition 1 in the case  $\bar{\mathbf{X}}$  is a stationary point. In view of (18), the term that we can simplify is  $\|\mathcal{L}_t^* \mathcal{A}^*(\bar{\epsilon})\|_F$ . Since  $\bar{\mathbf{X}}$  is a stationary point, we know  $P_{\bar{\mathbf{X}}}(\mathcal{A}^*(\bar{\epsilon})) = P_{\bar{\mathbf{X}}}(\mathcal{A}^*(\mathbf{y} - \mathcal{A}(\bar{\mathbf{X}}))) = 0$ . Then

$$\|\mathcal{L}_t^* \mathcal{A}^*(\bar{\epsilon})\|_F^2 = \|P_{\mathbf{X}^t} \mathcal{A}^*(\bar{\epsilon})\|_F^2 = \|(P_{\mathbf{X}^t} - P_{\bar{\mathbf{X}}}) \mathcal{A}^*(\bar{\epsilon})\|_F^2 \leq \|P_{\mathbf{X}^t} - P_{\bar{\mathbf{X}}}\|^2 \|\mathcal{A}^*(\bar{\epsilon})\|_F^2, \quad (45)$$

where the first equality is by the definition of  $P_{\mathbf{X}^t}$  in (39) and equation (17). Meanwhile, it holds that

$$\begin{aligned} \|P_{\mathbf{X}^t} - P_{\bar{\mathbf{X}}}\| &= \sup_{\|\mathbf{Z}\|_F \leq 1} \|(P_{\mathbf{X}^t} - P_{\bar{\mathbf{X}}})(\mathbf{Z})\|_F \\ &\stackrel{(a)}{=} \sup_{\|\mathbf{Z}\|_F \leq 1} \|(P_{\mathbf{U}^t} - P_{\bar{\mathbf{U}}})\mathbf{Z}(\mathbf{I} - P_{\bar{\mathbf{V}}})\|_F + \|(\mathbf{I} - P_{\mathbf{U}^t})\mathbf{Z}(P_{\mathbf{V}^t} - P_{\bar{\mathbf{V}}})\|_F \\ &\stackrel{(b)}{\leq} \sup_{\|\mathbf{Z}\|_F \leq 1} \frac{2\|\mathbf{X}^t - \bar{\mathbf{X}}\|}{\sigma_r(\bar{\mathbf{X}})} \|\mathbf{Z}\|_F \leq \frac{2\|\mathbf{X}^t - \bar{\mathbf{X}}\|}{\sigma_r(\bar{\mathbf{X}})}, \end{aligned}$$

here (a) is because  $(P_{\mathbf{X}^t} - P_{\bar{\mathbf{X}}})(\mathbf{Z}) = (P_{\mathbf{U}^t} - P_{\bar{\mathbf{U}}})\mathbf{Z}(\mathbf{I} - P_{\bar{\mathbf{V}}}) + (\mathbf{I} - P_{\bar{\mathbf{U}}})\mathbf{Z}(P_{\mathbf{V}^t} - P_{\bar{\mathbf{V}}})$  by a similar argument in (42) and (b) is by Lemma 9. Then, from (45), we see that

$$\|\mathcal{L}_t^* \mathcal{A}^*(\bar{\epsilon})\|_F^2 \leq \frac{4\|\mathbf{X}^t - \bar{\mathbf{X}}\|^2}{\sigma_r^2(\bar{\mathbf{X}})} \|\mathcal{A}^*(\bar{\epsilon})\|_F^2,$$

which, together with (18), implies that

$$\begin{aligned} \|(\mathcal{L}_t^* \mathcal{A}^* \mathcal{A} \mathcal{L}_t)^{-1} \mathcal{L}_t^* \mathcal{A}^* \epsilon^t\|_F^2 &\leq \frac{\|\mathbf{X}^t - \bar{\mathbf{X}}\|^2}{(1 - R_{2r})^2 \sigma_r^2(\bar{\mathbf{X}})} \\ &\quad \cdot (R_{3r}^2 \|\mathbf{X}^t - \bar{\mathbf{X}}\|_F^2 + 4\|\mathcal{A}^*(\bar{\epsilon})\|_F^2 + 4R_{3r} \|\mathcal{A}^*(\bar{\epsilon})\|_F \|\mathbf{X}^t - \bar{\mathbf{X}}\|_F). \end{aligned} \quad (46)$$

**Step 2.** In this step, we start using induction to show the convergence of  $\mathbf{X}^t$  in (20). First, we introduce  $\theta_t$  to measure the goodness of the current iterate in terms of subspace estimation:

$$\theta_t = \max\{\|\sin \Theta(\mathbf{U}^t, \bar{\mathbf{U}})\|, \|\sin \Theta(\mathbf{V}^t, \bar{\mathbf{V}})\|\}, \quad (47)$$

where  $\bar{\mathbf{U}}, \bar{\mathbf{V}}$  are the left and right singular vectors of  $\bar{\mathbf{X}}$  and here  $\|\sin \Theta(\mathbf{U}^t, \bar{\mathbf{U}})\| := |\sin(\cos^{-1}(\sigma_r(\mathbf{U}^{t\top} \bar{\mathbf{U}})))|$  measures the largest angle between subspaces  $\mathbf{U}^t, \bar{\mathbf{U}}$ .

Recall the definition of  $\tilde{\mathbf{B}}^t, \tilde{\mathbf{D}}_1^t$  and  $\tilde{\mathbf{D}}_2^t$  in (7). The induction we want to show is: given  $\theta_t \leq 1/2$ ,  $\tilde{\mathbf{B}}^t$  is invertible and  $\|\mathbf{X}^t - \bar{\mathbf{X}}\|_F \leq \|\mathbf{X}^0 - \bar{\mathbf{X}}\|_F$ , we prove  $\theta_{t+1} \leq 1/2$ ,  $\tilde{\mathbf{B}}^{t+1}$  is invertible,  $\|\mathbf{X}^{t+1} - \bar{\mathbf{X}}\|_F \leq \|\mathbf{X}^0 - \bar{\mathbf{X}}\|_F$  as well as  $\mathbf{B}^{t+1}$  is invertible and

$$\begin{aligned} \|\mathbf{X}^{t+1} - \bar{\mathbf{X}}\|_F^2 &\leq 5 \|(\mathcal{L}_t^* \mathcal{A}^* \mathcal{A} \mathcal{L}_t)^{-1} \mathcal{L}_t^* \mathcal{A}^* \epsilon^t\|_F^2 \\ &\leq \frac{5\|\mathbf{X}^t - \bar{\mathbf{X}}\|^2}{(1 - R_{2r})^2 \sigma_r^2(\bar{\mathbf{X}})} (R_{3r}^2 \|\mathbf{X}^t - \bar{\mathbf{X}}\|_F^2 + 4R_{3r} \|\mathcal{A}^*(\bar{\epsilon})\|_F \|\mathbf{X}^t - \bar{\mathbf{X}}\|_F + 4\|\mathcal{A}^*(\bar{\epsilon})\|_F^2) \\ &\leq \frac{9}{16} \|\mathbf{X}^t - \bar{\mathbf{X}}\|_F^2. \end{aligned} \quad (48)$$

For the rest of this step, we show when  $t = 0$ , the induction assumption holds, i.e.  $\theta_0 \leq 1/2$  and  $\tilde{\mathbf{B}}^0$  is invertible. Since  $\frac{\|\mathbf{X}^0 - \bar{\mathbf{X}}\|}{\sigma_r(\bar{\mathbf{X}})} \leq \frac{1}{4}$ , it holds by Lemma 9 that  $\theta_0 = \max\{\|\sin \Theta(\mathbf{U}^0, \bar{\mathbf{U}})\|, \|\sin \Theta(\mathbf{V}^0, \bar{\mathbf{V}})\|\} \leq 2 \frac{\|\mathbf{X}^0 - \bar{\mathbf{X}}\|}{\sigma_r(\bar{\mathbf{X}})} \leq \frac{1}{2}$ . Then, we have

$$\sigma_r(\tilde{\mathbf{B}}^0) \stackrel{(a)}{\geq} \sigma_r(\mathbf{U}^{0\top} \bar{\mathbf{U}}) \sigma_r(\bar{\mathbf{X}}) \sigma_r(\bar{\mathbf{V}}^\top \mathbf{V}^0) \stackrel{(b)}{=} (1 - \theta_0^2) \sigma_r(\bar{\mathbf{X}}) \geq 3/4 \cdot \sigma_r(\bar{\mathbf{X}}) > 0, \quad (49)$$

where (a) is because  $\mathbf{U}^{0\top} \bar{\mathbf{U}}, \bar{\mathbf{X}}, \bar{\mathbf{V}}^\top \mathbf{V}^0$  are all rank  $r$  matrices and (Luo and Zhang, 2020, Lemma 5) and (b) is by the definition of  $\|\sin \Theta(\mathbf{U}^t, \bar{\mathbf{U}})\|$ .

**Step 3.** In this step, we first show given  $\theta_t \leq 1/2$  and  $\|\mathbf{X}^t - \bar{\mathbf{X}}\|_F \leq \|\mathbf{X}^0 - \bar{\mathbf{X}}\|_F$ ,  $\mathbf{B}^{t+1}$  is invertible. Then we also do some preparation to show the main contraction (48). Notice that

$$\begin{aligned}\sigma_r(\mathbf{B}^{t+1}) &\geq \sigma_r(\tilde{\mathbf{B}}^t) - \|\mathbf{B}^{t+1} - \tilde{\mathbf{B}}^t\| \geq \sigma_r(\mathbf{U}^{t\top} \bar{\mathbf{U}}) \sigma_r(\bar{\mathbf{X}}) \sigma_r(\mathbf{V}^{t\top} \bar{\mathbf{V}}) - \|\mathbf{B}^{t+1} - \tilde{\mathbf{B}}^t\| \\ &\geq (1 - \theta_t^2) \sigma_r(\bar{\mathbf{X}}) - \|\mathbf{B}^{t+1} - \tilde{\mathbf{B}}^t\|,\end{aligned}\quad (50)$$

and

$$\begin{aligned}\max\{\|\mathbf{B}^{t+1} - \tilde{\mathbf{B}}^t\|, \|\mathbf{D}_1^{t+1} - \tilde{\mathbf{D}}_1^t\|, \|\mathbf{D}_2^{t+1} - \tilde{\mathbf{D}}_2^t\|\} &\stackrel{(a)}{\leq} \|(\mathcal{L}_t^* \mathcal{A}^* \mathcal{A} \mathcal{L}_t)^{-1} \mathcal{L}_t^* \mathcal{A}^* \epsilon^t\| \\ &\leq \|(\mathcal{L}_t^* \mathcal{A}^* \mathcal{A} \mathcal{L}_t)^{-1} \mathcal{L}_t^* \mathcal{A}^* \epsilon^t\|_F,\end{aligned}\quad (51)$$

where (a) is due to (11).

Under the induction assumption  $\|\mathbf{X}^t - \bar{\mathbf{X}}\|_F \leq \|\mathbf{X}^0 - \bar{\mathbf{X}}\|_F$ , the initialization condition (19) and  $\|\mathcal{A}^*(\bar{\epsilon})\|_F \leq \frac{1-R_{2r}}{4\sqrt{5}} \sigma_r(\bar{\mathbf{X}})$ , we have

$$\frac{R_{3r}^2 \|\mathbf{X}^t - \bar{\mathbf{X}}\|_F^2}{(1 - R_{2r})^2 \sigma_r^2(\bar{\mathbf{X}})} \leq 1/80, \quad \frac{4 \|\mathcal{A}^*(\bar{\epsilon})\|_F^2}{(1 - R_{2r})^2 \sigma_r^2(\bar{\mathbf{X}})} \leq 1/20, \quad \frac{4R_{3r} \|\mathbf{X}^t - \bar{\mathbf{X}}\|_F \|\mathcal{A}^*(\bar{\epsilon})\|_F}{(1 - R_{2r})^2 \sigma_r^2(\bar{\mathbf{X}})} \leq 1/20.$$

By combining these inequalities with (46), we obtain

$$\|(\mathcal{L}_t^* \mathcal{A}^* \mathcal{A} \mathcal{L}_t)^{-1} \mathcal{L}_t^* \mathcal{A}^* \epsilon^t\|_F \leq \frac{3}{4\sqrt{5}} \|\mathbf{X}^0 - \bar{\mathbf{X}}\| \leq \frac{3}{16} \sigma_r(\bar{\mathbf{X}}).$$

Thus, from (51) we have

$$\max\{\|\mathbf{B}^{t+1} - \tilde{\mathbf{B}}^t\|, \|\mathbf{D}_1^{t+1} - \tilde{\mathbf{D}}_1^t\|, \|\mathbf{D}_2^{t+1} - \tilde{\mathbf{D}}_2^t\|\} \leq \frac{3}{16} \sigma_r(\bar{\mathbf{X}}), \quad (52)$$

and  $\sigma_r(\mathbf{B}^{t+1}) \geq \frac{9}{16} \sigma_r(\bar{\mathbf{X}}) > 0$  because of (50). This shows the invertibility of  $\mathbf{B}^{t+1}$ .

With the invertibility of  $\mathbf{B}^{t+1}$ , we also introduce  $\rho_{t+1}$  to measure the goodness of the current iterate in the following way

$$\rho_{t+1} = \max\{\|\mathbf{D}_1^{t+1}(\mathbf{B}^{t+1})^{-1}\|, \|(\mathbf{B}^{t+1})^{-1} \mathbf{D}_2^{t+1\top}\|\}. \quad (53)$$

Notice  $\tilde{\mathbf{D}}_1^t(\tilde{\mathbf{B}}^t)^{-1} = \mathbf{U}_\perp^{t\top} \bar{\mathbf{X}} \mathbf{V}^t (\mathbf{U}^{t\top} \bar{\mathbf{X}} \mathbf{V}^t)^{-1} = \mathbf{U}_\perp^{t\top} \bar{\mathbf{U}} (\mathbf{U}^{t\top} \bar{\mathbf{U}})^{-1}$ , so

$$\|\tilde{\mathbf{D}}_1^t(\tilde{\mathbf{B}}^t)^{-1}\| \leq \|\mathbf{U}_\perp^{t\top} \bar{\mathbf{U}}\| \|(\mathbf{U}^{t\top} \bar{\mathbf{U}})^{-1}\| \stackrel{(a)}{=} \frac{\|\sin \Theta(\mathbf{U}^t, \bar{\mathbf{U}})\|}{\sqrt{1 - \|\sin \Theta(\mathbf{U}^t, \bar{\mathbf{U}})\|^2}} \stackrel{(b)}{\leq} \frac{\theta_t}{\sqrt{1 - \theta_t^2}}, \quad (54)$$

where (a) is due to the  $\sin \Theta$  property in Lemma 1 of Cai and Zhang (2018) and (b) is due to (47). The same bound also holds for  $\|(\tilde{\mathbf{B}}^t)^{-1} \tilde{\mathbf{D}}_2^{t\top}\|$ . Meanwhile, it holds that

$$\begin{aligned}\|\mathbf{D}_1^{t+1}(\mathbf{B}^{t+1})^{-1}\| &\leq \|(\mathbf{D}_1^{t+1} - \tilde{\mathbf{D}}_1^t)(\mathbf{B}^{t+1})^{-1}\| + \|\tilde{\mathbf{D}}_1^t(\mathbf{B}^{t+1})^{-1}\| \\ &\stackrel{(a)}{\leq} \frac{\|\mathbf{D}_1^{t+1} - \tilde{\mathbf{D}}_1^t\|}{\sigma_r(\mathbf{B}^{t+1})} + \|\tilde{\mathbf{D}}_1^t(\tilde{\mathbf{B}}^t)^{-1}\| + \|\tilde{\mathbf{D}}_1^t(\tilde{\mathbf{B}}^t)^{-1}(\mathbf{B}^{t+1} - \tilde{\mathbf{B}}^t)(\mathbf{B}^{t+1})^{-1}\| \\ &\stackrel{(b)}{\leq} \frac{\|\mathbf{D}_1^{t+1} - \tilde{\mathbf{D}}_1^t\|}{\sigma_r(\mathbf{B}^{t+1})} + \frac{\theta_t}{\sqrt{1 - \theta_t^2}} + \frac{\theta_t}{\sqrt{1 - \theta_t^2}} \frac{\|\mathbf{B}^{t+1} - \tilde{\mathbf{B}}^t\|}{\sigma_r(\mathbf{B}^{t+1})},\end{aligned}\quad (55)$$

where (a) is because  $(\mathbf{B}^{t+1})^{-1} = (\tilde{\mathbf{B}}^t)^{-1} - (\tilde{\mathbf{B}}^t)^{-1}(\mathbf{B}^{t+1} - \tilde{\mathbf{B}}^t)(\mathbf{B}^{t+1})^{-1}$  and (b) is due to the bound for  $\|\tilde{\mathbf{D}}_1^t(\tilde{\mathbf{B}}^t)^{-1}\|$  in (54). We can also bound  $\|(\mathbf{B}^{t+1})^{-1}\mathbf{D}_2^{t+1\top}\|$  in a similar way.

Thus, by plugging  $\sigma_r(\mathbf{B}^{t+1}) \geq \frac{9}{16}\sigma_r(\bar{\mathbf{X}})$ ,  $\theta_t \leq 1/2$  and the upper bound in (52) into (55), we have

$$\rho_{t+1} \leq \frac{1}{3} + \frac{1}{\sqrt{3}} + \frac{1}{3\sqrt{3}} \leq \frac{4 + \sqrt{3}}{3\sqrt{3}}.$$

**Step 4.** In the last step, we show the contraction inequality (48). Note from Lemma 9 that  $\theta_t$  decreases as  $\|\mathbf{X}^t - \bar{\mathbf{X}}\|_F$  decreases. So after we show the contraction of  $\|\mathbf{X}^{t+1} - \bar{\mathbf{X}}\|_F$ , it automatically implies that  $\theta_{t+1} \leq 1/2$ , which, together with similar arguments in (49), further guarantees the invertibility of  $\tilde{\mathbf{B}}^{t+1}$ .

Since  $\bar{\mathbf{X}}$  is a rank  $r$  matrix and  $\tilde{\mathbf{B}}^t, \mathbf{B}^{t+1}$  are invertible, a quick calculation asserts  $\tilde{\mathbf{D}}_1^t(\tilde{\mathbf{B}}^t)^{-1}\tilde{\mathbf{D}}_2^{t\top} = \mathbf{U}_\perp^{t\top}\bar{\mathbf{X}}\mathbf{V}_\perp^{t\top}$ . Therefore,

$$\begin{aligned}\bar{\mathbf{X}} &= [\mathbf{U}^t \quad \mathbf{U}_\perp^t][\mathbf{U}^t \quad \mathbf{U}_\perp^t]^\top \bar{\mathbf{X}} [\mathbf{V}^t \quad \mathbf{V}_\perp^t][\mathbf{V}^t \quad \mathbf{V}_\perp^t]^\top \\ &= [\mathbf{U}^t \quad \mathbf{U}_\perp^t] \begin{bmatrix} \tilde{\mathbf{B}}^t & \tilde{\mathbf{D}}_2^{t\top} \\ \tilde{\mathbf{D}}_1^t & \tilde{\mathbf{D}}_1^t(\tilde{\mathbf{B}}^t)^{-1}\tilde{\mathbf{D}}_2^{t\top} \end{bmatrix} [\mathbf{V}^t \quad \mathbf{V}_\perp^t]^\top.\end{aligned}$$

At the same time, it is easy to check

$$\mathbf{X}^{t+1} = \mathbf{X}_U^{t+1}(\mathbf{B}^{t+1})^{-1}\mathbf{X}_V^{t+1\top} = [\mathbf{U}^t \quad \mathbf{U}_\perp^t] \begin{bmatrix} \mathbf{B}^{t+1} & \mathbf{D}_2^{t+1\top} \\ \mathbf{D}_1^{t+1} & \mathbf{D}_1^{t+1}(\mathbf{B}^{t+1})^{-1}\mathbf{D}_2^{t+1\top} \end{bmatrix} [\mathbf{V}^t \quad \mathbf{V}_\perp^t]^\top.$$

So

$$\|\mathbf{X}^{t+1} - \bar{\mathbf{X}}\|_F^2 = \left\| \begin{bmatrix} \mathbf{B}^{t+1} - \tilde{\mathbf{B}}^t & \mathbf{D}_2^{t+1\top} - \tilde{\mathbf{D}}_2^{t\top} \\ \mathbf{D}_1^{t+1} - \tilde{\mathbf{D}}_1^t & \Delta^{t+1} \end{bmatrix} \right\|_F^2, \quad (56)$$

where  $\Delta^{t+1} = \mathbf{D}_1^{t+1}(\mathbf{B}^{t+1})^{-1}\mathbf{D}_2^{t+1\top} - \tilde{\mathbf{D}}_1^t(\tilde{\mathbf{B}}^t)^{-1}\tilde{\mathbf{D}}_2^{t\top}$ . Recall that (12) gives a precise error characterization for  $\|\mathbf{B}^{t+1} - \tilde{\mathbf{B}}^t\|_F^2 + \sum_{k=1}^2 \|\mathbf{D}_k^{t+1} - \tilde{\mathbf{D}}_k^t\|_F^2$ . Hence, to bound  $\|\mathbf{X}^{t+1} - \bar{\mathbf{X}}\|_F^2$  from (56), we only need to obtain an upper bound of  $\|\Delta^{t+1}\|_F^2$ .

Combining (53), (54) and Lemma 7, we have

$$\|\Delta^{t+1}\|_F \leq \rho_{t+1}\|\mathbf{D}_1^{t+1} - \tilde{\mathbf{D}}_1^t\|_F + \frac{\theta_t}{\sqrt{1-\theta_t^2}}\|\mathbf{D}_2^{t+1} - \tilde{\mathbf{D}}_2^t\|_F + \frac{\theta_t\rho_{t+1}}{\sqrt{1-\theta_t^2}}\|\mathbf{B}^{t+1} - \tilde{\mathbf{B}}^t\|_F.$$

Moreover, since  $(a+b+c)^2 \leq 3(a^2 + b^2 + c^2)$  and (12), it holds that

$$\|\Delta^{t+1}\|_F^2 \leq 3(\rho_{t+1} \vee \frac{\theta_t}{\sqrt{1-\theta_t^2}} \vee \frac{\theta_t\rho_{t+1}}{\sqrt{1-\theta_t^2}})^2 \|(\mathcal{L}_t^* \mathcal{A}^* \mathcal{A} \mathcal{L}_t)^{-1} \mathcal{L}_t^* \mathcal{A}^* \epsilon^t\|_F^2. \quad (57)$$

In summary, combining (56), (12) and (57), we get

$$\|\mathbf{X}^{t+1} - \bar{\mathbf{X}}\|_F^2 \leq (1 + 3(\rho_{t+1} \vee \frac{\theta_t}{\sqrt{1-\theta_t^2}} \vee \frac{\theta_t\rho_{t+1}}{\sqrt{1-\theta_t^2}})^2) \|(\mathcal{L}_t^* \mathcal{A}^* \mathcal{A} \mathcal{L}_t)^{-1} \mathcal{L}_t^* \mathcal{A}^* \epsilon^t\|_F^2. \quad (58)$$

Plugging in the upper bounds for  $\theta_t$  and  $\rho_{t+1}$ , we have  $1 + 3(\rho_{t+1} \vee \frac{\theta_t}{\sqrt{1-\theta_t^2}} \vee \frac{\theta_t\rho_{t+1}}{\sqrt{1-\theta_t^2}})^2 \leq 5$ , and thus

$$\begin{aligned}\|\mathbf{X}^{t+1} - \bar{\mathbf{X}}\|_F^2 &\leq 5 \|(\mathcal{L}_t^* \mathcal{A}^* \mathcal{A} \mathcal{L}_t)^{-1} \mathcal{L}_t^* \mathcal{A}^* \epsilon^t\|_F^2 \\ &\stackrel{(a)}{\leq} \frac{5\|\mathbf{X}^t - \bar{\mathbf{X}}\|^2}{(1 - R_{2r})^2 \sigma_r^2(\bar{\mathbf{X}})} (R_{3r}^2 \|\mathbf{X}^t - \bar{\mathbf{X}}\|_F^2 + 4\|\mathcal{A}^*(\bar{\epsilon})\|_F^2 + 4R_{3r}\|\mathcal{A}^*(\bar{\epsilon})\|_F \|\mathbf{X}^t - \bar{\mathbf{X}}\|_F) \\ &\stackrel{(b)}{\leq} \frac{9}{16} \|\mathbf{X}^t - \bar{\mathbf{X}}\|_F^2,\end{aligned}$$

where (a) is due to (46) and (b) is because under the initialization condition (19) and  $\|\mathcal{A}^*(\bar{\epsilon})\|_F \leq \frac{1-R_{2r}}{4\sqrt{5}}\sigma_r(\bar{\mathbf{X}})$ , the following inequalities hold

$$\frac{5R_{3r}^2\|\mathbf{X}^t - \bar{\mathbf{X}}\|_F^2}{(1-R_{2r})^2\sigma_r^2(\bar{\mathbf{X}})} \leq 1/16, \quad \frac{20\|\mathcal{A}^*(\bar{\epsilon})\|_F^2}{(1-R_{2r})^2\sigma_r^2(\bar{\mathbf{X}})} \leq 1/4, \quad \frac{20R_{3r}\|\mathbf{X}^t - \bar{\mathbf{X}}\|_F\|\mathcal{A}^*(\bar{\epsilon})\|_F}{(1-R_{2r})^2\sigma_r^2(\bar{\mathbf{X}})} \leq 1/4.$$

This completes the induction and finishes the proof of this theorem.  $\blacksquare$

**Proof of Theorem 2.** In view of the Riemannian Gauss-Newton equation in (29), to prove the claim, we only need to show

$$P_{T_{\mathbf{X}^t}}(\mathcal{A}^*(\mathcal{A}(\eta^t + \mathbf{X}^t) - \mathbf{y})) = 0. \quad (59)$$

From the optimality condition of the least squares problem (10), we know that  $\mathbf{B}^{t+1}$ ,  $\mathbf{D}_1^{t+1}$  and  $\mathbf{D}_2^{t+1}$  obtained in (5) satisfy

$$\mathcal{L}_t^*\mathcal{A}^*(\mathcal{A}\mathcal{L}_t \begin{bmatrix} \mathbf{B}^{t+1} & (\mathbf{D}_2^{t+1})^\top \\ \mathbf{D}_1^{t+1} & \mathbf{0} \end{bmatrix} - \mathbf{y}) = 0. \quad (60)$$

Then, the updating formula in (23), together with the definition of  $\mathcal{L}_t$ , implies that

$$\eta^t + \mathbf{X}^t = \mathcal{L}_t \begin{bmatrix} \mathbf{B}^{t+1} & (\mathbf{D}_2^{t+1})^\top \\ \mathbf{D}_1^{t+1} & \mathbf{0} \end{bmatrix}. \quad (61)$$

Hence, (60) implies  $\mathcal{L}_t^*\mathcal{A}^*(\mathcal{A}(\eta^t + \mathbf{X}^t) - \mathbf{y}) = 0$ . Note from the proof of Theorem 1 that for all  $t \geq 1$ ,  $\mathbf{B}^t$  is invertible. Then, it is not difficult to verify that  $\mathbf{U}^t, \mathbf{V}^t$  are orthonormal bases of the column and row spans of  $\mathbf{X}^t$  and  $P_{T_{\mathbf{X}^t}} = \mathcal{L}_t\mathcal{L}_t^*$  for all  $t \geq 0$ . We thus proved (59).  $\blacksquare$

**Proof of Proposition 3.** We compute the inner product between the update direction  $\eta^t$  in (23) and the Riemannian gradient:

$$\begin{aligned} \langle \text{grad}f(\mathbf{X}^t), \eta^t \rangle &= \langle P_{T_{\mathbf{X}^t}}\mathcal{A}^*(\mathcal{A}(\mathbf{X}^t) - \mathbf{y}), \eta^t \rangle \\ &\stackrel{(a)}{=} \langle -P_{T_{\mathbf{X}^t}}\mathcal{A}^*\mathcal{A}\eta^t, \eta^t \rangle \\ &\stackrel{(b)}{=} -\langle \mathcal{A}^*\mathcal{A}\eta^t, \eta^t \rangle = -\|\mathcal{A}(\eta^t)\|_2^2, \end{aligned}$$

here (a) is due to (59) and (b) is because  $\eta^t$  lies in  $T_{\mathbf{X}^t}\mathcal{M}_r$ . With this, we conclude the update direction  $\eta^t$  has negative inner product with the Riemannian gradient unless it is 0. Thus the update  $\eta^t$  is a descent direction.

If  $\mathcal{A}$  satisfies the  $2r$ -RIP, by similar arguments as in Lemma 2, we see that  $P_{T_{\mathbf{X}^t}}\mathcal{A}^*\mathcal{A}P_{T_{\mathbf{X}^t}}$  is symmetric positive definite over  $T_{\mathbf{X}^t}\mathcal{M}_r$  for all  $t \geq 0$ . Since  $\eta^t$  solves the Riemannian Gauss-Newton equation (29), we know that  $\eta^t = -(P_{T_{\mathbf{X}^t}}\mathcal{A}^*\mathcal{A}P_{T_{\mathbf{X}^t}})^{-1}\text{grad}f(\mathbf{X}^t)$  for all  $t \geq 0$ . For any subsequence  $\{\mathbf{X}^t\}_{t \in \mathcal{K}}$  that converges to a nonstationary point  $\tilde{\mathbf{X}}$ , it is not difficult to show that

$$\lim_{t \rightarrow \infty, t \in \mathcal{K}} P_{T_{\mathbf{X}^t}}\mathcal{A}^*\mathcal{A}P_{T_{\mathbf{X}^t}} = P_{T_{\tilde{\mathbf{X}}}}\mathcal{A}^*\mathcal{A}P_{T_{\tilde{\mathbf{X}}}} \quad \text{and} \quad \tilde{\eta} = \lim_{t \rightarrow \infty, t \in \mathcal{K}} \eta^t = -(P_{T_{\tilde{\mathbf{X}}}}\mathcal{A}^*\mathcal{A}P_{T_{\tilde{\mathbf{X}}}})^{-1}\text{grad}f(\tilde{\mathbf{X}}).$$

Hence,  $\{\eta^t\}_{t \in \mathcal{K}}$  is bounded,  $\tilde{\eta} \neq 0$  and

$$\lim_{t \rightarrow \infty, t \in \mathcal{K}} \langle \text{grad}f(\mathbf{X}^t), \eta^t \rangle = \langle \text{grad}f(\tilde{\mathbf{X}}), \tilde{\eta} \rangle = -\|\mathcal{A}(\tilde{\eta})\|_2^2 \stackrel{(\text{RIP condition})}{\leq} -(1-R_{2r})\|\tilde{\eta}\|_2^2 < 0,$$

i.e., the direction sequence  $\{\eta^t\}$  is gradient related by (Absil et al., 2009, Definition 4.2.1).  $\blacksquare$

**Proof of Theorem 3.** The proof of (34) shares many similar ideas to the proof of Theorem 1. Hence, we point out the main difference first and then give the complete proof. Compared to Theorem 1 where the target matrix is a stationary point, here the target matrix is  $\mathbf{X}^*$ . So when we apply Proposition 1,  $\bar{\mathbf{X}} = \mathbf{X}^*$ ,  $\bar{\epsilon} = \epsilon$  and we no longer have (45). Due to this difference, here we have an unavoidable statistical error term in the upper bound.

We begin by proving (34). We first apply Proposition 1 to bound  $\|(\mathcal{L}_t^* \mathcal{A}^* \mathcal{A} \mathcal{L}_t)^{-1} \mathcal{L}_t^* \mathcal{A}^* \epsilon^t\|_F^2$  in this setting. Set  $\bar{\mathbf{X}} = \mathbf{X}^*$  and  $\bar{\epsilon} = \epsilon$ , by Proposition 1, we have

$$\begin{aligned} & \|(\mathcal{L}_t^* \mathcal{A}^* \mathcal{A} \mathcal{L}_t)^{-1} \mathcal{L}_t^* \mathcal{A}^* \epsilon^t\|_F^2 \\ & \leq \frac{R_{3r}^2 \|\mathbf{X}^t - \mathbf{X}^*\|^2 \|\mathbf{X}^t - \mathbf{X}^*\|_F^2}{(1 - R_{2r})^2 \sigma_r^2(\mathbf{X}^*)} + \frac{\|\mathcal{L}_t^* \mathcal{A}^*(\epsilon)\|_F^2}{(1 - R_{2r})^2} + \|\mathcal{L}_t^* \mathcal{A}^*(\epsilon)\|_F \frac{2R_{3r} \|\mathbf{X}^t - \mathbf{X}^*\| \|\mathbf{X}^t - \mathbf{X}^*\|_F}{\sigma_r(\mathbf{X}^*) (1 - R_{2r})^2} \\ & \stackrel{(a)}{\leq} 2 \frac{R_{3r}^2 \|\mathbf{X}^t - \mathbf{X}^*\|^2 \|\mathbf{X}^t - \mathbf{X}^*\|_F^2}{(1 - R_{2r})^2 \sigma_r^2(\mathbf{X}^*)} + 2 \frac{\|\mathcal{L}_t^* \mathcal{A}^*(\epsilon)\|_F^2}{(1 - R_{2r})^2}, \end{aligned} \quad (62)$$

where (a) is by Cauchy-Schwarz inequality. Recall  $P_{\mathbf{X}^t}$  in (39),  $P_{\mathbf{X}^t}(\mathcal{A}^*(\epsilon))$  is a at most rank  $2r$  matrix and  $\sigma_i(P_{\mathbf{X}^t} \mathcal{A}^*(\epsilon)) \leq \sigma_i(\mathcal{A}^*(\epsilon))$  for  $1 \leq i \leq p_1 \wedge p_2$  by the projection property of  $P_{\mathbf{X}^t}$ . Then we have

$$\|\mathcal{L}_t^* \mathcal{A}^*(\epsilon)\|_F^2 = \|P_{\mathbf{X}^t} \mathcal{A}^*(\epsilon)\|_F^2 \leq \|(\mathcal{A}^*(\epsilon))_{\max(2r)}\|_F^2 \leq 2 \|(\mathcal{A}^*(\epsilon))_{\max(r)}\|_F^2. \quad (63)$$

Recall in this setting, the target matrix is  $\mathbf{X}^*$ . We replace  $\bar{\mathbf{X}}$  in (7) by  $\mathbf{X}^*$  and obtain  $\tilde{\mathbf{B}}^t := \mathbf{U}^{t\top} \mathbf{X}^* \mathbf{V}^t, \tilde{\mathbf{D}}_1^t := \mathbf{U}_{\perp}^{t\top} \mathbf{X}^* \mathbf{V}^t, \tilde{\mathbf{D}}_2^{t\top} := \mathbf{U}^{t\top} \mathbf{X}^* \mathbf{V}_{\perp}^t$ . Next, we use the induction to prove the main results. Define  $\theta_t, \rho_{t+1}$  in the same way as in the proof of Theorem 1. We aim to show: given  $\theta_t \leq 1/2$ ,  $\tilde{\mathbf{B}}^t$  is invertible,  $\|\mathbf{X}^t - \mathbf{X}^*\|_F \leq \|\mathbf{X}^0 - \mathbf{X}^*\|_F \vee \frac{2\sqrt{10}}{(1-R_{2r})} \|(\mathcal{A}^*(\epsilon))_{\max(r)}\|_F$ , then  $\theta_{t+1} \leq 1/2$ ,  $\tilde{\mathbf{B}}^{t+1}$  is invertible,  $\|\mathbf{X}^{t+1} - \mathbf{X}^*\|_F \leq \|\mathbf{X}^0 - \mathbf{X}^*\|_F \vee \frac{2\sqrt{10}}{(1-R_{2r})} \|(\mathcal{A}^*(\epsilon))_{\max(r)}\|_F$ , as well as  $\mathbf{B}^{t+1}$  is invertible and (34).

First we can easily check the assumption is true when  $t = 0$  under the initialization condition. Now, suppose the induction assumption is true at iteration  $t$ . Under the conditions (32), (33), from (62) and (63), we have

$$\|(\mathcal{L}_t^* \mathcal{A}^* \mathcal{A} \mathcal{L}_t)^{-1} \mathcal{L}_t^* \mathcal{A}^* \epsilon^t\|_F \leq \frac{3}{16} \sigma_r(\mathbf{X}^*).$$

Then following the same proof as the Step 3,4 of Theorem 1, we have  $\mathbf{B}^{t+1}$  is invertible,  $\rho_{t+1} \leq (4 + \sqrt{3})/3\sqrt{3}$  and

$$\begin{aligned} \|\mathbf{X}^{t+1} - \mathbf{X}^*\|_F^2 & \leq (1 + 3(\rho_{t+1} \vee \frac{\theta_t}{\sqrt{1 - \theta_t^2}} \vee \frac{\theta_t \rho_{t+1}}{\sqrt{1 - \theta_t^2}})^2)^2 \|(\mathcal{L}_t^* \mathcal{A}^* \mathcal{A} \mathcal{L}_t)^{-1} \mathcal{L}_t^* \mathcal{A}^* \epsilon^t\|_F^2 \\ & \leq 5 \|(\mathcal{L}_t^* \mathcal{A}^* \mathcal{A} \mathcal{L}_t)^{-1} \mathcal{L}_t^* \mathcal{A}^* \epsilon^t\|_F^2. \end{aligned} \quad (64)$$

Plugging (63) and (62) into (64), we arrive at

$$\begin{aligned} \|\mathbf{X}^{t+1} - \mathbf{X}^*\|_F^2 & \leq 10 \frac{R_{3r}^2 \|\mathbf{X}^t - \mathbf{X}^*\|^2 \|\mathbf{X}^t - \mathbf{X}^*\|_F^2}{(1 - R_{2r})^2 \sigma_r^2(\mathbf{X}^*)} + \frac{20 \|(\mathcal{A}^*(\epsilon))_{\max(r)}\|_F^2}{(1 - R_{2r})^2} \\ & \stackrel{(a)}{\leq} \frac{1}{2} \|\mathbf{X}^t - \mathbf{X}^*\|_F^2 + \frac{20}{(1 - R_{2r})^2} \|(\mathcal{A}^*(\epsilon))_{\max(r)}\|_F^2, \end{aligned} \quad (65)$$

where (a) is because under conditions (32), (33) and induction assumption at iteration  $t$ , it holds that

$$\frac{10R_{3r}^2 \|\mathbf{X}^t - \mathbf{X}^*\|_F^2}{(1 - R_{2r})^2 \sigma_r^2(\mathbf{X}^*)} \leq 1/2.$$

By (65), we get  $\|\mathbf{X}^{t+1} - \mathbf{X}^*\|_F \leq \|\mathbf{X}^0 - \mathbf{X}^*\|_F \vee \frac{2\sqrt{10}}{(1-R_{2r})} \|(\mathcal{A}^*(\epsilon))_{\max(r)}\|_F$ . Under the initialization conditions, Lemma 9 also implies  $\theta_{t+1} \leq 1/2$  and  $\tilde{\mathbf{B}}^{t+1}$  is invertible. This finishes the proof of (34).

Next, we proof the guarantee of RISRO under the Gaussian ensemble design with spectral initialization. Throughout the proof, we use various  $c, C, C_1$  to denote constants and they may vary from line to line. First we give the guarantee for the initialization  $\mathbf{X}^0 = (\mathcal{A}^*(\mathbf{y}))_{\max(r)}$ . Define  $\mathbf{Q}_0 \in \mathbb{R}^{p_1 \times 2r}$  as an orthogonal matrix which spans the column subspaces of  $\mathbf{X}^0$  and  $\mathbf{X}^*$ . Let  $\mathbf{Q}_{0\perp}$  be the orthogonal complement of  $\mathbf{Q}_0$ . Since

$$\|\mathbf{X}^0 - \mathcal{A}^*(\mathbf{y})\|_F^2 = \|\mathbf{X}^0 - P_{\mathbf{Q}_0}(\mathcal{A}^*(\mathbf{y}))\|_F^2 + \|P_{\mathbf{Q}_{0\perp}}(\mathcal{A}^*(\mathbf{y}))\|_F^2$$

and

$$\|\mathbf{X}^* - \mathcal{A}^*(\mathbf{y})\|_F^2 = \|\mathbf{X}^* - P_{\mathbf{Q}_0}(\mathcal{A}^*(\mathbf{y}))\|_F^2 + \|P_{\mathbf{Q}_{0\perp}}(\mathcal{A}^*(\mathbf{y}))\|_F^2,$$

the SVD property  $\|\mathbf{X}^0 - \mathcal{A}^*(\mathbf{y})\|_F^2 \leq \|\mathbf{X}^* - \mathcal{A}^*(\mathbf{y})\|_F^2$  implies that

$$\|\mathbf{X}^0 - P_{\mathbf{Q}_0}(\mathcal{A}^*(\mathbf{y}))\|_F^2 \leq \|\mathbf{X}^* - P_{\mathbf{Q}_0}(\mathcal{A}^*(\mathbf{y}))\|_F^2.$$

Note that

$$\begin{aligned} \|P_{\mathbf{Q}_0} - P_{\mathbf{Q}_0} \mathcal{A}^* \mathcal{A} P_{\mathbf{Q}_0}\| &\stackrel{(a)}{=} \sup_{\|\mathbf{Z}\|_F \leq 1} \langle (P_{\mathbf{Q}_0} - P_{\mathbf{Q}_0} \mathcal{A}^* \mathcal{A} P_{\mathbf{Q}_0}) \mathbf{Z}, \mathbf{Z} \rangle \\ &= \sup_{\|\mathbf{Z}\|_F \leq 1} \left| \|P_{\mathbf{Q}_0} \mathbf{Z}\|_F^2 - \|\mathcal{A} P_{\mathbf{Q}_0} \mathbf{Z}\|_F^2 \right| \\ &\stackrel{(b)}{\leq} \sup_{\|\mathbf{Z}\|_F \leq 1} R_{2r} \|P_{\mathbf{Q}_0} \mathbf{Z}\|_F^2 \leq R_{2r}, \end{aligned} \tag{66}$$

where (a) is because  $P_{\mathbf{Q}_0} - P_{\mathbf{Q}_0} \mathcal{A}^* \mathcal{A} P_{\mathbf{Q}_0}$  is symmetric and (b) is by the  $2r$ -RIP of  $\mathcal{A}$ . Hence,

$$\begin{aligned} \|\mathbf{X}^0 - \mathbf{X}^*\|_F &\leq \|\mathbf{X}^0 - P_{\mathbf{Q}_0}(\mathcal{A}^*(\mathbf{y}))\|_F + \|\mathbf{X}^* - P_{\mathbf{Q}_0}(\mathcal{A}^*(\mathbf{y}))\|_F \\ &\leq 2\|\mathbf{X}^* - P_{\mathbf{Q}_0}(\mathcal{A}^*(\mathbf{y}))\|_F \\ &\stackrel{(a)}{=} 2\|\mathbf{X}^* - P_{\mathbf{Q}_0}(\mathcal{A}^*(\mathcal{A}(\mathbf{X}^*) + \epsilon))\|_F \\ &= 2\|P_{\mathbf{Q}_0} \mathbf{X}^* - P_{\mathbf{Q}_0} \mathcal{A}^* \mathcal{A}(P_{\mathbf{Q}_0} \mathbf{X}^*) - P_{\mathbf{Q}_0}(\mathcal{A}^*(\epsilon))\|_F \\ &\leq 2(\|(P_{\mathbf{Q}_0} - P_{\mathbf{Q}_0} \mathcal{A}^* \mathcal{A} P_{\mathbf{Q}_0}) \mathbf{X}^*\|_F + \|P_{\mathbf{Q}_0}(\mathcal{A}^*(\epsilon))\|_F) \\ &\stackrel{(b)}{\leq} 2R_{2r} \|\mathbf{X}^*\|_F + 2\sqrt{2} \|(\mathcal{A}^*(\epsilon))_{\max(r)}\|_F \\ &\leq 2R_{2r} \sqrt{r} \kappa \sigma_r(\mathbf{X}^*) + 2\sqrt{2} \|(\mathcal{A}^*(\epsilon))_{\max(r)}\|_F, \end{aligned} \tag{67}$$

where (a) is due to the model of  $\mathbf{y}$  and (b) is due to that  $P_{\mathbf{Q}_0}(\mathcal{A}^*(\epsilon))$  is a at most rank  $2r$  matrix and the spectral norm bound for the operator  $(P_{\mathbf{Q}_0} - P_{\mathbf{Q}_0} \mathcal{A}^* \mathcal{A} P_{\mathbf{Q}_0})$  in (66). Hence, there exists  $c_1, c_2, C > 0$  such that when

$$R_{2r} \leq c_1 \frac{1}{\kappa \sqrt{r}}, \quad R_{3r} < \frac{1}{2}, \quad \text{and } \sigma_r(\mathbf{X}^*) \geq C \|(\mathcal{A}^*(\epsilon))_{\max(r)}\|_F, \tag{68}$$

we have  $\|\mathbf{X}^0 - \mathbf{X}^*\|_F \leq c_2 \sigma_r(\mathbf{X}^*)$  by (67) and the conditions in (32) and (33) are satisfied.

Next we show under the sample complexity indicated in the Theorem, (68) are satisfied with high probability. First by (Zhang et al., 2020, Lemma 6), for the Gaussian ensemble design considered

here, we have with probability at least  $1 - \exp(-c(p_1 + p_2))$  for some  $c > 0$  that  $\|\mathcal{A}^*(\epsilon)\| \leq c' \sqrt{\frac{p_1 + p_2}{n}} \sigma$ . So with the same high probability, we have

$$\|(\mathcal{A}^*(\epsilon))_{\max(r)}\|_{\text{F}} \leq c' \sqrt{\frac{(p_1 + p_2)r}{n}} \sigma, \quad (69)$$

and when  $n \geq C(p_1 + p_2)r \frac{\sigma^2}{\sigma_r^2(\mathbf{X}^*)}$ , we have  $\sigma_r(\mathbf{X}^*) \geq C \|(\mathcal{A}^*(\epsilon))_{\max(r)}\|_{\text{F}}$ . At the same time, by (Candès and Plan, 2011, Theorem 2.3), there exists  $C > 0$  when  $n \geq C(p_1 + p_2)\kappa^2 r^2$ ,  $R_{2r} \leq c_1 \frac{1}{\kappa\sqrt{r}}$  and  $R_{3r} < \frac{1}{2}$  are satisfied with probability at least  $1 - \exp(-c(p_1 + p_2))$  for some  $c > 0$ .

In summary, there exists  $C > 0$  such that when  $n \geq C(p_1 + p_2)r(\frac{\sigma^2}{\sigma_r^2(\mathbf{X}^*)} \vee r\kappa^2)$ , (68) holds with probability at least  $1 - \exp(-c(p_1 + p_2))$  for some  $c > 0$ . So by the first part of the Theorem, we have with the same high probability:

$$\|\mathbf{X}^{t+1} - \mathbf{X}^*\|_{\text{F}}^2 \leq 10 \frac{R_{3r}^2 \|\mathbf{X}^t - \mathbf{X}^*\|_{\text{F}}^4}{(1 - R_{2r})^2 \sigma_r^2(\mathbf{X}^*)} + \frac{20 \|(\mathcal{A}^*(\epsilon))_{\max(r)}\|_{\text{F}}^2}{(1 - R_{2r})^2}, \quad \forall t \geq 0.$$

More specifically, the above convergence can be divided into two phases. Let

- (Phase I) When  $\|\mathbf{X}^t - \mathbf{X}^*\|_{\text{F}}^2 \geq \frac{\sqrt{2}}{R_{3r}} \|(\mathcal{A}^*(\epsilon))_{\max(r)}\|_{\text{F}} \sigma_r(\mathbf{X}^*)$ ,

$$\|\mathbf{X}^{t+1} - \mathbf{X}^*\|_{\text{F}} \leq 2\sqrt{5} \frac{R_{3r} \|\mathbf{X}^t - \mathbf{X}^*\|_{\text{F}}^2}{(1 - R_{2r}) \sigma_r(\mathbf{X}^*)}$$

- (Phase II) When  $\|\mathbf{X}^t - \mathbf{X}^*\|_{\text{F}}^2 \leq \frac{\sqrt{2}}{R_{3r}} \|(\mathcal{A}^*(\epsilon))_{\max(r)}\|_{\text{F}} \sigma_r(\mathbf{X}^*)$ ,

$$\|\mathbf{X}^{t+1} - \mathbf{X}^*\|_{\text{F}} \leq \frac{2\sqrt{10} \|(\mathcal{A}^*(\epsilon))_{\max(r)}\|_{\text{F}}}{1 - R_{2r}}$$

Combining Phase I, II and (69), by induction we have  $\|\mathbf{X}^t - \mathbf{X}^*\|_{\text{F}} \leq 2^{-2t} \|\mathbf{X}^0 - \mathbf{X}^*\|_{\text{F}} + c\sqrt{\frac{r(p_1 + p_2)\sigma^2}{n}}$  and this implies the desired error bound for  $\|\mathbf{X}^t - \mathbf{X}^*\|_{\text{F}}$  after double-logarithmic number of iterations. ■

**Proof of Theorem 4.** In the phase retrieval example, the mapping  $\mathcal{A}$  no longer satisfies a proper RIP condition and the strategy we use is to show the contraction of  $\mathbf{X}^t - \mathbf{X}^*$  in terms of its nuclear norm and then transform it back to Frobenius norm.

We also use the induction to show the main results. Specifically, we show: given  $|\mathbf{u}^{*\top} \mathbf{u}^t| > 0$  where  $\mathbf{u}^* = \frac{\mathbf{x}^*}{\|\mathbf{x}^*\|_2}$  and  $\|\mathbf{X}^t - \mathbf{X}^*\|_{\text{F}} \leq \|\mathbf{X}^0 - \mathbf{X}^*\|_{\text{F}}$ , then  $|\mathbf{u}^{*\top} \mathbf{u}^{t+1}| > 0$ ,  $\|\mathbf{X}^{t+1} - \mathbf{X}^*\|_{\text{F}} \leq \|\mathbf{X}^0 - \mathbf{X}^*\|_{\text{F}}$  and (37).

First, the induction assumption is true when  $t = 0$  by the initialization condition and the perturbation bound in Lemma 9. Assume it is also correct at iteration  $t$ . Let  $\tilde{\mathbf{b}}^t = \mathbf{u}^{t\top} \mathbf{X}^* \mathbf{u}^t$ ,  $\tilde{\mathbf{d}}^t = (\mathbf{u}_\perp)^{t\top} \mathbf{X}^* \mathbf{u}^t$ . It is easy to verify  $\tilde{\mathbf{d}}^t (\tilde{\mathbf{b}}^t)^{-1} \tilde{\mathbf{d}}^t = \mathbf{u}_\perp^{t\top} \mathbf{X}^* \mathbf{u}_\perp^t$  and  $\mathbf{X}^* = [\mathbf{u}^t \mathbf{u}_\perp^t] \begin{bmatrix} \tilde{\mathbf{b}}^t & \tilde{\mathbf{d}}^{t\top} \\ \tilde{\mathbf{d}}^t & \tilde{\mathbf{d}}^t (\tilde{\mathbf{b}}^t)^{-1} \tilde{\mathbf{d}}^t \end{bmatrix} [\mathbf{u}^t \mathbf{u}_\perp^t]^\top$ . Define the linear operator  $\mathcal{L}_t$  similar as (9) in this setting in the following way

$$\mathcal{L}_t : \mathbf{W} = \begin{bmatrix} w_0 \in \mathbb{R} & \mathbf{w}_1^\top \in \mathbb{R}^{1 \times (p-1)} \\ \mathbf{w}_1 \in \mathbb{R}^{(p-1) \times 1} & \mathbf{0} \end{bmatrix} \rightarrow [\mathbf{u}^t \mathbf{u}_\perp^t] \begin{bmatrix} w_0 & \mathbf{w}_1^\top \\ \mathbf{w}_1 & \mathbf{0} \end{bmatrix} [\mathbf{u}^t \mathbf{u}_\perp^t]^\top, \quad (70)$$

and it is easy to compute its adjoint  $\mathcal{L}_t^*(\mathbf{M}) = \begin{bmatrix} \mathbf{u}^{t\top} \mathbf{M} \mathbf{u}^t & \mathbf{u}^{t\top} \mathbf{M} \mathbf{u}_\perp^t \\ \mathbf{u}_\perp^{t\top} \mathbf{M} \mathbf{u}^t & 0 \end{bmatrix}$ , where  $\mathbf{M}$  is a rank 2 symmetric matrix. Define operator  $P_{\mathbf{X}^t}$  similar as (39) over the space of  $p \times p$  symmetric matrices

$$P_{\mathbf{X}^t}(\mathbf{W}) := \mathcal{L}_t \mathcal{L}_t^*(\mathbf{W}) = \mathbf{u}^t \mathbf{u}^{t\top} \mathbf{W} \mathbf{u}^t \mathbf{u}^{t\top} + \mathbf{u}_\perp^t \mathbf{u}_\perp^{t\top} \mathbf{W} \mathbf{u}^t \mathbf{u}^{t\top} + \mathbf{u}^t \mathbf{u}^{t\top} \mathbf{W} \mathbf{u}_\perp^t \mathbf{u}_\perp^{t\top}.$$

It is easy to verify that  $P_{\mathbf{X}^t}$  is an orthogonal projector. Meanwhile, let  $P_{(\mathbf{X}^t)_\perp}(\mathbf{W}) = \mathbf{W} - P_{\mathbf{X}^t}(\mathbf{W}) = \mathbf{u}_\perp^t \mathbf{u}_\perp^{t\top} \mathbf{W} \mathbf{u}_\perp^t \mathbf{u}_\perp^{t\top}$ .

By using the operator  $\mathcal{L}_t$ , the least squares solution in Step 4 can be rewritten in the following way

$$\begin{aligned} \begin{bmatrix} b^{t+1} & \mathbf{d}^{t+1\top} \\ \mathbf{d}^{t+1} & \mathbf{0} \end{bmatrix} &= \arg \min_{b \in \mathbb{R}, \mathbf{d} \in \mathbb{R}^{p-1}} \left\| \mathbf{y} - \mathcal{A} \mathcal{L}_t \begin{bmatrix} b & \mathbf{d}^\top \\ \mathbf{d} & \mathbf{0} \end{bmatrix} \right\|_2^2 \\ &= (\mathcal{L}_t^* \mathcal{A}^* \mathcal{A} \mathcal{L}_t)^{-1} \mathcal{L}_t^* \mathcal{A}^* \mathbf{y} \\ &= (\mathcal{L}_t^* \mathcal{A}^* \mathcal{A} \mathcal{L}_t)^{-1} \mathcal{L}_t^* \mathcal{A}^* (\mathcal{A}(P_{\mathbf{X}^t} \mathbf{X}^*) + \mathcal{A}(P_{(\mathbf{X}^t)_\perp}(\mathbf{X}^*))) \\ &= \begin{bmatrix} \tilde{b}^t & \tilde{\mathbf{d}}^{t\top} \\ \tilde{\mathbf{d}}^t & \mathbf{0} \end{bmatrix} + (\mathcal{L}_t^* \mathcal{A}^* \mathcal{A} \mathcal{L}_t)^{-1} \mathcal{L}_t^* \mathcal{A}^* \mathcal{A}(P_{(\mathbf{X}^t)_\perp}(\mathbf{X}^*)). \end{aligned} \tag{71}$$

Here,  $\mathcal{L}_t^* \mathcal{A}^* \mathcal{A} \mathcal{L}_t$  is invertible is due to the lower bound of the spectrum of  $\mathcal{L}_t^* \mathcal{A}^* \mathcal{A} \mathcal{L}_t$  in Lemma 5. So

$$\begin{aligned} \|\mathbf{X}^{t+1} - \mathbf{X}^*\|_* &\leq \left\| \mathbf{X}^{t+1} - [\mathbf{u}^t \mathbf{u}_\perp^t] \begin{bmatrix} b^{t+1} & \mathbf{d}^{t+1\top} \\ \mathbf{d}^{t+1} & \mathbf{0} \end{bmatrix} [\mathbf{u}^t \mathbf{u}_\perp^t]^\top \right\|_* \\ &\quad + \left\| [\mathbf{u}^t \mathbf{u}_\perp^t] \begin{bmatrix} b^{t+1} & \mathbf{d}^{t+1\top} \\ \mathbf{d}^{t+1} & \mathbf{0} \end{bmatrix} [\mathbf{u}^t \mathbf{u}_\perp^t]^\top - (\mathbf{u}^t \mathbf{u}_\perp^t) \begin{bmatrix} \tilde{b}^t & \tilde{\mathbf{d}}^{t\top} \\ \tilde{\mathbf{d}}^t & \tilde{\mathbf{d}}^t (\tilde{b}^t)^{-1} \tilde{\mathbf{d}}^{t\top} \end{bmatrix} [\mathbf{u}^t \mathbf{u}_\perp^t]^\top \right\|_* \\ &\stackrel{(a)}{\leq} 2 \left\| [\mathbf{u}^t \mathbf{u}_\perp^t] \begin{bmatrix} b^{t+1} & \mathbf{d}^{t+1\top} \\ \mathbf{d}^{t+1} & \mathbf{0} \end{bmatrix} [\mathbf{u}^t \mathbf{u}_\perp^t]^\top - [\mathbf{u}^t \mathbf{u}_\perp^t] \begin{bmatrix} \tilde{b}^t & \tilde{\mathbf{d}}^{t\top} \\ \tilde{\mathbf{d}}^t & \tilde{\mathbf{d}}^t (\tilde{b}^t)^{-1} \tilde{\mathbf{d}}^{t\top} \end{bmatrix} [\mathbf{u}^t \mathbf{u}_\perp^t]^\top \right\|_* \\ &\leq 2 \left\| \begin{bmatrix} b^{t+1} - \tilde{b}^t & \mathbf{d}^{t+1\top} - \tilde{\mathbf{d}}^{t\top} \\ \mathbf{d}^{t+1} - \tilde{\mathbf{d}}^t & \mathbf{0} \end{bmatrix} \right\|_* + 2 \|\tilde{\mathbf{d}}^t (\tilde{b}^t)^{-1} \tilde{\mathbf{d}}^{t\top}\|_* \\ &\stackrel{(b)}{=} 2 \|(\mathcal{L}_t^* \mathcal{A}^* \mathcal{A} \mathcal{L}_t)^{-1} \mathcal{L}_t^* \mathcal{A}^* \mathcal{A}(P_{(\mathbf{X}^t)_\perp}(\mathbf{X}^*))\|_* + 2 \|\tilde{\mathbf{d}}^t (\tilde{b}^t)^{-1} \tilde{\mathbf{d}}^{t\top}\|_*, \end{aligned} \tag{72}$$

here (a) is due to Lemma 4 and (b) is due to (71).

First notice  $\|\tilde{\mathbf{d}}^t (\tilde{b}^t)^{-1} \tilde{\mathbf{d}}^{t\top}\|_* = \|P_{(\mathbf{X}^t)_\perp} \mathbf{X}^*\|_*$ . Next we give bound for  $\|(\mathcal{L}_t^* \mathcal{A}^* \mathcal{A} \mathcal{L}_t)^{-1} \mathcal{L}_t^* \mathcal{A}^* \mathcal{A}(P_{(\mathbf{X}^t)_\perp}(\mathbf{X}^*))\|_*$ . With probability at least  $1 - C_1 \exp(-C_2(\delta_1, \delta_2)p) - C_3 n^{-p}$  ( $C_1, C_2, C_3 > 0$ ), we have

$$\begin{aligned} &\|(\mathcal{L}_t^* \mathcal{A}^* \mathcal{A} \mathcal{L}_t)^{-1} \mathcal{L}_t^* \mathcal{A}^* \mathcal{A}(P_{(\mathbf{X}^t)_\perp}(\mathbf{X}^*))\|_* \\ &\stackrel{(a)}{\leq} \frac{4}{(1 - \delta_1)n} \|\mathcal{L}_t^* \mathcal{A}^* \mathcal{A} P_{(\mathbf{X}^t)_\perp}(\mathbf{X}^*)\|_* \\ &\stackrel{(b)}{\leq} C \frac{4p}{(1 - \delta_1)n} \|\mathcal{A} P_{(\mathbf{X}^t)_\perp}(\mathbf{X}^*)\|_1 \\ &\stackrel{(c)}{\leq} C' \frac{1 + \delta_2}{1 - \delta_1} p \|P_{(\mathbf{X}^t)_\perp}(\mathbf{X}^*)\|_* \end{aligned}$$

for some  $C, C' > 0$ . Here  $\|\cdot\|_1$  denotes the  $\ell_1$  norm of a vector, (a) is due to Lemma 5, (b) is due to Lemma 6 and (c) is due to (Candès et al., 2013, Lemma 3.1) and  $P_{(\mathbf{X}^t)_\perp}(\mathbf{X}^*)$  is a symmetric matrix.

Putting above results into (72), we have with probability at least  $1 - C_1 \exp(-C_2(\delta_1, \delta_2)p) - C_3 n^{-p}$ ,

$$\begin{aligned} \|\mathbf{X}^{t+1} - \mathbf{X}^*\|_{\text{F}} &\leq \|\mathbf{X}^{t+1} - \mathbf{X}^*\|_* \leq C \frac{1 + \delta_2}{1 - \delta_1} p \|P_{(\mathbf{X}^t)^\perp}(\mathbf{X}^*)\|_* \stackrel{(a)}{=} C \frac{1 + \delta_2}{1 - \delta_1} p \|P_{(\mathbf{X}^t)^\perp}(\mathbf{X}^*)\|_{\text{F}} \\ &\stackrel{(b)}{\leq} C \frac{1 + \delta_2}{1 - \delta_1} p \frac{\|\mathbf{X}^t - \mathbf{X}^*\|_{\text{F}}^2}{\sigma_1(\mathbf{X}^*)}, \end{aligned}$$

where (a) is because  $P_{(\mathbf{X}^t)^\perp}(\mathbf{X}^*)$  is a symmetric rank 1 matrix, (b) is due to the same argument as (43). Since  $\sigma_1(\mathbf{X}^*) = \|\mathbf{X}^*\|_{\text{F}}$ , when  $\|\mathbf{X}^0 - \mathbf{X}^*\|_{\text{F}} \leq \frac{(1-\delta_1)}{C(1+\delta_2)p} \|\mathbf{X}^*\|_{\text{F}}$  for some large enough  $C$ , we have  $\|\mathbf{X}^{t+1} - \mathbf{X}^*\|_{\text{F}} \leq \|\mathbf{X}^t - \mathbf{X}^*\|_{\text{F}} \leq \|\mathbf{X}^0 - \mathbf{X}^*\|_{\text{F}}$ . Also  $|\mathbf{u}^{t+1\top} \mathbf{u}^*| > 0$  as it is a non-decreasing function of  $\|\mathbf{X}^{t+1} - \mathbf{X}^*\|_{\text{F}}$  by Lemma 9. This finishes the induction and the proof. ■

## 10 Additional Proofs and Technical Lemmas

We collect the additional proofs and technical lemmas that support the main technical results in this section.

**Proof of Equation (16).** First, we denote

$$\mathbf{U}^t = [\mathbf{u}_1, \dots, \mathbf{u}_{p_1}]^\top, \mathbf{V}^t = [\mathbf{v}_1, \dots, \mathbf{v}_{p_2}]^\top, \mathbf{M} = [\mathbf{m}_1, \dots, \mathbf{m}_{p_1}]^\top, \mathbf{N} = [\mathbf{n}_1, \dots, \mathbf{n}_{p_2}]^\top.$$

Then

$$\arg \min_{\substack{\mathbf{M} \in \mathbb{R}^{p_1 \times r}, \mathbf{N} \in \mathbb{R}^{p_2 \times r} \\ (\mathbf{M}, \mathbf{N}) \in \Omega}} \sum_{(i,j) \in \Omega} \left\{ (\mathbf{U}^t \mathbf{N}^\top + \mathbf{M} \mathbf{V}^{t\top} - \mathbf{X})_{[i,j]} \right\}^2 = \arg \min_{\substack{\mathbf{M} \in \mathbb{R}^{p_1 \times r}, \mathbf{N} \in \mathbb{R}^{p_2 \times r} \\ (\mathbf{M}, \mathbf{N}) \in \Omega}} \sum_{(i,j) \in \Omega} (\mathbf{u}_i^\top \mathbf{n}_j + \mathbf{m}_i^\top \mathbf{v}_j - \mathbf{X}_{[i,j]})^2. \quad (73)$$

If  $(i, j) \in \Omega$ , then the corresponding design matrix  $\mathbf{A}^{ij}$  has 1 at location  $(i, j)$  and 0 at the rest of locations. Then

$$\mathbf{A}^{ij} \mathbf{V}^t = [0, \dots, \overbrace{\mathbf{v}_j}^{i^{\text{th}}}, \dots, 0]^\top, \quad \mathbf{A}^{ij\top} \mathbf{U}^t = [0, \dots, \overbrace{\mathbf{u}_i}^{j^{\text{th}}}, \dots, 0]^\top.$$

So on the sketching perspective of R2RILS, we have

$$\begin{aligned} &\arg \min_{\substack{\mathbf{M} \in \mathbb{R}^{p_1 \times r}, \mathbf{N} \in \mathbb{R}^{p_2 \times r} \\ (\mathbf{M}, \mathbf{N}) \in \Omega}} \sum_{(i,j) \in \Omega} (\langle \mathbf{U}^{t\top} \mathbf{A}^{ij}, \mathbf{N}^\top \rangle + \langle \mathbf{M}, \mathbf{A}^{ij} \mathbf{V}^t \rangle - \mathbf{X}_{[i,j]})^2 \\ &= \arg \min_{\substack{\mathbf{M} \in \mathbb{R}^{p_1 \times r}, \mathbf{N} \in \mathbb{R}^{p_2 \times r} \\ (\mathbf{M}, \mathbf{N}) \in \Omega}} \sum_{(i,j) \in \Omega} (\langle \mathbf{N}, [0, \dots, \overbrace{\mathbf{u}_i}^{j^{\text{th}}}, \dots, 0]^\top \rangle + \langle \mathbf{M}, [0, \dots, \overbrace{\mathbf{v}_j}^{i^{\text{th}}}, \dots, 0]^\top \rangle - \mathbf{X}_{ij})^2 \\ &= \arg \min_{\substack{\mathbf{M} \in \mathbb{R}^{p_1 \times r}, \mathbf{N} \in \mathbb{R}^{p_2 \times r} \\ (\mathbf{M}, \mathbf{N}) \in \Omega}} \sum_{(i,j) \in \Omega} (\mathbf{u}_i^\top \mathbf{n}_j + \mathbf{m}_i^\top \mathbf{v}_j - \mathbf{X}_{[i,j]})^2, \end{aligned}$$

which is exactly the same as (73) and this finishes the proof. ■

**Proof of Lemma 3.** The proof is the same as the proof of Proposition 2.3 [Vandereycken \(2013\)](#), except here we need to replace the gradient in the matrix completion setting to the gradient  $\mathcal{A}^*(\mathcal{A}(\mathbf{X}) - \mathbf{y})$  in our setting. ■

**Lemma 4 (Projection onto the Positive Semidefinite Cone in the Nuclear norm)** *Given any symmetric matrix  $\mathbf{A} \in \mathbb{R}^{p \times p}$ , and denotes its eigenvalue decomposition as  $\sum_{i=1}^p \lambda_i \mathbf{v}_i \mathbf{v}_i^\top$  with  $\lambda_1 \geq \dots \geq \lambda_p$ . Let  $\mathbf{A}_0 = \sum_{i=1}^p (\lambda_i \vee 0) \mathbf{v}_i \mathbf{v}_i^\top$ , then*

$$\mathbf{A}_0 = \arg \min_{\mathbf{X} \in \mathbf{S}_+^p} \|\mathbf{A} - \mathbf{X}\|_*,$$

here  $\mathbf{S}_+^p$  is the set of  $p \times p$  positive semidefinite (PSD) matrices.

**Proof of Lemma 4** Here the main property we use is the variational representation of nuclear norm from. Let  $m = \max\{i : \lambda_i \geq 0\}$ . For any PSD matrix  $\mathbf{X}$ ,

$$\begin{aligned} \|\mathbf{X} - \mathbf{A}\|_* &\geq \sum_{i=1}^{p-m} \sigma_i(\mathbf{X} - \mathbf{A}) = \sup_{\mathbf{U} \in \mathbb{O}_{p,(p-m)}, \mathbf{V} \in \mathbb{O}_{p,(p-m)}} \text{tr}(\mathbf{U}^\top (\mathbf{X} - \mathbf{A}) \mathbf{V}) \\ &\geq \sup_{\mathbf{U} \in \mathbb{O}_{p,(p-m)}} \text{tr}(\mathbf{U}^\top (\mathbf{X} - \mathbf{A}) \mathbf{U}) \geq 0 - \inf_{\mathbf{U} \in \mathbb{O}_{p,(p-m)}} \text{tr}(\mathbf{U}^\top \mathbf{A} \mathbf{U}) \\ &\geq -\left(\sum_{i=m+1}^p \lambda_i\right). \end{aligned}$$

On the other hand,  $\|\mathbf{A}_0 - \mathbf{A}\|_* = -(\sum_{i=m+1}^p \lambda_i)$  and this finishes the proof.  $\blacksquare$

**Lemma 5 (Bounds for spectrum of  $\mathcal{L}^* \mathcal{A}^* \mathcal{A} \mathcal{L}$  in Phase Retrieval)** *For any given unit vector  $\mathbf{u} \in \mathbb{R}^p$ , define the linear map*

$$\mathcal{L} : \mathbf{W} = \begin{bmatrix} w_0 \in \mathbb{R} & \mathbf{w}_1^\top \in \mathbb{R}^{1 \times (p-1)} \\ \mathbf{w}_1 \in \mathbb{R}^{(p-1) \times 1} & \mathbf{0} \end{bmatrix} \rightarrow [\mathbf{u} \mathbf{u}_\perp] \begin{bmatrix} w_0 & \mathbf{w}_1^\top \\ \mathbf{w}_1 & \mathbf{0} \end{bmatrix} [\mathbf{u} \mathbf{u}_\perp]^\top.$$

It is easy to compute  $\mathcal{L}^*(\mathbf{M}) = \begin{bmatrix} \mathbf{u}^\top \mathbf{M} \mathbf{u} & \mathbf{u}^\top \mathbf{M} \mathbf{u}_\perp \\ \mathbf{u}_\perp^\top \mathbf{M} \mathbf{u} & 0 \end{bmatrix}$ , where  $\mathbf{M} \in \mathbb{R}^{p \times p}$  is a symmetric matrix.

Suppose  $\mathbf{a}_i \stackrel{i.i.d.}{\sim} N(0, \mathbf{I}_p)$ . Then  $\forall \delta \in (0, 1)$ ,  $\exists C(\delta) > 0$  such that when  $n \geq C(\delta)p \log p$ , with probability at least  $1 - c_1 \exp(-c_2(\delta)p) - c_3 n^{-p}$ , we have for any  $\mathbf{u}$  and  $\mathbf{M} \in \text{Ran}(\mathcal{L}^*)$

$$\|\mathcal{L}^* \mathcal{A}^* \mathcal{A} \mathcal{L}(\mathbf{M})\|_{\text{F}} \geq \frac{1 - \delta}{2} n \|\mathbf{M}\|_{\text{F}}. \quad (74)$$

where  $\mathcal{A}$  is the linear map in (36) generated by  $\{\mathbf{a}_i\}_{i=1}^n$ . Also for any  $\mathbf{u}$  and matrix  $\mathbf{M} \in \text{Ran}(\mathcal{L}^*)$ , with the same high probability, we have

$$\|(\mathcal{L}^* \mathcal{A}^* \mathcal{A} \mathcal{L})^{-1}(\mathbf{M})\|_* \leq \frac{4}{(1 - \delta)n} \|\mathbf{M}\|_*, \quad (75)$$

**Proof of Lemma 5** Note that (74) is true when  $\mathbf{M}$  is a zero matrix. When  $\mathbf{M}$  is non-zero,  $\mathcal{L}(\mathbf{M}) = \mathbf{u} \mathbf{m}^\top + \mathbf{m} \mathbf{u}^\top$  for some  $\mathbf{m}$ . Then  $\frac{1}{n} \|\mathcal{A} \mathcal{L}(\mathbf{M})\|_2^2 = \frac{1}{n} \sum_{i=1}^n |\mathbf{a}_i^\top \mathbf{u}|^2 |\mathbf{a}_i^\top \mathbf{m}|^2$  and  $\|\mathbf{M}\|_{\text{F}}^2 = \|\mathcal{L}(\mathbf{M})\|_{\text{F}}^2 = 2(|\mathbf{m}^\top \mathbf{u}|^2 + \|\mathbf{m}\|_2^2 \|\mathbf{u}\|_2^2)$ . For any  $\mathcal{L}$  and  $\mathbf{M}$ , with probability  $1 - c_1 \exp(-c_2(\delta)p) - c_3 n^{-p}$ , we have

$$\|\mathcal{L}^* \mathcal{A}^* \mathcal{A} \mathcal{L}(\mathbf{M})\|_{\text{F}} = \|\mathcal{A} \mathcal{L}(\mathbf{M})\|_2^2 / \|\mathbf{M}\|_{\text{F}} \stackrel{(a)}{\geq} \frac{1 - \delta}{2} n \|\mathcal{L}(\mathbf{M})\|_{\text{F}}^2 / \|\mathbf{M}\|_{\text{F}} = \frac{1 - \delta}{2} n \|\mathcal{L}(\mathbf{M})\|_{\text{F}}, \quad (76)$$

where (a) is due to the (Sun et al., 2018, Lemma 6.4).

Next, we prove (75). First suppose  $\mathbf{W} \in \text{Ran}(\mathcal{L}^*)$  satisfies  $(\mathcal{L}^* \mathcal{A}^* \mathcal{A} \mathcal{L})(\mathbf{W}) = \mathbf{M}$ , then we have

$$\frac{\|(\mathcal{L}^* \mathcal{A}^* \mathcal{A} \mathcal{L})^{-1} \mathbf{M}\|_*}{\|\mathbf{M}\|_*} = \frac{\|\mathbf{W}\|_*}{\|\mathcal{L}_t^* \mathcal{A}^* \mathcal{A} \mathcal{L}_t(\mathbf{W})\|_*}. \quad (77)$$

Hence, to prove the desired result, we only need to obtain a lower bound of  $\|\mathcal{L}_t^* \mathcal{A}^* \mathcal{A} \mathcal{L}_t(\mathbf{W})\|_*$ :

$$\begin{aligned} \|\mathcal{L}^* \mathcal{A}^* \mathcal{A} \mathcal{L}(\mathbf{W})\|_* &= \sup_{\|\mathbf{Z}\| \leq 1} \langle \mathcal{A} \mathcal{L}(\mathbf{W}), \mathcal{A} \mathcal{L}(\mathbf{Z}) \rangle \geq \langle \mathcal{A} \mathcal{L}(\mathbf{W}), \mathcal{A} \mathcal{L}\left(\frac{\mathbf{W}}{\|\mathbf{W}\|}\right) \rangle \\ &= \|\mathcal{A} \mathcal{L}(\mathbf{W})\|_2^2 / \|\mathbf{W}\| \\ &\stackrel{(a)}{\geq} \frac{(1-\delta)}{2} n \|\mathcal{L}(\mathbf{W})\|_{\text{F}}^2 / \|\mathbf{W}\| \stackrel{(b)}{\geq} \frac{1-\delta}{4} n \|\mathbf{W}\|_*, \end{aligned} \quad (78)$$

where (a) holds for any  $\mathcal{L}, \mathbf{W}$  with probability  $1 - c_1 \exp(-c_2(\delta)p) - c_3 n^{-p}$  by the same reason as (a) in (76); (b) is true because  $\mathbf{W} \in \text{Ran}(\mathcal{L}^*)$  and  $\|\mathcal{L}(\mathbf{W})\|_{\text{F}} = \|\mathbf{W}\|_{\text{F}} \geq \|\mathbf{W}\|_* / \sqrt{2}$ .  $\blacksquare$

**Lemma 6 (Upper Bound for  $\|\mathcal{L}^* \mathcal{A}^*(\mathbf{z})\|_*$  in Phase Retrieval)** *Consider the same linear operator  $\mathcal{L}$  as in Lemma 5. Suppose  $\mathbf{a}_i \stackrel{i.i.d.}{\sim} N(0, \mathbf{I}_p)$  and  $\mathcal{A}$  is the linear map in (36) generated by  $\{\mathbf{a}_i\}_{i=1}^n$ . Then there exists  $C, c_1, c_2 > 0$  such that when  $n \geq Cp$ , with probability at least  $1 - c_1 \exp(-c_2 p)$ , for any  $\mathcal{L}$  and  $\mathbf{z}$ , we have  $\|\mathcal{L}^* \mathcal{A}^*(\mathbf{z})\|_* \leq cp \|\mathbf{z}\|_1$  for some  $c > 0$ , where  $\|\mathbf{z}\|_1$  denotes the  $\ell_1$  norm of  $\mathbf{z}$ .*

**Proof of Lemma 6.** The proof is based on concentration of sub-exponential random variables. First, for fixed  $\mathcal{L}$ , we have

$$\begin{aligned} \sup_{\|\mathbf{z}\|_1 \leq 1} \|\mathcal{L}^* \mathcal{A}^*(\mathbf{z})\|_* &= \sup_{\|\mathbf{z}\|_1 \leq 1} \sup_{\mathbf{W} \in \mathbf{S}, \|\mathbf{W}\| \leq 1} \langle \mathcal{L}^* \mathcal{A}^*(\mathbf{z}), \mathbf{W} \rangle \\ &= \sup_{\|\mathbf{z}\|_1 \leq 1} \sup_{\mathbf{W} \in \mathbf{S}, \|\mathbf{W}\| \leq 1} \langle \mathbf{z}, \mathcal{A} \mathcal{L}(\mathbf{W}) \rangle = \sup_{\mathbf{W} \in \mathbf{S}, \|\mathbf{W}\| \leq 1} \sup_{\|\mathbf{z}\|_1 \leq 1} \langle \mathbf{z}, \mathcal{A} \mathcal{L}(\mathbf{W}) \rangle = \sup_{\mathbf{W} \in \mathbf{S}, \|\mathbf{W}\| \leq 1} \|\mathcal{A} \mathcal{L}(\mathbf{W})\|_{\infty}, \end{aligned}$$

here  $\mathbf{S}$  is the set of symmetric matrices and  $\|\mathcal{A} \mathcal{L}(\mathbf{W})\|_{\infty}$  denotes the largest absolute value in the vector  $\mathcal{A} \mathcal{L}(\mathbf{W})$ .

Notice  $\mathcal{L}(\mathbf{W})$  is a symmetric rank-2 matrix with spectral norm bounded by 1, without loss of generality, we can consider the bound for  $\|\mathcal{A}(\mathbf{M})\|_{\infty}$  for fixed rank 2 matrix  $\mathbf{M}$  with eigenvalue decomposition  $\mathbf{u}_1 \mathbf{u}_1^T - t \mathbf{u}_2 \mathbf{u}_2^T$  and  $t \in [-1, 1]$ . In this case  $\|\mathcal{A}(\mathbf{M})\|_{\infty} = \max_i |\mathbf{a}_i^T \mathbf{u}_1|^2 - t |\mathbf{a}_i^T \mathbf{u}_2|^2|$  and  $|\mathbf{a}_i^T \mathbf{u}_1|^2 - t |\mathbf{a}_i^T \mathbf{u}_2|^2|$  is a subexponential random variable. By the concentration of subexponential random variable [Vershynin \(2010\)](#), we have

$$\mathbb{P}(|\mathbf{a}_i^T \mathbf{u}_1|^2 - t |\mathbf{a}_i^T \mathbf{u}_2|^2| - \xi > x) \leq \exp(-c \min(x^2, x)),$$

where  $\xi = \mathbb{E}|\mathbf{a}_i^T \mathbf{u}_1|^2 - t |\mathbf{a}_i^T \mathbf{u}_2|^2|$ . And a union bound yields

$$\mathbb{P}(\max_i |\mathbf{a}_i^T \mathbf{u}_1|^2 - t |\mathbf{a}_i^T \mathbf{u}_2|^2| - \xi > x) \leq n \exp(-c \min(x^2, x)). \quad (79)$$

Next, we use the  $\epsilon$ -net argument to extend the bound to hold for any symmetric rank 2 matrix  $\mathbf{M}$  with spectral norm bounded by 1. Notice that by proving that, we also prove the desired inequality for any  $\mathcal{L}$ . Let  $S_{\epsilon}$  be an  $\epsilon$ -net on the unit sphere,  $T_{\epsilon}$  be an  $\epsilon$  net on  $[-1, 1]$  and set

$$N_{\epsilon} = \{\mathbf{M} = \mathbf{u}_1 \mathbf{u}_1^T - t \mathbf{u}_2 \mathbf{u}_2^T : (\mathbf{u}_1, \mathbf{u}_2, t) \in S_{\epsilon} \times S_{\epsilon} \times T_{\epsilon}\}.$$

Since  $|S_\epsilon| \leq (3/\epsilon)^p$ , we have  $|N_\epsilon| \leq (3/\epsilon)^{2p+1}$ . A union bound yields

$$\mathbb{P}(\forall \mathbf{M} \in N_\epsilon, \max_i \{|\mathbf{a}_i^\top \mathbf{u}_1|^2 - t|\mathbf{a}_i^\top \mathbf{u}_2|^2| - \xi\} > x) \leq n \exp(-c \min(x^2, x) + (2p+1) \log(3/\epsilon)). \quad (80)$$

Now suppose  $(\mathbf{u}_1^*, \mathbf{u}_2^*, t^*) = \arg \max_{\mathbf{u}_1, \mathbf{u}_2, t \in [-1, 1]} \|\mathcal{A}(\mathbf{M})\|_\infty$  and denote  $\mathbf{M}^* = \mathbf{u}_1^* \mathbf{u}_1^{*\top} - t^* \mathbf{u}_2^* \mathbf{u}_2^{*\top}$ ,  $\mu = \|\mathcal{A}(\mathbf{M}^*)\|_\infty$ . Then find the approximation  $\mathbf{M}_0 = \mathbf{u}_0 \mathbf{u}_0^\top - t_0 \mathbf{v}_0 \mathbf{v}_0^\top \in N_\epsilon$  such that  $\|\mathbf{u}_0 - \mathbf{u}^*\|_2, \|\mathbf{v}^* - \mathbf{v}_0\|_2, |t^* - t_0|$  are each at most  $\epsilon$ . First notice

$$\begin{aligned} \|\mathbf{u}^* \mathbf{u}^{*\top} - \mathbf{u}_0 \mathbf{u}_0^\top\| &= \sup_{\|\mathbf{x}\|_2=1} |\|\mathbf{u}_0^\top \mathbf{x}\|^2 - |\mathbf{u}^{*\top} \mathbf{x}\|^2| \\ &= \sup_{\|\mathbf{x}\|_2=1} |(\mathbf{u}_0 - \mathbf{u}^*)^\top \mathbf{x}| |(\mathbf{u}_0 + \mathbf{u}^*)^\top \mathbf{x}| \\ &\leq \|\mathbf{u}^* - \mathbf{u}_0\|_2 \|\mathbf{u}^* + \mathbf{u}_0\|_2 \leq 2\|\mathbf{u}^* - \mathbf{u}_0\|_2 \leq 2\epsilon. \end{aligned}$$

Using the above bound, we have

$$\|\mathbf{M}^* - \mathbf{M}_0\| \leq \|\mathbf{u}^* \mathbf{u}^{*\top} - \mathbf{u}_0 \mathbf{u}_0^\top\| + |t^* - t_0| \|\mathbf{v}^* \mathbf{v}^{*\top}\| + |t_0| \|\mathbf{v}^* \mathbf{v}^{*\top} - \mathbf{v}_0 \mathbf{v}_0^\top\| \leq 5\epsilon. \quad (81)$$

Now take  $x \geq cp$  for some  $c > 0$ , then from (80), we have the event  $\{\|\mathcal{A}(\mathbf{M}_0)\|_\infty \leq cp\}$  happens with probability at least  $1 - \exp(-Cp)$ . And on this event, we have

$$\mu \leq \|\mathcal{A}(\mathbf{M}^* - \mathbf{M}_0)\|_\infty + \|\mathcal{A}(\mathbf{M}_0)\|_\infty \stackrel{(a)}{\leq} 5\epsilon \cdot 2\mu + cp \implies \mu \leq \frac{cp}{(1 - 10\epsilon)},$$

where (a) is by triangle inequality and the fact that  $\mathbf{M}^* - \mathbf{M}_0$  can be decomposed into the sum of two rank 2 symmetric matrices with spectral norm bounded by  $5\epsilon$  (81). Take  $\epsilon < 1/10$ , we get  $\|\mathcal{A}(\mathbf{M}^*)\|_\infty < cp$  for some  $c > 0$  with probability at least  $1 - \exp(-Cp)$ . This finishes the proof.  $\blacksquare$

**Lemma 7** (Zhang et al., 2020, Lemma 3) Suppose  $\mathbf{F}, \hat{\mathbf{F}} \in \mathbb{R}^{p_1 \times r}, \mathbf{G}, \hat{\mathbf{G}} \in \mathbb{R}^{r \times r}, \mathbf{H}, \hat{\mathbf{H}} \in \mathbb{R}^{r \times p_2}$ . If  $\mathbf{G}$  and  $\hat{\mathbf{G}}$  are invertible,  $\|\mathbf{F}\mathbf{G}^{-1}\| \leq \lambda_1$ , and  $\|\hat{\mathbf{G}}^{-1}\hat{\mathbf{H}}\| \leq \lambda_2$ , we have

$$\|\hat{\mathbf{F}}\hat{\mathbf{G}}^{-1}\hat{\mathbf{H}} - \mathbf{F}\mathbf{G}^{-1}\mathbf{H}\|_F \leq \lambda_2 \|\hat{\mathbf{F}} - \mathbf{F}\|_F + \lambda_1 \|\hat{\mathbf{H}} - \mathbf{H}\|_F + \lambda_1 \lambda_2 \|\hat{\mathbf{G}} - \mathbf{G}\|_F. \quad (82)$$

**Lemma 8** (Candès and Plan, 2011, Lemma 3.3) Let  $\mathbf{Z}_1, \mathbf{Z}_2 \in \mathbb{R}^{p_1 \times p_2}$  be two low rank matrices with  $r_1 = \text{rank}(\mathbf{Z}_1), r_2 = \text{rank}(\mathbf{Z}_2)$ . Suppose  $\langle \mathbf{Z}_1, \mathbf{Z}_2 \rangle = 0$  and  $r_1 + r_2 \leq \min(p_1, p_2)$ . If  $\mathcal{A}$  satisfies the  $(r_1 + r_2)$ -RIP condition, then

$$|\langle \mathcal{A}(\mathbf{Z}_1), \mathcal{A}(\mathbf{Z}_2) \rangle| \leq R_{r_1+r_2} \|\mathbf{Z}_1\|_F \|\mathbf{Z}_2\|_F.$$

**Lemma 9** Let  $\mathbf{X}_1 = \mathbf{U}_1 \boldsymbol{\Sigma}_1 \mathbf{V}_1^\top$  and  $\mathbf{X}_2 = \mathbf{U}_2 \boldsymbol{\Sigma}_2 \mathbf{V}_2^\top$  be two rank  $r$  matrices with corresponding singular value decompositions. Then

$$\begin{cases} \|\mathbf{U}_1 \mathbf{U}_1^\top - \mathbf{U}_2 \mathbf{U}_2^\top\| \leq \frac{\|\mathbf{X}_1 - \mathbf{X}_2\|}{\sigma_r(\mathbf{X}_1) \vee \sigma_r(\mathbf{X}_2)}, \\ \max\{\|\sin \Theta(\mathbf{U}_1, \mathbf{U}_2)\|, \|\sin \Theta(\mathbf{V}_1, \mathbf{V}_2)\|\} \leq \frac{2\|\mathbf{X}_1 - \mathbf{X}_2\|}{\sigma_r(\mathbf{X}_1) \vee \sigma_r(\mathbf{X}_2)}. \end{cases}$$

**Proof.** See Lemma 4.2 of Wei et al. (2016) and Theorem 6 of Luo and Zhang (2020).  $\blacksquare$